M.Sc. Thesis

entitled

Time Resolved Measurements in the Post - Discharge of an RF Plasma.

James C. Molloy

Bachelor of Engineering (Electronic)

Department of Physics, Dublin City University,

Glasnevin, Dublin 9.

June 1990

Supervisor Dr. Mike Hopkins,

Department of Physics,

Dublin City University,

Glasnevin, Dublin 9.

TABLE OF CONTENTS

List of Appendices

Appendix A

A paper submitted to The 7th International Colloquium on Plasma Sputtering, June 5 - 9, 1989, Antibes, France, entitled *'Characterisation of RF plasmas using Langmuir probes'*

Appendix B

Circuit diagrams for the data acquisition system

Appendix C

Circuit and timing diagrams for the pulsing circuitry

Appendix D

Program listing and flowchart of 'vals1.asm', the assembly routine for data acquisition

Appendix E

Program listing for 'myfuncs6.c', the C function to experimentally take a characteristic and analyse it

Appendix F

The connections between the PIO - 48 input/output board and the 50 - way connector

Appendix G

An introduction to the modelling of discharges using the Boltzmann Equation

ACKNOWLEDGEMENTS

I would like to thank a number of people at the outset of this thesis. Firstly, Mike Hopkins for his enthusiasm, help, accessibility and encouragement; also for giving me the chance of 'doing a post-grad.', an experience through which I learned much and will never forget. Secondly, all the post-graduate students and staff in the physics department for their friendship and advice but especially John Scanlan for his willingless to help at all times, his patience and understanding; Paul Jenkins for his listening ear and his sympathetic taste in music, and Mark Daly for the initial plots and his 'sense of humour'.

I must also mention the technician staff (Al Devine for the photos), but especially Alan Hughes, the head technician, who was always there with his motivation, knowledge, and his cool - headedness. A word of thanks must be given to the humble, hard working heroines of the department, the secretaries - Barbara and Marion. Finally, I would like to thank my entire family for their constant support and interest throughout my entire student life.

There is a tide in the affairs of men,
which, taken at the flood,
leads on to fortune; omitted,
all the voyage of their life is bound
in shallows and in miseries.
On such a full sea are we now afloat,
and we must take the current when it
serves, or lose our ventures.

Brutus to Cassius on
the plains of Phillipi.

ABSTRACT

The development and use of a computerised data acquisition system for the study of the temporal variations of the plasma parameters in pulsed Helium and Argon afterglows using a single Langmuir probe. The controlling software and electronics were developed to a level that enabled plasma characteristics to be analysed and presented on a number of output devices.

A novel technique was developed to pulse the probe which limits plasma depletion during the measurement process. A non - Maxwellian electron energy distribution was found at early times in the afterglow with two distinct 'temperature' or energy groups. The 'faster' or 'hotter' electrons 'blended' with the cold group at late times in the afterglow, giving a single group which could be characterised by a unique temperature. This temperature was seen to approach room temperature in the temporal limit. The decay of bulk electron temperature and density was modelled using the diffusion equation and reasonable agreement was found to exist between the theoretical and experimental data.

LIST OF SYMBOLS USED

V_p plasma potential

V_f floating potential

n_e electron density

n_i positive ion density

n_0 neutral gas density ($\cong 10^5\ n_e$)

m_i ionic mass - He = 6.7×10^{-27} Kg
Ar = 67×10^{-27} Kg

λ_D Debye length

D_a Ambipolar Diffusion coefficient

Λ Characteristic diffusion length

E Electric field strength

ω_p Plasma frequency

ω Operating frequency

ρ Charge density

λ, λ_{emfp} Electron-neutral collision mean free path

σ Collision cross section or Plasma conductivity

ν Electron collision frequency

γ Secondary electron coefficient

μ Electron mobility

$\langle\bar{K}\rangle$	Average kinetic energy of an electron
R_{pr}	Probe radius
A, A_p	Probe area
I_e, i_e	Electron current to the probe
I_{+sat}	Saturation ion current
I_{esat}	Saturation electron current
Vol	Volume taken up by the plasma
τ_d	Depletion time constant for the probe
$\tau_n^{\pm}$	Density decay times for the different modes the solutions to the diffusion equation
I(V)	Current to the probe at a given applied voltage V
I'(V)	First derivative of the characteristic
f(r,v,t)	Electron velocity distribution function EVDF
f(ε)	Electron energy distribution function EEDF
k	Boltzmann constant
e	electronic charge
m_e	electronic mass
ε_0	permittivity of free space

CHAPTER I

THE THEORY OF LOW PRESSURE GAS DISCHARGES

1.1 What is a plasma?

A plasma is a collection of charged particles,[1] of sufficiently high density so that the Coulomb forces between the charged particles is an important factor in determining their statistical properties, yet of sufficiently low density so that the nearest - neighbour interaction is dominated by the long range Coulomb force exerted by the many distant particles. It is important to note that the word plasma is more applicable to the fully ionised, high density, high temperature state (thermonuclear fusion), however, this word is used interchangibly with 'discharge' throughout the following discussion.

One of the reasons that a plasma behaves collectively[2] rather than as if its particles behave individually is the appearance of very strong electrostatic forces as soon as an attempt is made to separate artificially the positive charges from the negative ones. The electric field, **E**, created by the separation of positive and negative charges gives rise to a restoring force which attempts to bring the particles in question (here positive ions and electrons) back into spatial coincidence. The electronic motion (in the collisionless case) is governed by:

$$m_e \frac{d^2 \mathbf{x}}{dt^2} = -e\,\mathbf{E} = -\frac{n_e e^2}{\varepsilon_0}\,\mathbf{x}\,, \qquad (1.1)$$

where m_e and e are the electron mass and charge, **x** the magnitude of oscillation, **E** the induced electric field, n_e the number density of carrier pairs in the plasma and ε_0 the permittivity of free space.

Equation (1.1) is of course the equation for the simple harmonic oscillator and implies an oscillatory motion at an angular frequency

$$\omega_p = \left(\frac{n_e e^2}{\varepsilon_0 m_e} \right)^{1/2} \qquad (1.2)$$

The parmater, ω_p, is known as the plasma frequency, and is of the order of GigaHertz for the plasmas in question here.

1.2 The Debye Length and Shielding

The above frequency (which is characteristic of all attempts in natural systems to depart from neutrality) is usually much greater than the frequency of collisions between electrons and the neutral gas atoms. The electrons thus have time to undergo numerous oscillations between collisions, and although the oscillatory motion will eventually be destroyed (damped out) as a result of collisions, they (and therefore the collision induced damping) can be neglected to yield an excellent first approximation. Looking at a particular electron during the initial transient with random speed v, it will travel a distance of the order v/ω_p; and since v is of the order $(k\ T_e/m_e)^{1/2}$, it follows that

$$\lambda_D = \left(\varepsilon_0\ k\ T_e\ /\ e^2\ n_e \right)^{1/2} \qquad (1.3)$$

The parameter λ_D is known as the Debye length and is the order of magnitude for the distance over which a significant departure from neutrality can be maintained (λ_D is approximately 100μm here).

In the above derivations it is assumed that the ions are stationary due to their inertia (since $m_e << m_i$) and that the plasma is bounded by an electrode which is biased relative to the bulk plasma, say, negatively. This negative electrode will rarify the electrons in its vicinity, and thus create a local positive space charge. Equation (1.4) governs the electron density in the vicinity of a biased electrode which is immersed in the discharge. The equation holds for between the bulk of the plasma (where neutrality is assumed to hold - $n_e \cong n_i = n_\infty$ and V = 0, E = 0) and a point close to the electrode (n, V)

$$\frac{n_e}{n_\infty} = \exp\,(eV / kT_e) \qquad (1.4)$$

When a potential V_0 is introduced[3] at the point x = 0 (the biased electrode in this case) in the plasma of unperturbed density n_0, Poisson's equation in one dimension is

$$d^2V/dx^2 = -\rho/\varepsilon_0 = -e(n_i - n_e)/\varepsilon_0 \qquad (1.5)$$

It can be shown that for small V the solution is

$$V(x) = V_0 \exp(-x/\lambda_D), \qquad (1.5a)$$

The parameter λ_D is the Debye length which was mentioned already!. It is obvious that any externally introduced potential decays exponentially away from the source and is effectively "shielded" within the distance λ_D; refer to Figure (1.1) for the density and potential distributions in the vicinity of an applied potential.

Electron collisions are essential for maintaining an electrical discharge[4], and because of their small mass, they are the species to which the energy of an external power source couples.

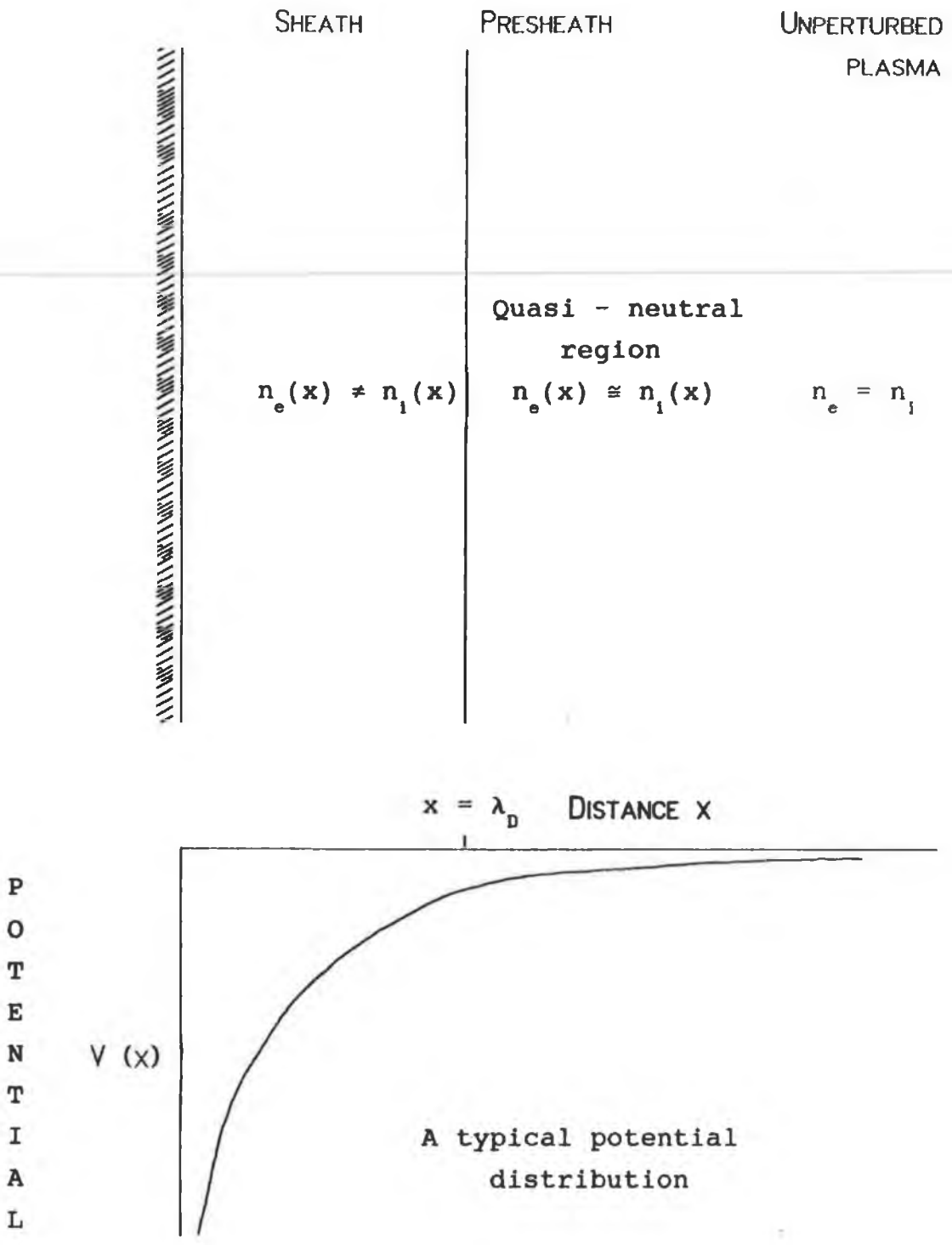

Figure (1.1)
Schematic of a large plane probe immersed in a weak, neutral plasma

Species with high potential energy, such as ions or excited atoms are produced by the collision of electrons with neutral atoms and hence the role of electron - particle collisions is of the utmost importance in the study of gas discharges.

1.3 Introduction to Low Pressure Discharges

A low pressure discharge is created by passing a current through the gas; this current can be supplied directly from electrodes immersed in the gas (as is the case for this work), and such a plasma is shown in Photograph (1.1) - note the electrodes and their sheaths, and also the probe at the rear being heated in order to clean it. The other important method for producing a discharge is by the absorption of electromagnetic energy as in the case of the electrodeless discharge.

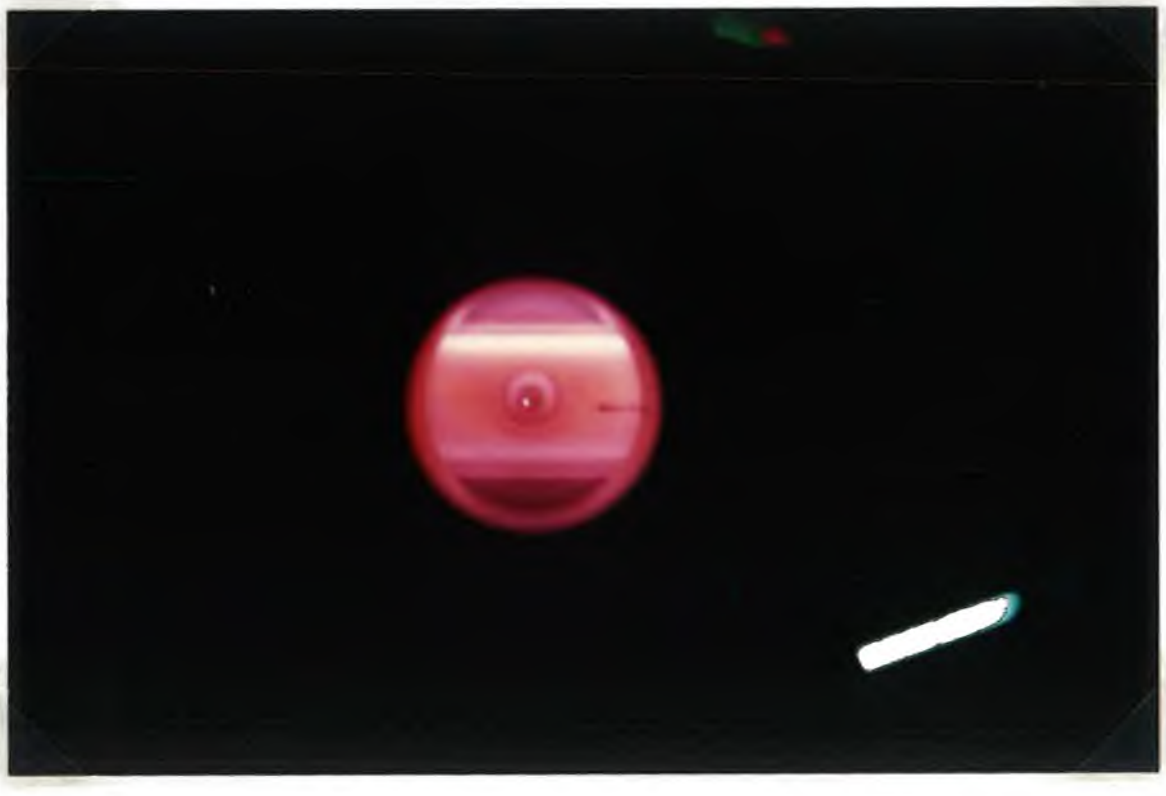

Photograph (1.1)
An RF helium discharge

An important feature from the plasma processing point of view[4] is the existence of an extreme non - equilibrium between the temperature of the heavy (ions) and light particles (electrons). A useful parameter[34] called the reactivity (a measure of how effective the discharge is at etching a sample) is determined mainly by the electron temperature, T_e, which is much greater than the temperature of the ions (close to room temperature). and it quantifies the suitability of the discharge for processing.

This non - equilibrium between particle temperatures is a crucial factor to the success of plasma processing techniques since it allows a high reactivity without the high bulk heat content of a system in chemical equilibrium. Moreover, the background gas may not only have a low temperature, but also a low density which lends to greater deposition control. Also the substrate to be treated or covered can be selected to maximise product quality e.g. the adhesion of deposited layers.

A combination of chemical e.g. radical surface reactions, and physical methods e.g. ion bombardment can yield marked improvements in the essential characteristics of the etch, such as anisotropy, damage and mask selectivity[35]. In order to understand the means by which the discharges work and what physical properties / mechanisms occurring lend to their suitability for plasma processing purposes, it is necessary to examine them on a microscopic scale as well as in terms of bulk statistical parameters such as species densities and temperatures.

Experiments were carried out on three types of low pressure discharge, these being

1. DC (direct current)
2. RF (radio frequency)
3. Pulsed RF

Since types 2 and 3 are the most important in this study, only a brief sketch will be given of DC discharges, whereas both the RF and pulsed RF will be the subject of a more rigourous treatment. The literature is well stocked with papers and articles on type 1 discharges[5-9] which are also known as glow discharges and were studied in the early twentieth century by some of the pioneers of atomic physics.

1.4 DC Discharges

The structure of a DC discharge from visible emission is shown in Figure (1.2)

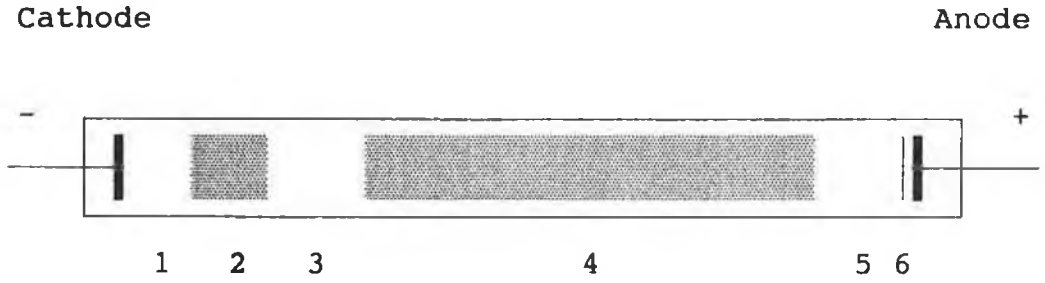

Figure (1.2)
The visible emission from a DC glow discharge

Region 1 is the cathode fall or cathode dark space. Energetic ion bombardment of the cathode results in secondary emission and these secondary electrons emitted from the cathode, are accelerated across the considerable cathode fall, and sustain the discharge through intense ionisation in the negative glow. This voltage drop (the cathode fall) is very sensitive to environmental conditions such as the state of the cathode, as well as the gas pressure and type.

Regions 2 and 3 are called the negative glow and Faraday Dark space respectively. They are responsible for current continuity between the cathode and the bulk of the discharge i.e. region 4. Region 4 is the most important and best studied part of the discharge. It is called the positive column and is usually treated as being uniform in the axial direction[10] i.e. in the direction of current flow. The average kinetic energy of an electron which undergoes collisions[4] in the positive column is

$$< \bar{K} > = (3/2)\ kT_i + (m_i / m_e)\ \kappa\ e\ \mathbf{E}\ \lambda \qquad (1.6)$$

where the subscripts i and e refer to the ions and electrons respectively, κ is a statistical parameter associated with the fact that the electron motion is random in any direction. Since $kT_i << kT_e$, the first term on the right hand side of Equation (1.6) can be neglected.

Also from the fact that λ, the mean free path, is given as

$$\lambda = (n_0 \sigma)^{-1} \qquad (1.7)$$

where n_0 is the neutral gas density and σ the atomic cross section for elastic collisions, it follows that

$$< \bar{K} > \propto E / n_0 \qquad (1.8)$$

The parameter E / n_0 is called the reduced field strength and is very important both in the modelling[11] and in practical approaches to studying discharges. If the inter - electrode spacing is increased the length of the positive column is seen to increase also; if decreased then the latter reduces in size until it disappears altogether.

The most important method of sustaining the discharge[15] is due to secondary emission of electrons from the cathode; this is caused by ions bombarding the cathode and releasing electrons, these being accelerated across the large potential drop of the cathode fall, and on entering the negative glow cause considerable ionisation. The electrons that are accelerated across the anode fall produce the ion current for the discharge; it is important to note that the main contributor to current in the cathode dark space is ions, whereas electrons form the dominant current carrying species in the rest of the discharge.

Since the plasma consists of charged particles an applied electric field will lead to the flow of charge, and the conductivity for the static field case is given by[1]

$$\sigma = \frac{n_e e^2}{m_e \nu} \qquad (1.9)$$

with ν being the electron collision frequency, $n_0 \sigma_c \mathbf{v}_e$, and σ_c the momentum transfer cross - section.

This yields a value of

$$\sigma = \frac{n_e e^2}{m_e n_0 \sigma_c v_e} \qquad (1.10)$$

This tells us that the plasma conductivity is proportional to the electronic density n_e. Dhali[10] considers the radial profile of the electron density for the positive column to be of the form

$$n_e(\mathbf{r}) = J_0(2.405\ \mathbf{r} / R_d) \qquad (1.11)$$

where J_0 is the first order Bessel function, $\mathbf{r}$ the radial distance and R_d the radius of the discharge tube. This is an approximation that is valid only when ambipolar diffusion sets in. Note the Bessel function is a power series in $\mathbf{r}$ which forms the solution of a differential equation of type

$$\mathbf{r}^2 \frac{d^2 n_e(\mathbf{r})}{d\mathbf{r}^2} + \mathbf{r} \frac{dn_e(\mathbf{r})}{d\mathbf{r}} + (\mathbf{r}^2 - n^2) = 0,\ n \in \mathbb{Z}$$

Regions 5 and 6 are known as the anode fall and anode glow respectively, and have been mentioned in the discussion on the positive column.

Unfortunately DC discharges are totally unsuited to plasma processing[15] for a number of reasons, such as their spatial inhomogeneity, their low current densities and probably most importantly the fact that the DC discharge depends on γ, the secondary emission coefficient, which will vary greatly with the surface condition of the electrodes. The very ions that cause the secondary emission are usually high energy, massive particles that can cause structural damage to the target.

1.5 RF Discharges

There is currently much interest in the mechanisms which produce and sustain RF discharges both from the academic and the applied viewpoints[12]. Early applications were sputter deposition of insulators and metals; more recently, planar dry etching for pattern transfer in IC fabrication has become a major topic[13]. Throughout the following discussion, the driving potential (the potential applied to the electrodes) takes the form

$$E(t) = E_0 \cos \omega t \qquad (1.12)$$

where ω is known as the operating frequency. This parameter is usually fixed for industrial applications at the value assigned to it by the communications community at 13.56 MHz. It was not chosen for academic reasons, and it is not a 'magic' frequency where physically interesting properties manifest themselves; the only reason for its choice was to minimize inter-system noise in communications (a problem that is not entirely overcome as its harmonics still lead to difficulties).

The inadequacies of DC discharges for processing applications have already been mentioned, and RF is the natural alternative. For ω < 50 kHz, the current - voltage characteristics are remarkably similar to the DC case. In effect, the discharges are still of the DC type, with the electrodes alternating functions as anode and cathode every half cycle; a change in terminology from anode and cathode falls to RF sheaths will be used from now on. It is important to remember that secondary emission is still the dominant sustaining mechanism for the discharge and for this reason, low frequency discharges are called 'γ discharges'.

It is known that the current density increases with increasing operating frequency and as ω becomes greater than $\sim$ 10MHz[15], the high current density and Joule heating generate adequate ionisation to sustain the discharge, and for this reason these discharges are termed 'α discharges'.

The 'classical' derivation of the voltage division (on the electrodes) in an assymetric RF discharge is by Koenig and Maissel[37]. They considered the relationship between the unequal electrode areas A_1 and A_2, the sheath voltages and thicknesses V_1, V_2, d_1 and d_2 respectively. They made a number of dubious simplifying assumptions in their derivation but their results give a reasonable quantative description for the voltage distribution.

The following emperical equation was derived

$$V_1 / V_2 = (A_2 / A_1)^4 \qquad (1.13)$$

The index of four in Equation (1.13) is only an approximation and in practice varies from between one and five, depending on the discharge geometry. From Equation (1.13), one can see that the larger voltage appears on the smaller of the two electrodes (this is an important result for plasma processing applications).

A large sheath voltage can appear at the grounded electrode, and the wall of the chamber is usually connected to this ground. This effectively makes the wall and grounded electrode one large electrode and the wafer for processing can thus be placed on the driven electrode. The opposite to the above mentioned set - up is sometimes used in plasma deposition systems.

Brown[16], derives an expression of the form

$$\langle \bar{K} \rangle = \frac{m_i e^2 E_0^2}{2 m_e (\langle \nu \rangle^2 + \omega^2)} \qquad (1.14)$$

for the average kinetic energy of an electron undergoing collisions. This is analogous to Equation (1.6) for the DC case. The parameter $\langle \nu \rangle$ is the average collision frequency that appears in Equation (1.9) and is given by

$$\langle \nu \rangle = n_0 \langle \sigma \, v_e \rangle \qquad (1.15)$$

where n_0 is the gas density. Equation (1.14) is very similar to that derived by Chapman[5] for a collisionless electron using $(m_e v_e^2) / 2$ = energy gained from the field

$$\langle \bar{K} \rangle = \int_0^{2\pi} \frac{e^2 E_0^2 \sin^2 \omega t}{2 \omega^2 m_e} \, dt$$

$$= (\pi e^2 E_0^2) / 2 \omega^2 m_e \qquad (1.16)$$

Practical bulk electron energies are of the order of an electron volt ($\cong 10^4$ K).

Boeuf[11] states that it is not realistic to assume that the ionisation rate in the glow is a function of the local mean electron energy and he considers it more appropriate to study the contributions of 'beam' and 'bulk' electrons separately in sustaining the discharge. He does agree however with the fact that secondary emission of electrons is not essential to self - sustain a discharge. The above mentioned groups of electrons are described in the following sections.

1.6 Beam electrons

If a blocking capacitor is used on the driven electrode, the actual driving potential (the potential after this capacitor) is seen to be greatly shifted towards the negative. This is a direct consequence of the fact that the ionic mass is much greater than that of the electron. So in order to equalise the species currents to the electrodes - the ionic contribution being much smaller due to its inertia and smaller mobility, a DC offset is developed (which in some ways is equivalent to using a larger surface area for ion collection). This ensures almost continuous ion bombardment of the electrode; a fact that can be used for efficient processing methods.

It is well known that when an energetic particle strikes a metal surface, electrons and other particles will be released. This electron emission is characterised by

$$n_i^{inc} = \gamma \, n_e^{emit} \qquad (1.17)$$

where n_e^{emi} gives the number of electrons emitted and n_i^{inc} the number of incident ions; the parameter γ is called the 'secondary emission coefficient'. γ is a representation of the number of electrons emitted for each incident ion, so if γ is unity then each incident ion causes the ejection of one electron. Usually, γ is less than one, and hence it takes a number of ions to release a single electron. It will obviously depend on the metal surface condition, as well as its density, temperature and binding energy, and also on the energy of the incident ion. These emitted electrons are accelerated by the sheath up to energies of e V_{RF} towards the temporary or momentary anode, but encounter the 'positive column' - like glow and give their energy up causing ionisation, thus degrading themselves to the low energy, cold or bulk electron group described below.

1.7 Bulk electrons

When the fast electrons from the cathode impinge on the plasma more positive ion / electron pairs are formed due to ionisation. There is obviously a lower limit for the energy required by a group of electrons to be considered part of a beam, and anything below this threshold is considered to be of the bulk kind. These bulk electrons can gain energy from the field and cause their own ionisation. Sheath oscillations are a very important and interesting property of RF discharges, and can act as a source of energy to the electrons.

When an electrode appears as a momentary anode, the electrons flow towards it and the electron density near the anode becomes increasingly large (equal to the ion density in the sheath). The electrode then switches polarity and becomes a temporary cathode, thus repelling the low energy electrons, while some of the hotter electrons may have enough energy to penetrate the sheath.

The low energy electrons are thus pushed back into the plasma; if the sheath expands rapidly enough, the electrons can gain energy from the sheath field. This energy is given by

$$m_e \mu^2 E^2 / 2 \qquad (1.18)$$

from $v_d = \mu E$ and $E = v_s / \mu$. Thus it is seen that the electron 'surfs' along with the **E** field of the expanding sheath. 'Wave riding[36]' becomes a very important mechanism of energy transfer as the operating frequency increases or for large sheath velocities.

Gogolides[21] states after a theoretical and experimental comparison for Argon at 13.56MHz that 'the primary ionisation occurs at the bulk - sheath interface, and is a result of electrons which diffuse into the sheath and then are energetically pushed into the discharge by the sheath field during the cathodic phase of the RF cycle'. The so called 'electron - sheath collision regime'[11] can also occur; the electron now has a greater chance of colliding with the sheath than with other particles. This is the opposite to the case described above, where many electron - particle collisions were possible during the sheath expansion period

If it is assumed that $E \propto V_{RF}$, $d_{max} \propto V^{-1}_{RF}$ and using the fact[13] that

$$\bar{v}_s^2 = \frac{\varepsilon_0 \omega^2 V_{RF}}{2 e n_e} \qquad (1.19)$$

we get the following relationship between the applied RF voltage and the sheath expansion time

$$\tau_s \propto V_{RF}^{-3/2} \qquad (1.20)$$

The sheath could now be considered as a massive particle[5], and the electron would increase its velocity to $v_e + 2 v_s$ i.e. the electrons are reflected by the sheaths. This of course leads to an increase in the electrons kinetic energy which can be deposited in the bulk of the discharge thus increasing further the ionisation in the plasma. The 'electron - sheath collision regime' would obviously hold only for low pressures and most practical situations would be somewhere between the two.

It should be noted that if one of the discharge parameters like pressure, operating frequency ω or the driving potential is changed and the others kept constant, a dramatic transition between the regimes can occur accompanied by a large increase in the plasma density. Boeuf gives the example, backed up by the experimental results of Godyak and Kanneh, of changing the driving potential and observing a dramatic increase in plasma density around a certain threshold value of potential. He also notes that the transition between the wave riding and beam regimes is denoted by a large increase in current density and a sharp decrease in sheath width[45].

There is also a difference of two orders of magnitude in the plasma density between the beam and wave riding scenarios (for driving potentials of 300V and 100V respectively). The separate contributions to the total power deposition in the discharge due to the ions, wave riding electrons and the beam electrons as the driving voltage is varied is also calculated by Boeuf and Belenguer. It shows that at low power densities (low driving potentials), most of the power is dissipated by the wave riding electrons, and as the power density increases, the beam electron contribution increases accordingly; this is accompanied by an increase in the ionic contribution, and a decrease in that of the wave riding electrons.

van Roosemalen, van den Hoek and Kalter have studied the power deposition in a high power, planar, 13.56 MHz oxygen discharge[13] and conclude that positive ion acceleration in the ion sheath and electron collisions with neutral gas particles in the bulk of the plasma glow account for only approximately 25 % of the deposited power. They consider three regions - the sheaths, the glow or plasma itself, and the sheath - glow boundary.

The main contribution comes from ion wall bombardment in the sheaths. In studying the glow region they have neglected secondary emission electrons and concentrated on drift electrons. They do take the wave riding electrons into account, and this as expected makes only a small contribution (4 %). They suggest some unobserved sheath phenomemon or perhaps plasma waves to account for the missing 75 % of the power.

Wiesemann gives the following approximation for the power deposited by electrons in the plasma as

$$P \propto \bar{n}_e \; n_0 \; \text{vol} \; \langle \bar{K} \rangle \qquad (1.21)$$

where $\bar{n}_e$ is the average electron density obtained by integrating Equation (1.11) over the volume of the plasma, vol is the volume in 3 - D space taken up by the glow and $\langle \bar{K} \rangle$ is given by Equation (1.14).

Unfortunately, compared to DC plasmas, there are great difficulties in obtaining a Langmuir probe current - voltage characteristic in an RF plasma. The RF tends to distort the characteristic by 'shoving' it to the right, thus making the temperature and plasma potential seem higher than they actually are, and the density smaller. In an RF discharge, the plasma potential fluctuates with time, often with an amplitude much greater than the electron energy (eV). Thus if the probe is maintained at a fixed DC bias, the fluctuating voltage across the probe - plasma sheath results in the collection of a time varying current. Since the temporal variation of the plasma potential is not usually known, the instantaneous probe current cannot be used to infer plasma parameters.

If the time varying potential on the probe mentioned above can be eliminated, a DC - like characteristic is obtained, thus enabling analysis to be carried out accurately. The tuned[44] and driven probe (see Schott or Chen) set - ups go some way to alleviate the problem and the literature is full of examples using these methods[3,15,25]. On the other hand if the RF plasma is periodically switched on and off a DC plasma exists after switch off, and so characteristics can be taken at any particular time relative to the switch off instant.

The plasma parameters obtained can be 'extrapolated back into the RF' to yield their values during RF operation. Figure (1.3) shows an RF characteristic and one taken 30μs after switch off; the resemblance of the latter to a DC characteristic is obvious and one can see the distorted nature of the RF characteristic. These 'pulsed RF' discharges are discussed in the following section.

1.7 Pulsed RF Discharges

Pulsed RF discharges have been studied by Webb et al[41] for processing purposes and they find that the power level, and thus the concentration of active species increases, while maintaining lower substrate temperatures (hence reducing thermal damage to the wafer). Precisely the same experimental set up is used as for the RF case, the only difference being that periodic bursts of RF are now applied to the electrodes. The driving potential is observed on a high speed oscilloscope and adjusted until the minimum RF voltage remains in the switch - off region; this is usually of the order 1 - 2 volts, and is too low to cause any ionisation in the post - discharge. The mark - space ratio of the RF modulating signal are variable.

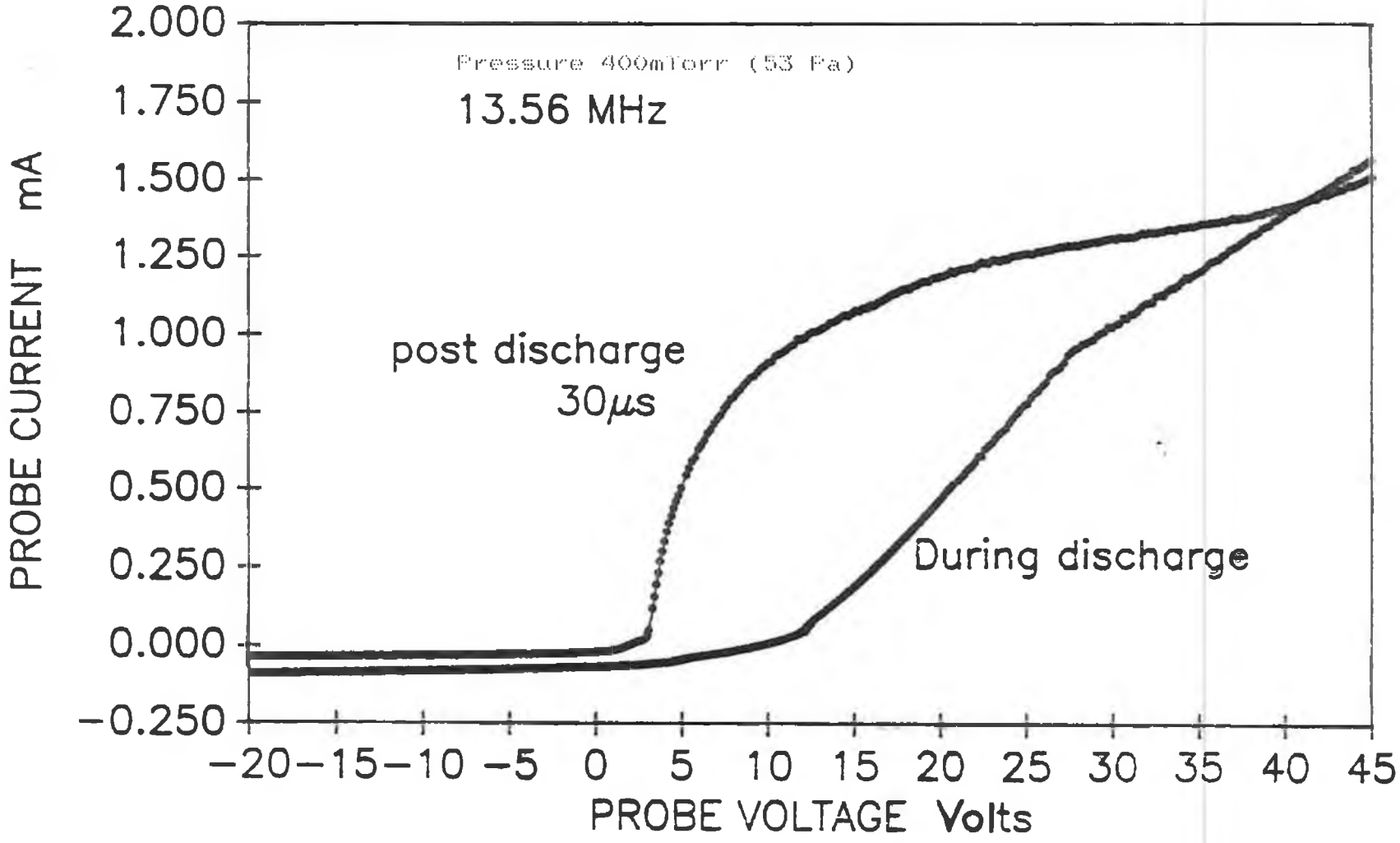

Figure (1.3)

A comparison of pulsed RF and continuous RF Langmuir probe characteristics in a Helium plasma

Photograph (1.2) shows this set up on the scope and one can see that the RF decays in approximately 1 μs (the probes used were x 10 and so voltages given on the photo must be multiplied by 10). The plasma is allowed to decay naturally and current - voltage measurements are taken at a time Δt after switch - off.

After the plasma is initiated, the transient oscillations reach steady state equilibrium, and when the plasma is switched off, the density and temperature decay exponentially. Helium and Argon afterglows are studied in this work and the experimental details and results will be dealt with at a later stage.

Blue and Stanko[17] investigated a pulsed Helium discharge and found that at late times in the afterglow, (when the electron temperature had reached the steady state value of 300K i.e. the electrons had thermalised with the ions, which were at ambient temperature) the main plasma loss mechanism is through ambipolar diffusion. The temporal diffusion is of the form

$$n(t) = n_0 \exp[-(D_a / \Lambda^2)\, t] \qquad (1.22)$$

where D_a is the ambipolar diffusion coefficient, and Λ^2 the characteristic diffusion length given by

$$\Lambda^{-2} = (2.405/ R)^2 + (\pi/ L)^2 \qquad (1.23)$$

Here they assume a Bessel function solution for the electron density as in Equation (1.11), R is the radius of the cylinder and L its length. Densities and temperature decays have been modelled for this work using the diffusion equation in one dimension, and the comparisons with experiment are reported in Chapter **IV**.

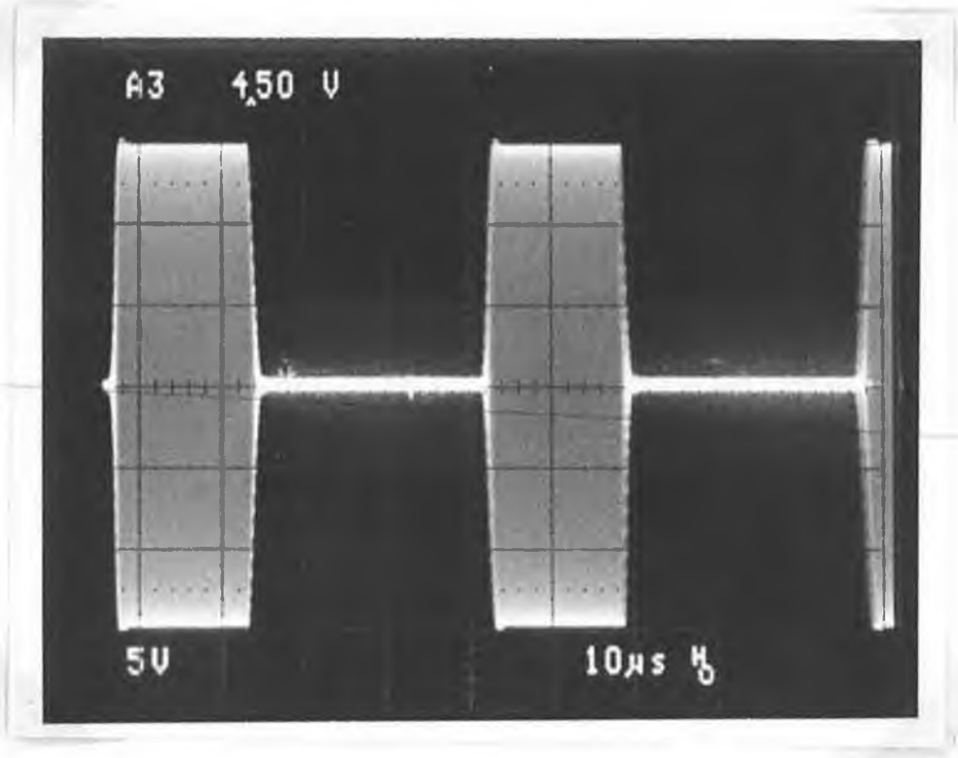

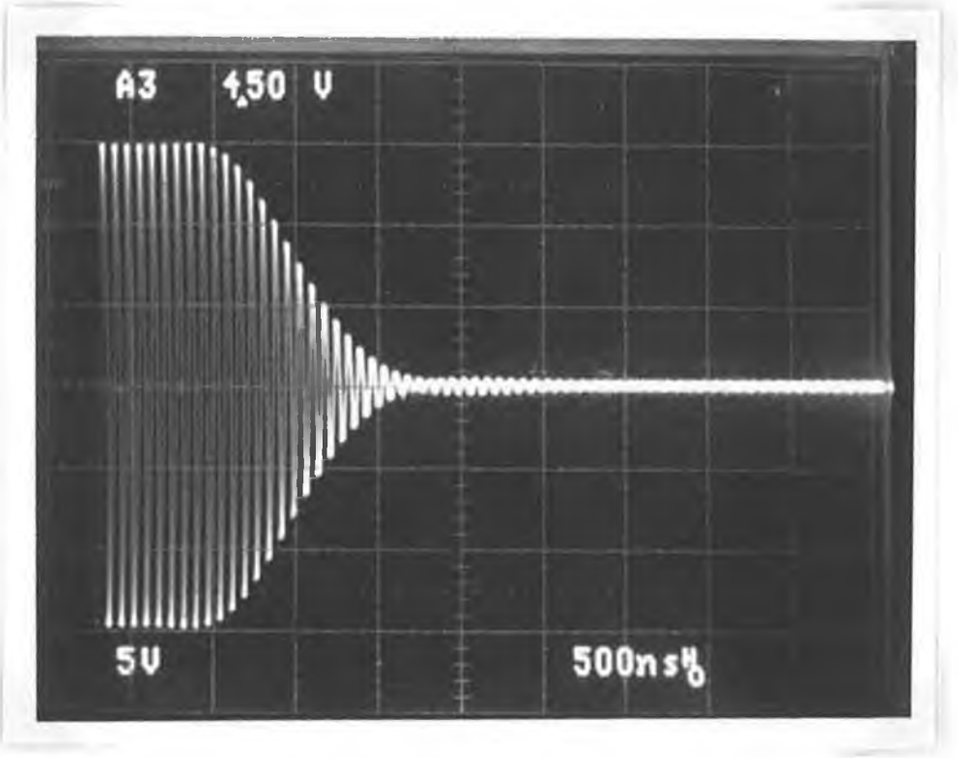

Photograph (1.2)
The driving potential (top) as measured on the top electrode, and the corresponding decay of the RF in the plasma

Smith, Goodall and Copsey[18] give an expression for the electron density in terms of the atomic (He^+) and molecular (He_2^+) ion densities:-

$$n_e = n_{10}\left[1 - \frac{\nu}{\lambda_1 - \lambda_2}\right]e^{-\lambda_1 t} + \left[n_{20} + \frac{\nu n_{10}}{\lambda_1 - \lambda_2}\right]e^{-\lambda_2 t} \quad (1.24)$$

Here, n_{10} and n_{20} are the initial He^+ and He_2^+ ion densities, ν is the conversion rate of the He^+ to He_2^+ ions, and λ_1 and λ_2 are the respective ion density decay constants given by

$$\lambda_1 = D_{a1} / \Lambda_1^2 + \nu$$

$$\lambda_2 = D_{a2} / \Lambda_2^2 \quad (1.25)$$

D_{a1} and D_{a2} are the ambipolar diffusion constants similar to that used in Equation (1.22), the diffusion length, Λ^{-2}, is given by Equation (1.23).

The above authors found that the electron temperatures were all greater than the wall temperature, and that they decayed slowly with time in the afterglow relative to the decay of the electron density. These results are in accord with those which will be discussed in Chapter **IV**. At later times in the afterglow the electron energy distribution is seen to relax, and the 'fast' or high energy electrons vanish leaving the 'cold' or low energy group which have a corresponding Maxwellian distribution. The temperatures decay to the ambient or room temperature in the temporal limit. A novel method which involves pulsing the probe is used in this work with impressive results and it will be described in Chapter **IV**. Clements and Skarsgard[20] use a double probe (see the chapter on Langmuir probes) to obtain a monotonically decreasing temperature with time and a final (latest time) temperature well above room temperature.

CHAPTER II

LANGMUIR PROBES

2.1 Introduction

An electrostatic probe is essentially a small electrode, usually made of metal, inserted into the plasma. The probe can be biased both positively and negatively with respect to the plasma depending on the charge of the species to be collected. The probes used for this work are single probes but a brief description of both double and emitting probes is also given here.

Originally these probes were thought to have very little perturbative effect on the plasma (at least in the absence of magnetic fields). This does not hold for the case of very weak plasmas such as afterglows (described below), but can be overcome to an extent by reducing the probe size. Probes have the advantage of being able to take localised measurements unlike spectroscopic or microwave techniques; unfortunately the theory of probe operation is not as simple as the actual device itself but much progress has been made in recent years to explain the different operating regimes.

2.2 Theory

The so called low pressure/ collisionless thin sheath model is used in the analysis of the data; the criteria needed for this theory to hold are[38]

$$\lambda_{coll} >> R_{pr} >> \lambda_D \qquad (2.1)$$

that is the Debye Length, given by Equation (1.3), is much less than the radius of the probe and the electron collision mean free path, e.m.f.p..

The e.m.f.p. is given as

$$\lambda_{coll} \cong \frac{.18\ \pi\ n_e \lambda_D^4}{\ln(12\ \pi\ n_0\ \lambda_D^3)} \qquad (2.2)$$

where the symbols have their usual meanings; this is of the order of millimeters, and so one can deduce that collisional losses in the afterglow will be negligible.

The theory originally devised by Irving Langmuir in the early part of this century now applies and the literature is full of reviews of this work e.g. Chen[3] and Schott.[25] A schematic of a typical probe current - voltage characteristic can be seen in Figure (2.1). Here total species current is plotted against the voltage applied to the probe, and three distinct regions can be seen. At V_p the probe is at the same potential as the plasma and hence no electric field exists; the charge carriers migrate to the probe as a result of their thermal energies.

This current is known as the electron saturation current and can be expressed as:

$$I_e(V_{app}) = - (n_e\ e < v_e > A) / 4 \text{ for } V_{app} \geq V_p \qquad (2.3)$$

where A is the probe area (≅ sheath area), $< v_e >$ is the average electron velocity, n_e and e are the electron density and charge respectively. Owing to the fact that electrons are much lighter than ions and hence have a higher mobility they will be the main contributor to the probe current. If the probe is now biased positively with respect to the plasma, the electrons are accelerated towards the probe and ions are repelled, thus making the ionic current negligible.

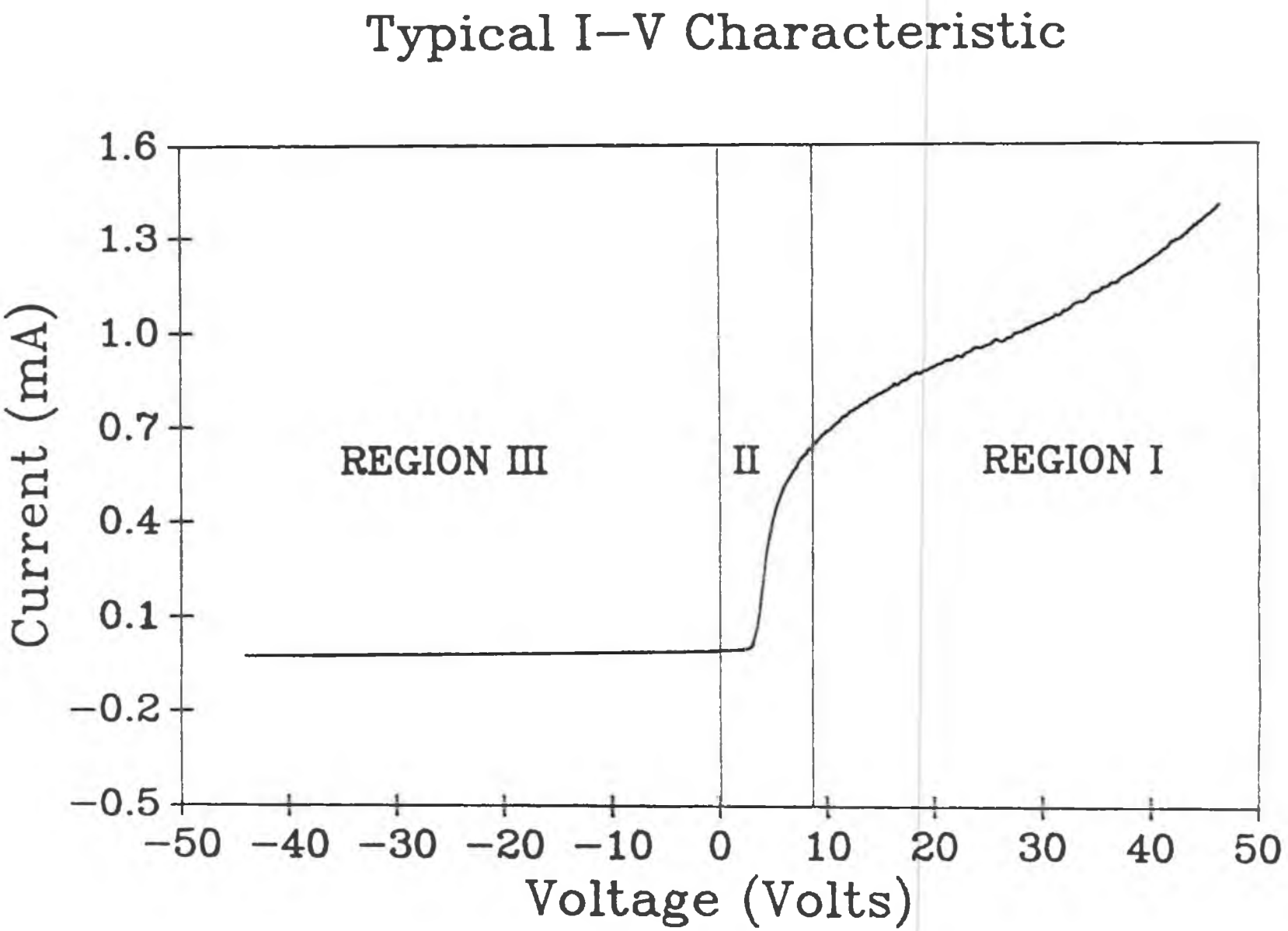
Typical I–V Characteristic
1.6
1.3
1.0
0.7
0.4
0.1
−0.2
−0.5
Current (mA)
REGION III
II
REGION I
−50 −40 −30 −20 −10 0 10 20 30 40 50
Voltage (Volts)

Figure (2.1)

Close to the probe there is an excess of negative charge and this negative charge density will increase until it equals the positive charge on the probe. This layer is called the sheath outside which the electric field is very small as is shown in Figure (1.1). The behaviour of the potential is governed by Equations (1.5) and (1.5a) where the field is seen to be shielded outside the distance λ_D. The only electronic current now is that which enters as a result of random thermal motions.

Region 2 occurs when the probe is biased negatively with respect to the plasma and now the electrons are repelled according to Equation (1.4), and ions collected. The electron current is now reduced by the Boltzmann factor according to

$$I_e(V_{app}) = -\frac{1}{4} n_e e \langle v_e \rangle A \exp (e V / k T_e) \qquad (2.4)$$

This region is of great importance as many of the plasma properties can be deduced here as will be seen later. Ideally the electron distribution can be characterised by a Maxwellian distribution, and the shape of the curve after the ionic contribution is subtracted is an exponential . Unfortunately, this is not the case in experimental situations, and two groups are to be seen (see the section on analysis). These groups correspond to the bulk (lower energy and cold), and the beam (high energy and hot) groups discussed in the previous chapter. At V_f the probe repels the vast majority of electrons except that flux of fast electrons equal to that of the ions, hence the probe draws no net current. Region 3 denotes ion saturation and the formation of an ion sheath; note that the magnitudes of the currents greatly differ between regions 1 and 3.

2.3 Other Probe Types

The Double Probe

Figures (2.2a and (2.2b)) show typical experimental probe set - ups. The double probe arrangement is used when no reference electrode is available such as inductively or capacitively coupled plasmas with external electrodes. Looking at the double probe scenario where the probes are inserted in the plasma and one arm is biased with respect to the other but insulated from ground; the system is 'floating' relative to the plasma and can follow changes in the plasma potential (the reason it was designed). By applying a positive voltage to P_1 with respect to P_2 that is $V_1 - V_2 > 0$, electrons are collected. Remembering that $\mu_e >> \mu_i$, the probes must be biased negatively with respect to the plasma to stop a net electron current from flowing through the 'circuit'. However, if $A_1 >> A_2$, the ion current to P_2 will balance the saturation electron current to P_1. The characteristic will be symmetric about the origin if $A_1 = A_2$.

Figure (2.3) gives a double probe characteristic for unequal probe areas. If $V_1 = V_2$, both probes are at the floating potential and hence I= 0; the current through the system is limited by the ion saturation current, since any electronic current must be balanced by an equal ionic current, hence only the electrons with high enough energy to reach the probe can be sampled.

The emissive probe

The fact that probes not only collect ions and electrons - characterised by their 'sticking coefficients', but also emit these is used in the emissive probe set up. The emission can be due to electron ejection by impinging particles or to direct heating.

Figure (2.2a)

Experimental set – up using a single probe

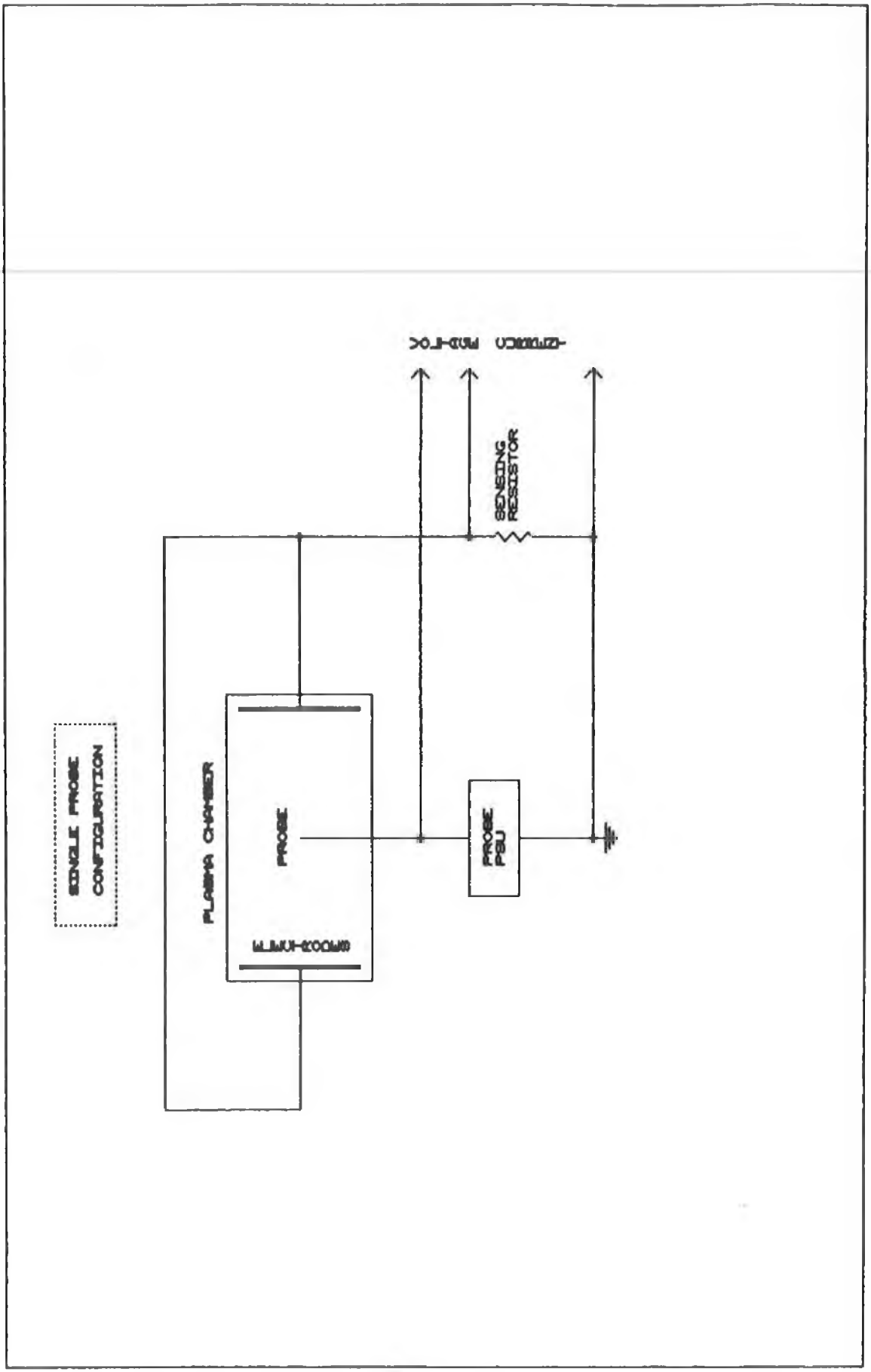

Figure (2.2b)

Experimental set – up using a double probe

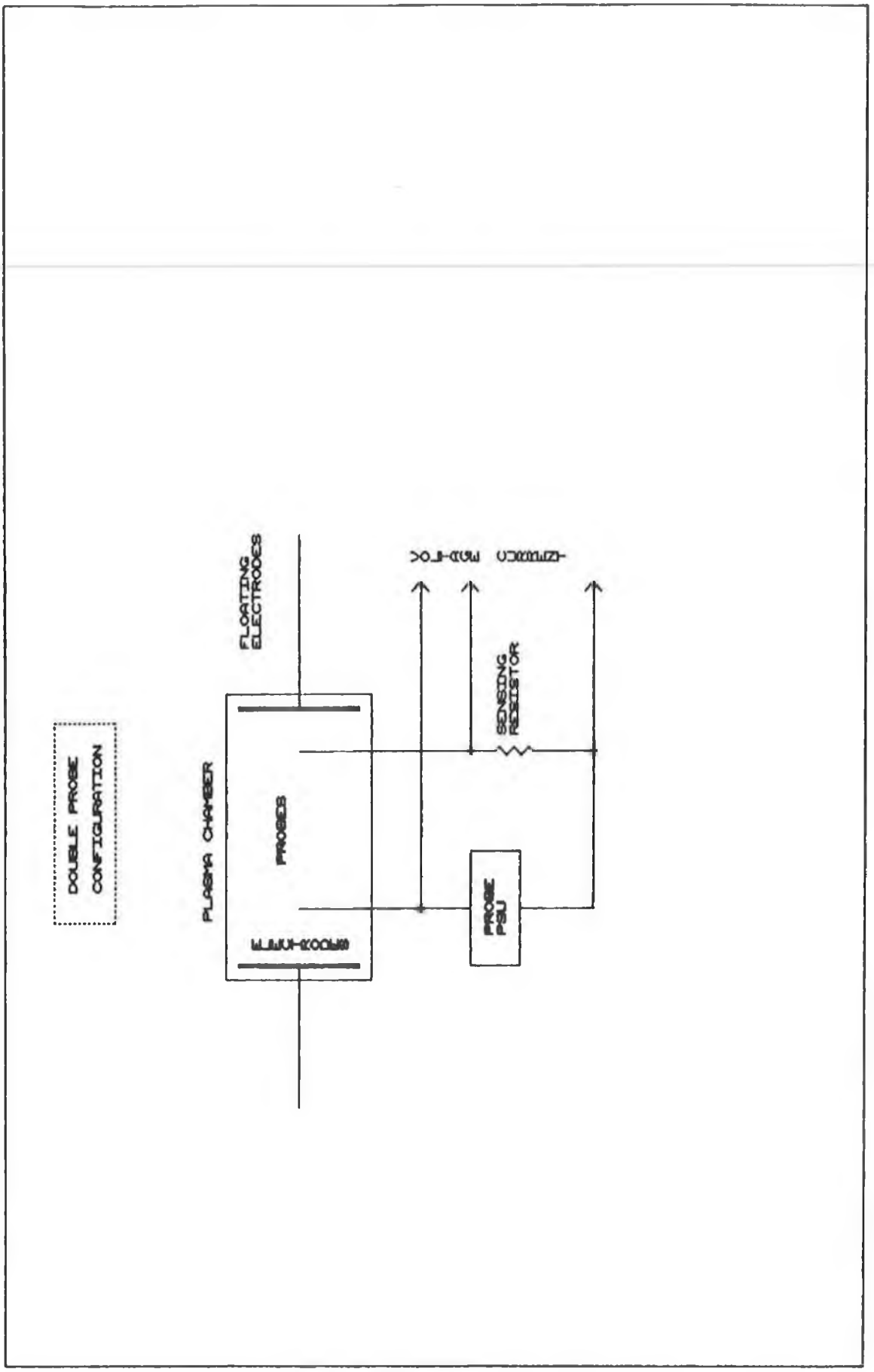

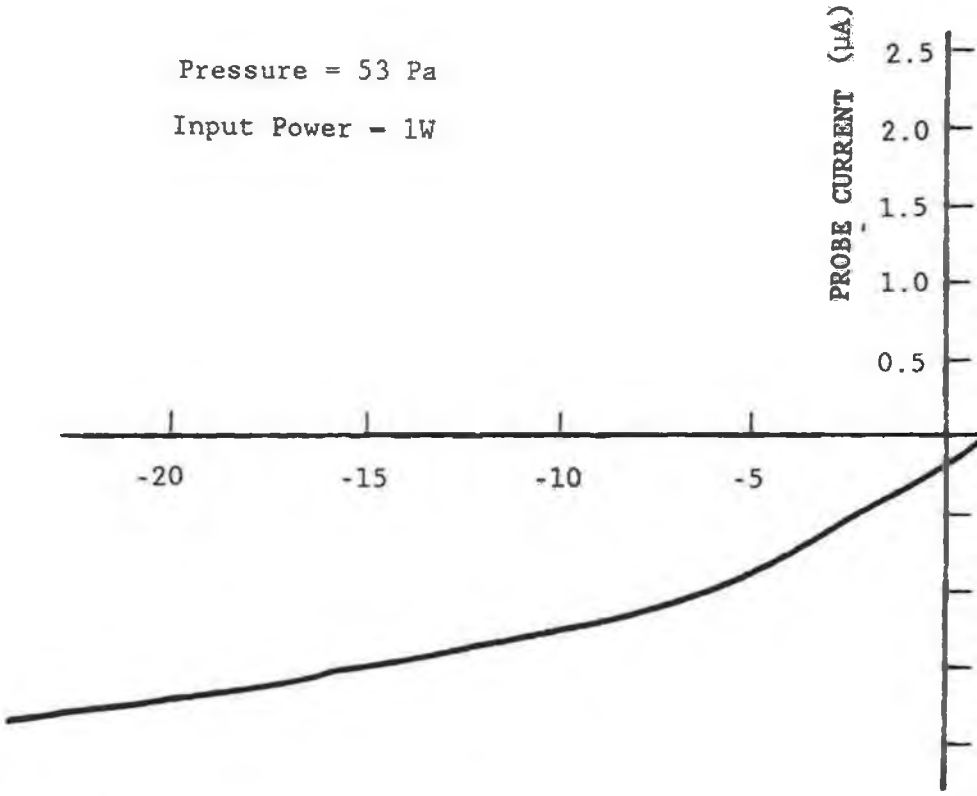

Figure (2.3)

A double probe characteristic taken in an RF

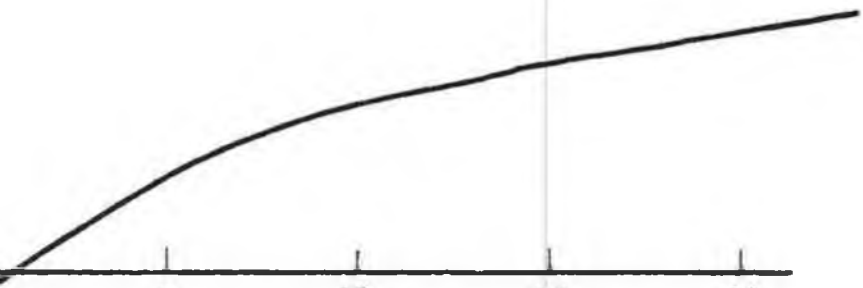

-0.5

PROBE VOLTAGE (Volts)

-1.0

-1.5

-2.0

plasma

These probes are a very important diagnostic tool in that the emission can be controlled by a simple current control to the filament and the difference between the 'cold' and 'hot' probe can be used to gain information about the floating and plasma potentials. The paper by Hopkins, Hughes, Scanlan and Molloy[27] (Appendix A) deals with the use of an electronic technique using a voltage follower to characterise low frequency RF plasmas.

2.4 Perturbative effect of the probe on the plasma

If a positive square wave is applied to a probe, an overshoot in I_e is apparent. This has been explained by Brenner[39] as follows: if the probe voltage is pulsed rapidly above the plasma potential, an excess of positive ions remains near the positive probe for a long time compared to that required for the electronic component of the current to reach a steady state. So one expects to see an overshoot in the electron current at the start of the pulse due to the decrease in the negative space charge about the probe. It is important to note that the overshoot only occurs for probe potentials above the plasma potential, and that the oscillations die out in approximately $1\mu s$.[3] In high density discharges, no overshoot is seen, and this is because there are numerous electron collisions in the plasma and the current cannot rise fast enough. It is useful to have a quantitive estimate of how much current can be drawn from the plasma without depleting it significantly. Smith et al[18] suggest the following equation in order that the probe current be less than x % of the total electron current in the plasma.

It provides a limiting condition on the current that can be drawn

$$i_e < \frac{x}{100} e \, Vol \frac{dn_e}{dt} \qquad (2.5)$$

where Vol is the volume occupied by the afterglow plasma in cm^3. In the present situation $i_e \cong 10mA$. Waymouth[28] found that if the high energy (beam) electrons were removed from the plasma (by using a probe) at a comparible rate to the generation rate, serious perturbation of the electron energy distribution occurred.

He quotes a depletion time constant, τ_d, such that half of the electron current drawn by the probe at potential - $m v_0^2 / 2 e$ (from electron kinetic energy = electric potential, $e V_{pr}$) is characterised by a depletion time constant shorter than τ_d. So half the electron current drawn by the probe is characterised by a time constant shorter than

$$\tau_d = (2.9 \, Vol / A_p v) \, m v^2 / k T_e$$

$$= 5.8 \, Vol \, e V_{pr} / A_p v \, k T_e \qquad (2.6)$$

$$= 3 \, Vol \, (3 m_e / k T_e)^{1/2} / A_p$$

with A_p the probe area and v the electron velocity. In the present case $\tau_d \cong 100ms$ (for a .5eV electron distribution).

It can be shown that the criterion for which no disturbance occurs

$$n_e >> 1.5 \times 10^4 T_e^2 A_p / Vol \qquad (2.7)$$

where T_e is in Kelvin.

For the present situation, assuming .5eV as the electron temperature, n_e must be much greater than 1×10^{14} m^{-3}. Even if the plasma does not satisfy the above condition, it is still possible to take 'non - perturbative' measurements by pulsing the probe with pulses of length τ_p if

$$1/\omega_p << \tau_p << \tau_d \qquad (2.8)$$

where ω_p is the electron plasma frequency (Equation (1.2)).

Blue and Stanko[17] pulsed the probe with 20μs pulses in a He afterglow and discovered the existence of two energy groups of electrons at early times, and also verified the suitability of pulsing the probe. This work and its benefits are echoed later on in this thesis.

Referring again to the above authors, the pulse width, τ_p was varied from wide (>5ms), to narrow (20μs), and when no changes occurred in plasma characteristics with successive changes in pulse width, they had reached an optimum value, above which perturbation would occur. They also noted that at large pulse widths i.e. plasma depletion, the electron temperatures were higher than expected and electron densities lower; these results are fully in accord with what one would expect if depletion was occurring, and they are supported in this work as will be seen in Chapter IV.

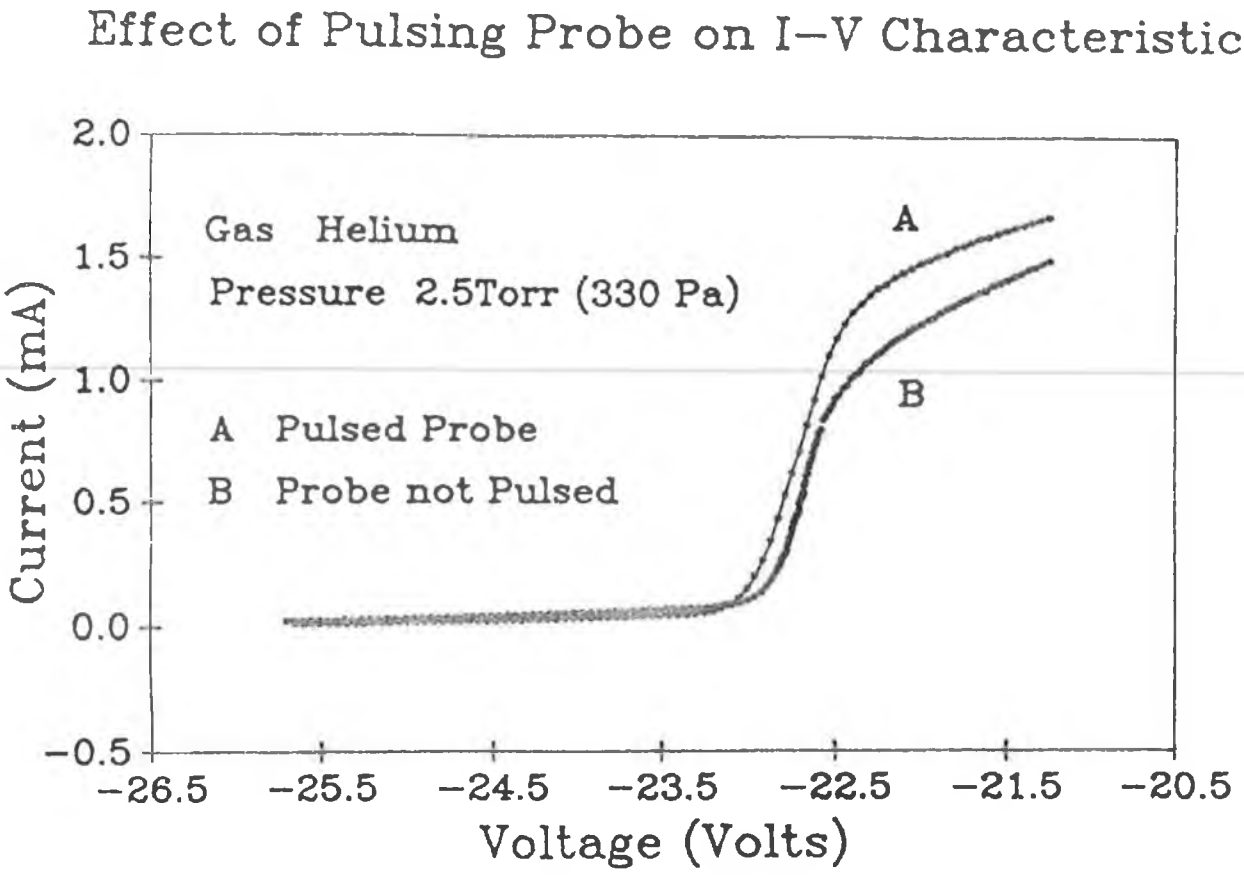

Figure (2.4)

Figure (2.4) - Fig's (2.4), (2.5) and (2.7) are DC characteristics and are used because of the clarity with which they portray the points being stressed, shows a current - voltage characteristic both when the probe is pulsed, and when it is not; the increase in density for the former is obvious, though the temperature change deduced from the difference in slopes of the exponential region is not so apparent.

2.5 Analysis

Some of the simplifying assumptions used in elementary probe theory for low pressure discharges are stated below:

1) The plasma is infinite, homogenous (the same at every point) and quasineutral in the absence of a probe i.e. $n_e \cong n_i$,

2) The electrons and ions have Maxwellian velocity distributions with temperatures T_e and T_i respectively, with $T_e >> T_i$; the Maxwellian distribution is of the form

$$f(u)du = 4\, u^2\, \pi^{-1/2}\, e^{-u^2} du \; ; \; u^2 = \frac{m\, v^2}{2kT_e} \qquad (2.9)$$

3) The mean free paths of ions and electrons given by Equation (2.2) must be large compared to the other relevant dimensions and lengths of the system, such as the Debye Length, λ_D, and the probe radius, R_p,

4) Each charged particle hitting the probe is absorbed and does not react with the probe material,

5) The space charge sheath is well defined and outside it, the space potential is assumed as constant,

6) The sheath thickness is small compared to the lateral dimensions of the probe.

Unfortunately, these assumptions are not very representitive of real plasma systems but do yield quite useful information when used in theories to explain plasma behaviour in the presence of a probe. There are deviations from quasineutrality, as well as the fact that the probe disturbs the plasma itself (see Section (2.4)), and the plasma-probe surface interaction can influence the immediate environment of the probe.

Schott states that the upper limit[25] of the applicability of low pressure theory is approximately 1 Torr; as long as Equation (2.1) holds, the density is not affected by collisional processes, and the theory can be used. When either R_p or λ_D > the mean free path, as is the case for high pressure discharges, particle diffusion to the probe has to be taken into account in order to yield meaningful results. High density theory will not be considered here.

Real Time

Figure (2.5) shows a typical I(V) scan with the corresponding first derivative, I'(V). Using elementary probe theory[3,25], the maximum of I'(V) occurs at the plasma potential, and also the ratio of the current to the first derivative at the plasma potential is equal to the electron temperature i.e.

$$\frac{I\ (V_p)}{I'(V_p)} = kT_e e^{-1} \qquad (2.10)$$

So one can accurately assume (using the notation of Hopkins[24]) the following to be good approximations

$$V_p = V_{maxderiv}$$

$$e^{-1}kT_e = I_{maxderiv} / I'(V)_{max}$$

and $$I_{0e} = I_{sat}.$$

Here I_{0e} is the random thermal flux of electrons per unit length of the probe.

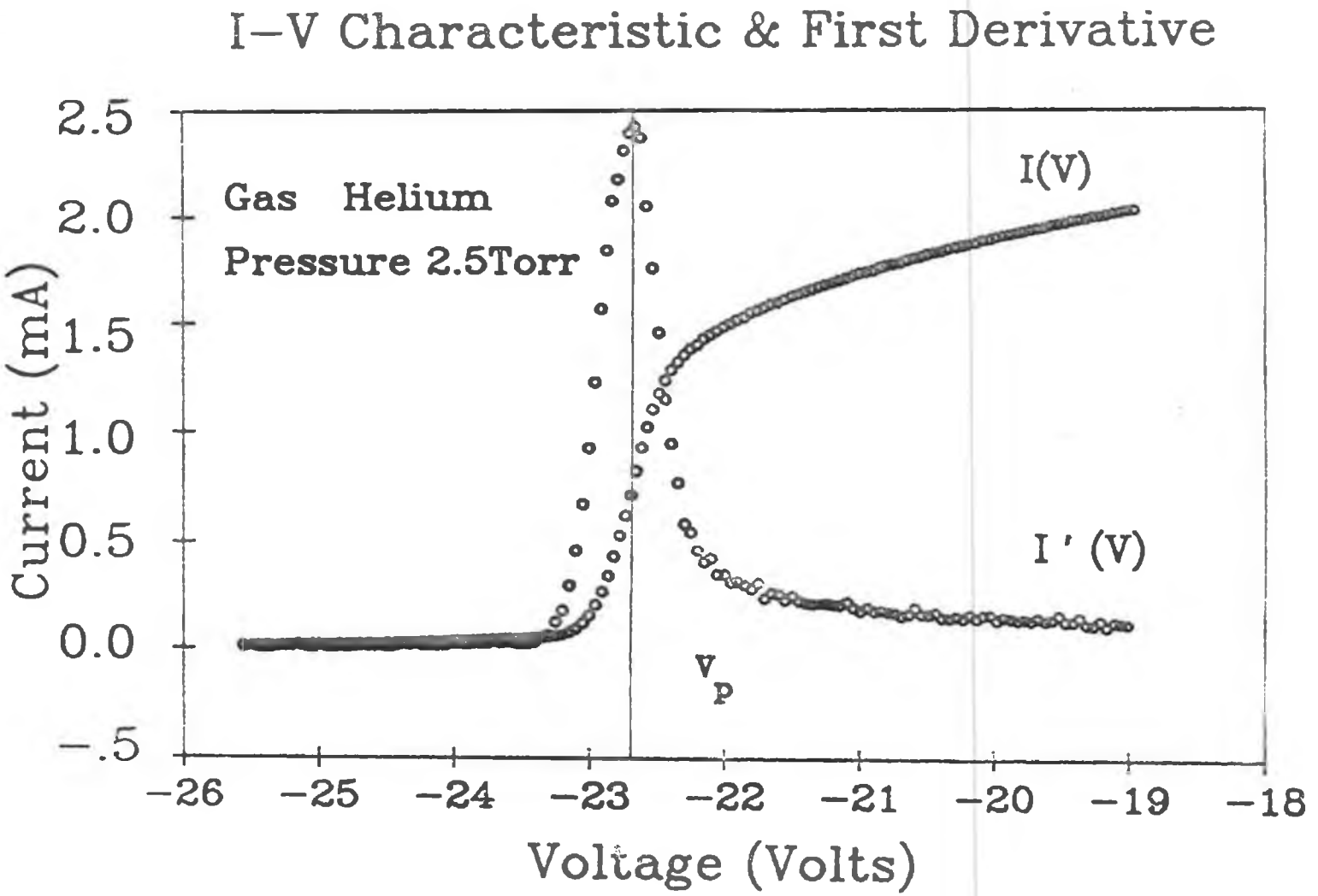
I–V Characteristic & First Derivative
Gas Helium
Pressure 2.5Torr
I(V)
I ' (V)
V_p
Current (mA)
2.5
2.0
1.5
1.0
0.5
0.0
−.5
−26
−25
−24
−23
−22
−21
−20
−19
−18
Voltage (Volts)

Figure (2.5)

Due to the fact that the maximum in I'(V) always occurs below the point where the electron saturation current is reached, V_p is corrected by the method of intersecting slopes. This gives

$$V_p = V_{max} + e^{-1}kT_e \ln(I_{sat} / I_{maxderiv}) \quad (2.11)$$

In effect, this extends the exponential region of the characteristic until it intersects with the electron current saturation. This intersection yields the new plasma potential. The smaller the voltage step size used in the scan, the more accurate the computed paramaters will be, and so a rough first or 'glance' scan is used to obtain the saturation current, and also the above estimates for the electron temperature etc. A more accurate scan can then be carried out, concentrating on the important region (exponential region) of the characteristic, thus yielding accurate values for the plasma parameters.

This more accurate second scan is then taken which only measures currents that are greater than twice the ionic current at a large negative probe bias - this has the effect of reducing noise. The upper limit of the scan is taken to be the voltage at which the derivative reaches one third of its maximum value i.e. $I'(V)_{max} / 3$, thus ensuring that the important exponential region is obtained, and that the probe does not go into saturation (depleting the plasma) or start to glow.

A single relay or sensing resistor is used throughout the second scan to avoid switch bounce, and to optimise the range of the A / D. Updates of the plasma parameters are constantly being printed on the screen, and the data can be saved to disk for analysis at a later date. This analysis (not real - time) is described in the next section.

The electron energy distribution function can also be obtained from the characteristic using the method of Laframboise (see Hopkins (PhD Thesis), Wiessemann[4] Anderson[26], Llewellyn - Jones[41] or Druyvesteyn). One useful result is quoted in Equation (2.12); this relates the second derivative to the EEDF. When studying volume and surface reactions in plasmas for processing purposes, one needs to know the various densities, potentials, cross sections and energies of the various constituent particles; all this information can be extracted from the EEDF. Provided the EEDF is isotropic, the second derivative of the probe characteristic is proportional to the EEDF.

The distribution function, $f(\varepsilon)$, at a given electron energy, ε is given by[31]

$$n_e f(\varepsilon) = \frac{2}{e} \frac{d^2 I}{d V_p^2} (2 m_e E/ e)^{1/2} \qquad (2.12)$$

$$\varepsilon = -e(V_{pr} - V_p) \qquad (2.13)$$

$$\int_0^\infty f(\varepsilon) d\varepsilon = 1 \qquad (2.14)$$

There is good agreement between the experimental and theoretical EEDF's with some deviation in the high energy tail. Once $f(\varepsilon)$ has been obtained (which is no mean feat) the mean electron energy, $\bar{\varepsilon}$, can be calculated from

$$\bar{\varepsilon} = \int_0^\infty \varepsilon f(\varepsilon) d\varepsilon \qquad (2.15)$$

Non Real Time Analysis

The C program, BF2, is used to analyse the data after it has been stored on disk. The gas type (Argon or Helium) is first input and then the name of the data file. The data is read, and the current and voltage maxima and minima are calculated; the electron saturation current is also found at this stage using the method described in the last section.

The data can now be plotted as

1 Current vs Voltage,

2 ln(Current) vs Voltage,

3 Saturation ion current vs Voltage,

where voltage corresponds to the probe voltage in volts. Each of these can also be plotted with or without the saturation ion current subtracted from the characteristic; this has the effect of shifting the characteristic upwards along the current axis, hence introducing more electron current (fast electron current as can be seen from Figure (2.6)).

The ion saturation current to be subtracted takes the form[25]

$$I_{+sat} \cong I_{esat}\left[\frac{2\,\pi\,m_e}{e\,m_i}\right]^{1/2} \qquad (2.16)$$

with e being the exponential, and the rest of the symbols having their usual meanings. The use of this quantity is a matter of some debate but is used here as a good approximation.

The analysis of the ion saturation current

If the square of the ion current is plotted vs the probe voltage, a straight line is obtained of the form

$$I_i^2 = \alpha V + \beta \qquad (2.17)$$

A least squares fit yields the slope, α, and the current intercept, β. The positive ion density and plasma potential can be obtained as follows:

The standard Orbit Motion Limit theory (OML) gives the positive ion current I_i as

$$I_i = e A_p n_i \left[\frac{-2 e (V - V_p)}{\pi^2 m_i} \right]^{1/2} \qquad (2.18)$$

where A_p is the probe area, V_p the plasma potential and m_i the mass of the ion. Squaring both sides and equating with Equation (2.18) gives

$$\alpha = - \frac{2 e^3 A_p^2 n_i^2 V}{m_i \pi^2} \qquad (3.19)$$

and

$$\beta = \frac{2 e^3 A_p^2 n_i^2 V_p}{m_i \pi^2} \qquad (3.19a)$$

hence $$n_i = \left[\frac{\alpha m_p \pi^2}{2 e^3 A_p^2} \right]^{1/2} \qquad (3.20)$$

and $$V_p = -\beta / \alpha \qquad (3.21)$$

Paranjpe claims that there is an acceptable error ($\cong$ 10 %) in the calculated ion density but has misgivings about the accuracy of the plasma potential deduced using this method. This author used the method of the semi - logarithmic plot described in the next section to analyse the characteristics. The same type of analysis used on the saturation ion current can also be used on the saturation electron current yielding n_e and V_p but there are problems associated with this method.

Analysis using the semi - logarithmic plot

For a Maxwellian EEDF, a plot of ln(Current) vs the probe voltage yields a straight line, with a slope equal to kT_e^{-1} $(eV)^{-1}$; the EEDF in low pressure discharges is unfortunately non - Maxwellian. Figure (2.7) shows such a semi - logarithmic plot for a DC discharge in which two distinct energy / temperature groups are evident. The 'fast' or 'hot' electrons reach the probe at lower applied voltages (i.e. less attractive) than the 'slow' or 'cold' group because of their higher energies. This high energy group corresponds to the 'beam' electrons discussed already, and are responsible for the ionisation in the discharge. The use of a 'temperature' to characterise this group is very dubious, and much more information would be obtained from an EEDF.

A temperature can also be assigned to the lower energy 'bulk' electrons; these control the electron transport properties of the discharge. The plasma potential can be obtained from the intersection of the electron saturation current and the extended exponential region. Schott states that 'uncertainties in ion current extrapolation may lead to inaccurate results with respect to the fast tail of the electron velocity distribution'.

Subtraction of Ion Saturation Current

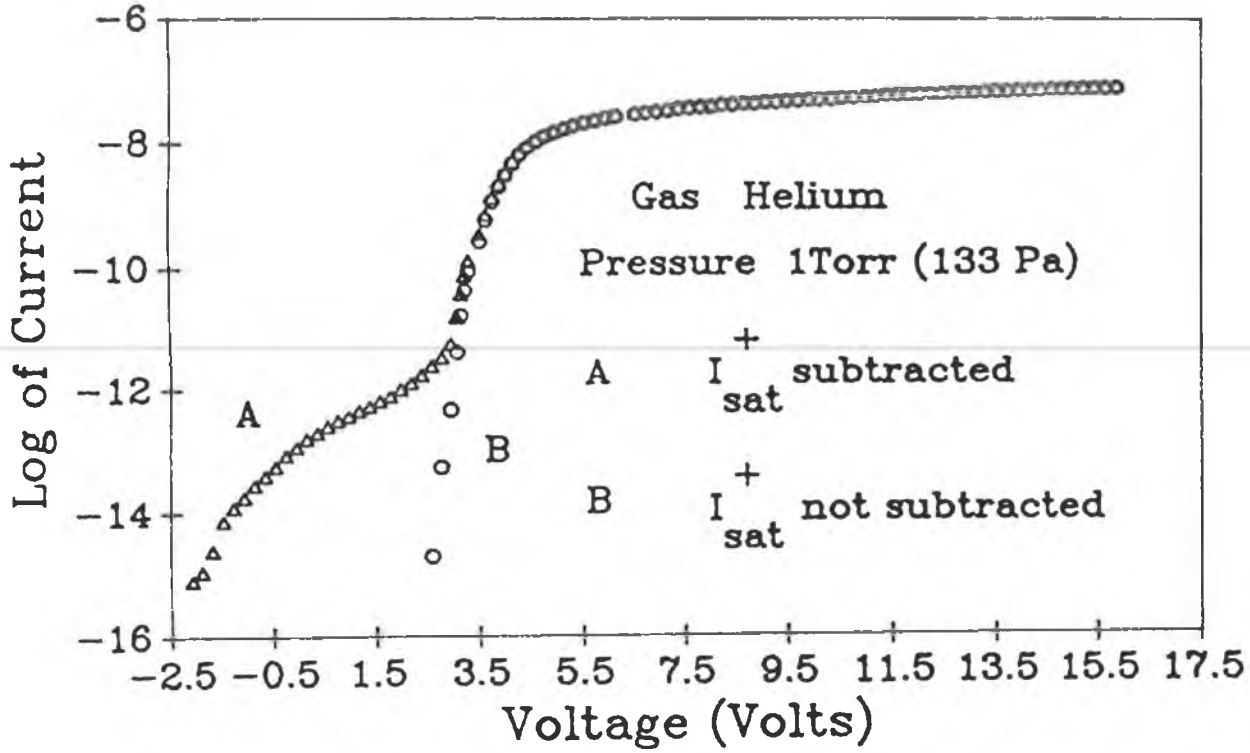

Figure (2.6)

Semi−Log Plot of an I−V characteristic

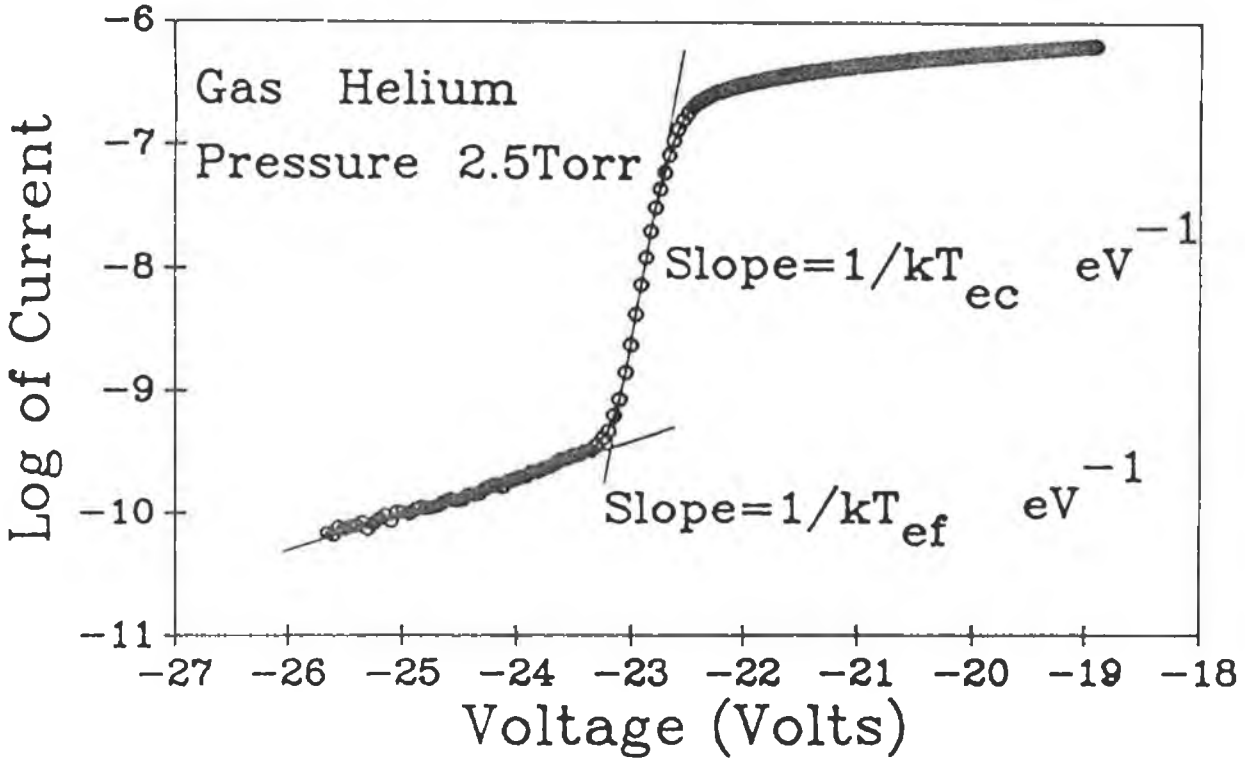

Figure (2.7)

So it can be seen that Langmuir probes can be used to obtain all the important plasma parameters accurately and cheaply. However, the assumptions used in the different theories must be understood as it is not just a case of sticking a biased wire into the plasma and obtaining meaningful results.

CHAPTER III

THE EXPERIMENTAL SET UP AND PROCEDURES

3.1 Introduction

The experiments are performed in a stainless - steel walled vacuum chamber (kindly donated by VG Quadrupoles Ltd) with two water cooled aluminium electrodes each 80 mm in diameter and 35 mm apart (see Photographs (3.1a) and (3.1b)). The bottom electrode is optionally grounded, whereas, the top one serves as the driven electrode. The chamber is pumped by a mechanical pump capable of obtaining a base pressure of 4 Pa; the flow of gases is controlled by MKS flow controllers, while the pressure is monitored by a 1.33×10^3 Pa Baratron pressure gauge, and regulated by an automatic pressure controller.

The pulse train modulated output of a HP 33141A function generator is fed via an RF power amp (ENI model 320L), and this is fed into either a matching network or a broadband transformer (see Figure (3.1) for the different arrangements used) to the top (driven) electrode. Unfortunately, no direct method of measuring the reflected and absorbed power is available, but the amplifier is capable of delivering approximately 20 Watts of power; the plasma is matched to minimise the reflected power. Two ports on the chamber are used, and on both occasions the probe tip was immersed in the centre of the glow (not true for DC since it was in the cathode glow).

The probe is regularly cleaned by applying a large positive bias with regard to the plasma, hence collecting electron saturation current, until red hot in a high density DC glow, and also by biasing it negatively when not in use to enable ion bombardment. The DC glow is produced using a KingsHill DC supply which produces a potential drop of 350V across the electrodes and 60mA. Measurements are performed in a wide range of conditions for both Ar and He gases. All measurements for this work are done using a single tungsten probe of radius .25mm.

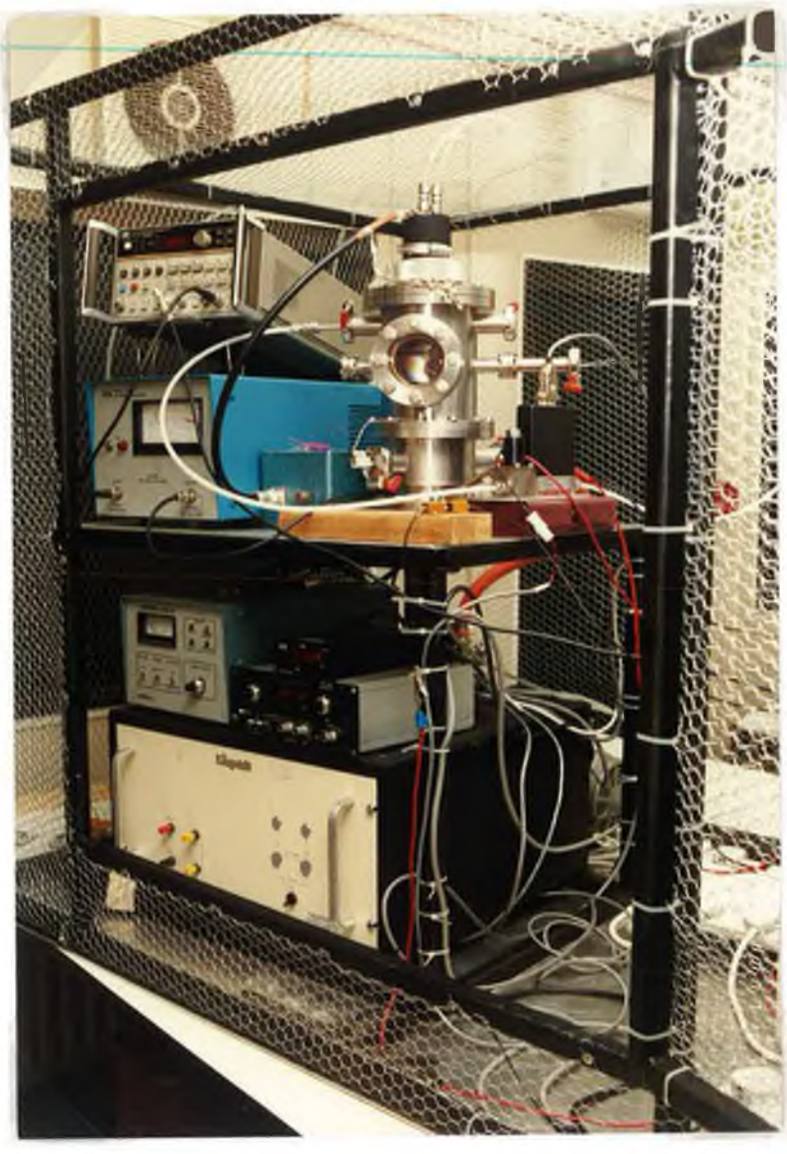

Photograph (3.1a)
The plasma chamber and associated equipment; note the Faraday cage

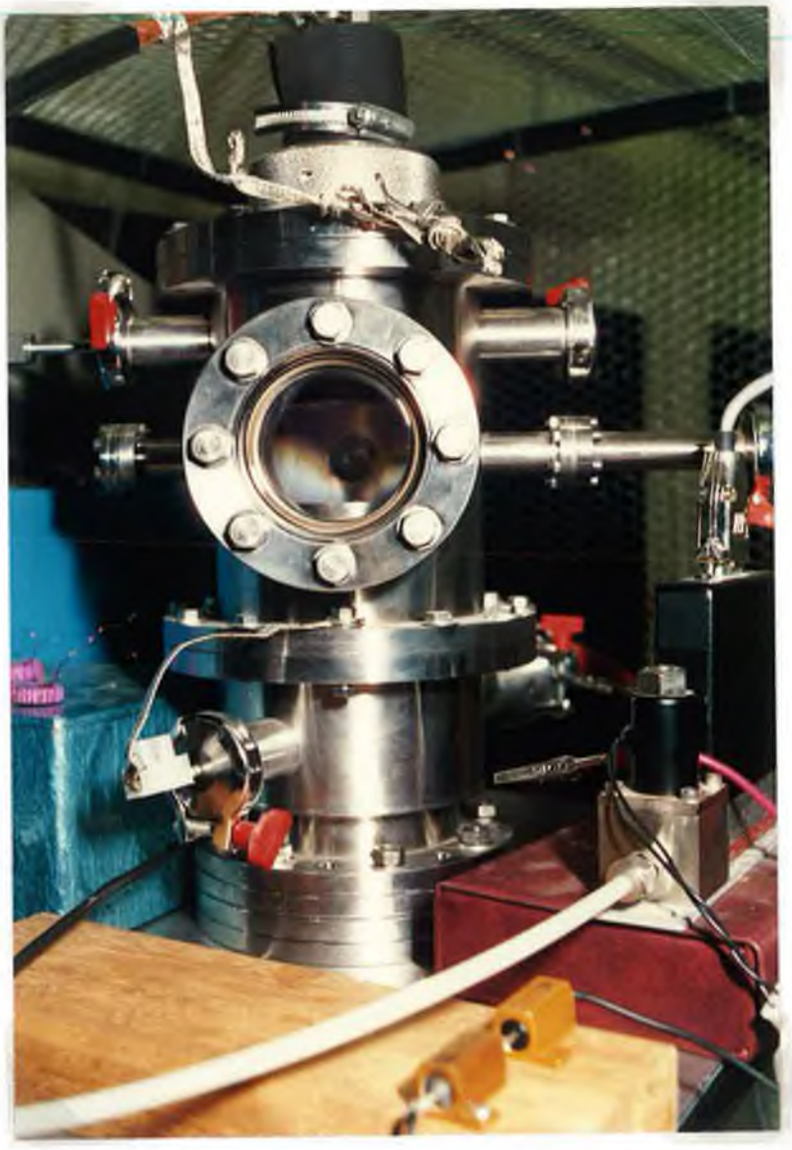

Photograph (3.1b)
A close up of the plasma chamber; the top electrode is the driven electrode

Figure (3.1) shows two typical experimental set-ups to produce an RF plasma. In the first diagram a source of alternating voltage connected to a power amplifier, which is in turn connected to a matching network. This couples the power from the amplifier into the plasma by matching the output impedance of the former to the natural or characteristic impedance of the plasma[14] (remember the maximum power theorem for complex impedances). The output of the matching network must come through a decoupling or blocking capacitor to ensure that no net DC current flows through the system. This output is applied directly to the top electrode with the other grounded.

The non-trivial nature of grounding in RF systems must be mentioned since a straight piece of wire will have an impedance $Z=R+j\omega L$, where R is its resistance given by $\rho l/ A$, ω is the operating frequency, and L the inductance of the length l of wire associated with it; this impedance can become apparent in the MHz operating frequency range. Due to the nonuniform distribution of current over the cross section of the conductors, 'the skin effect', I^2R losses are greater than if there was a uniform current distribution. This leads to an effective resistance, which becomes more pronounced at higher frequencies.

The impedance, $(j\omega C)^{-1}$, associated with the capacitance of oscilloscope probe leads becomes negligible at high frequencies and serious loading of signals by the scopes can occur. It is also found that ground loops are best avoided, and that the use of separate grounds is advisable. RF filters are installed on the mains sockets, and these greatly reduce RF noise in external equipment such as computers. Finally, to decrease the radiated power from the system, a Faraday cage was constructed about the chamber and all relevant equipment placed inside on a separate ground.

MATCHING NETWORK FOR RF PLASMAS

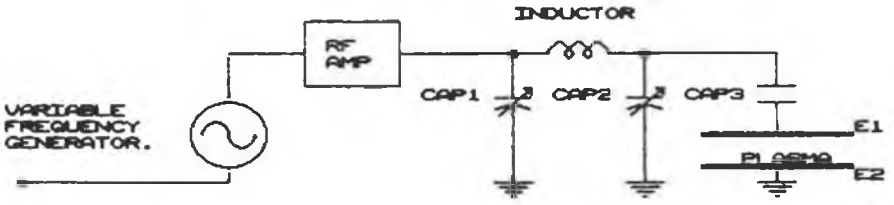

CAP1 & CAP2 ARE VARIABLE, PARALLEL PLATE CAPACITORS; CAP3 IS A FIXED VALUE CAPACITOR KNOWN AS THE DECOUPLING CAPACITOR. E1 & E2 ARE THE ELECTRODES AND IN THIS CASE E2 IS CONNECTED TO THE WALL OF THE CHAMBER, WHICH IS GROUNDED.

VARIABLE TRANSFORMER MATCHING UNIT FOR RF PLASMAS

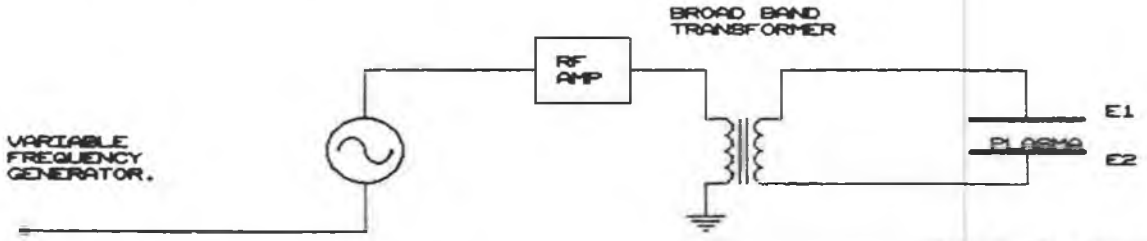

THE WALL OF THE CHAMBER IS GROUNDED BUT THE ELECTRODES FLOAT.

	JAMES MOLLOY	
Title: MATCHING N/W'S FOR RF/PULSED RF PLASMAS		
Size: A	Document Number	REV
Date: January 17, 2078	Sheet of	

Figure (3.1)

Photograph (3.2) shows the light output from the afterglow in a pulsed Argon plasma. The exponential decrease is suggesitive of an $e^{-t/\tau}$ loss mechanism and can be linked to the decay in plasma density.

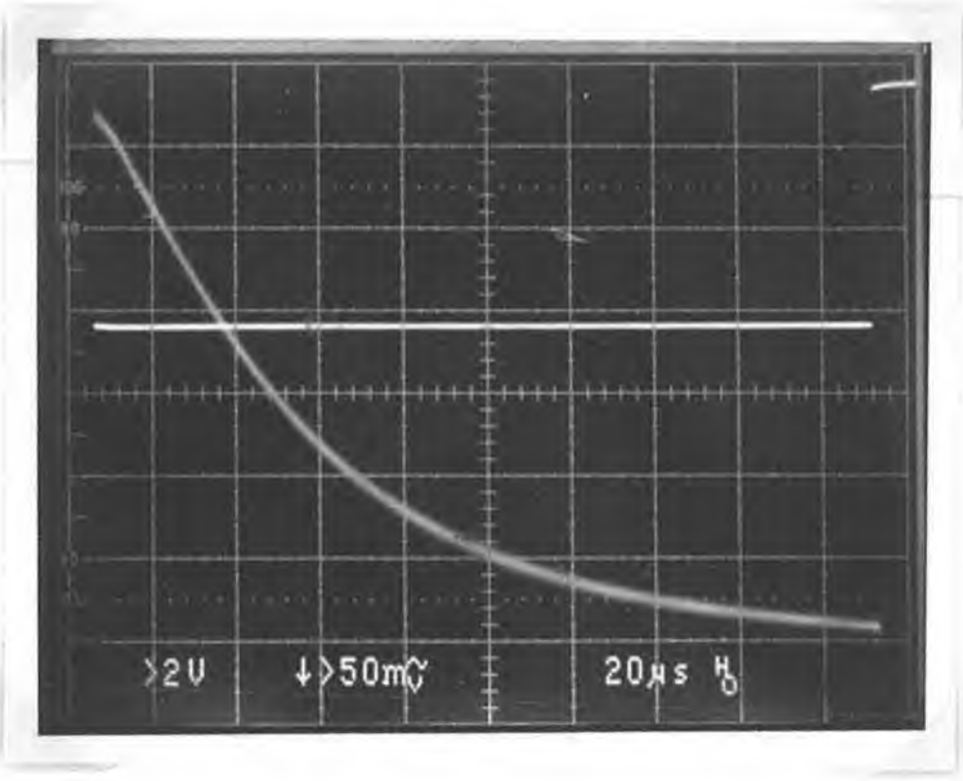

Photograph (3.2)
The light output from an Argon afterglow

3.2 The software

One of the first groups to analyse plasmas using the combination of minicomputer and Langmuir probes was Taylor and Leung[32]; they used a Hewlett - Packard 9820 calculator - plotter for their work. Hopkins and Graham[33] used an Apple IIe minicomputer in 1987. All programs used in this work are written on an IBM XT compatible. Assembly language routines, written in 8086 were interfaced to C calling programs, and this greatly speeded up the data acquisition process. A project file containing the C calling program and the assembly routines to be called is created and then compiled and linked.

The Assembly language routines

Microsoft Macro Assembler version 5.1 was used throughout and the standard assembly-interface method consists of these steps:

a) Setting up the procedure
b) Entering the procedure
c) Allocating local data (optional)
d) Preserving register variables
e) Accessing parameters
f) Returning a value (optional)
g) Exiting the procedure

Vals1.ASM

This is the data acquisition routine and its flow - chart is given in Appendix (D). It takes the parameters from the C calling program - the number of samples and the address in memory where storage of the converted voltage and current is to begin, and places them in the relevant registers to be accessed when needed.

A sample call from the C program is given below:

```
vals1(ii,ss);
```

with

```
ss=(unsigned int *) calloc(4,sizeof(unsigned int));
```

This reserves and zeros memory for four 16-bit numbers, which will contain the converted current and voltage readings. The number of samples is given by ii (≤ 256 at present). The C program loops through the probe voltage, calls the Assembly language routine described above for each voltage, and then retrieves the data to analyse it.

3.3 The electronics

A completely computerised system is used to measure the probe characteristics. This provides accurate control of the probe voltage, the ability to measure the probe currents in the μA to mA ranges, high speed calculation of the plasma parameters and neat, flexible presentation of the data. Figure (3.2) gives an overview of the electronics used. The probe current is measured by switching in current-sensing resistors with low tolerance and adequate power ratings. The voltage drop across this sensing resistor is a measure of the probe current; Figure (3.3) shows this set up. This drop is kept small (≅ 150 m V); this is necessary due to problems with V I heating giving resistance changes with temperature . This small voltage drop can be amplified by a fixed gain precision amplifier to utilise the full range of the A / D.

The accuracy of measurement of the basic plasma parameters such as electron and ion densities, electron temperatures, plasma and floating potentials all depend on the bit resolution of the A / D. The current is measured with the following resolution for a full scale input to a 16 - bit A / D :-

$$1 / 2^{n-1} = 1 / 2^{15} \approx 0.0003 \ \% \ \text{of full scale.}$$

Note 1 bit is used for the sign of the number, and also that the above accuracy is achievable using multiple averaging. So the current can be measured to an accuracy of 2 in 1 x 10^4. When analog voltages are being read in they are first stored in a sample and hold before conversion; the sample and hold must have a short acquisition time combined with low droop rate and very little feedthrough.

Figure (3.2)
An overview of the acquisition system

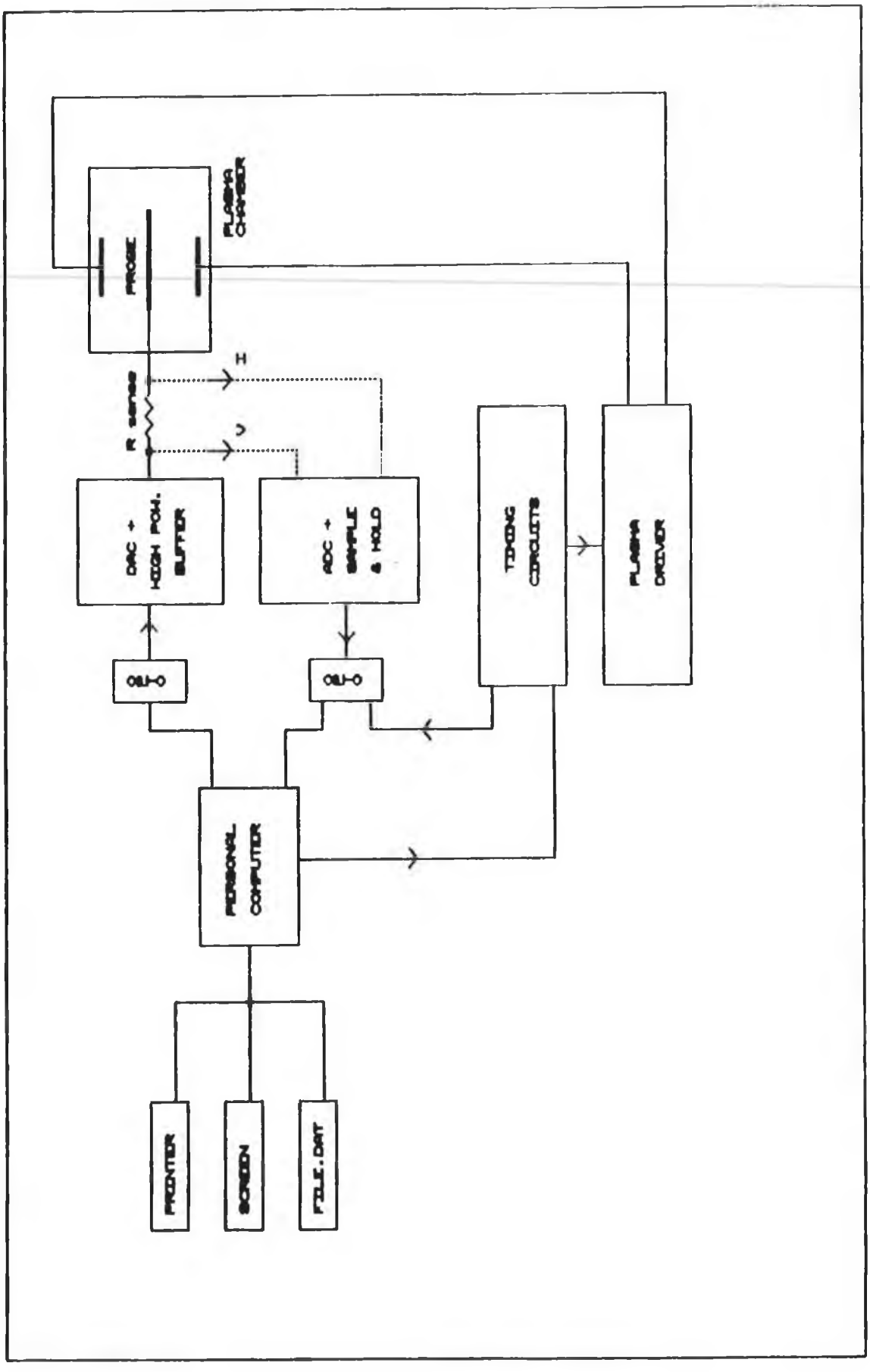

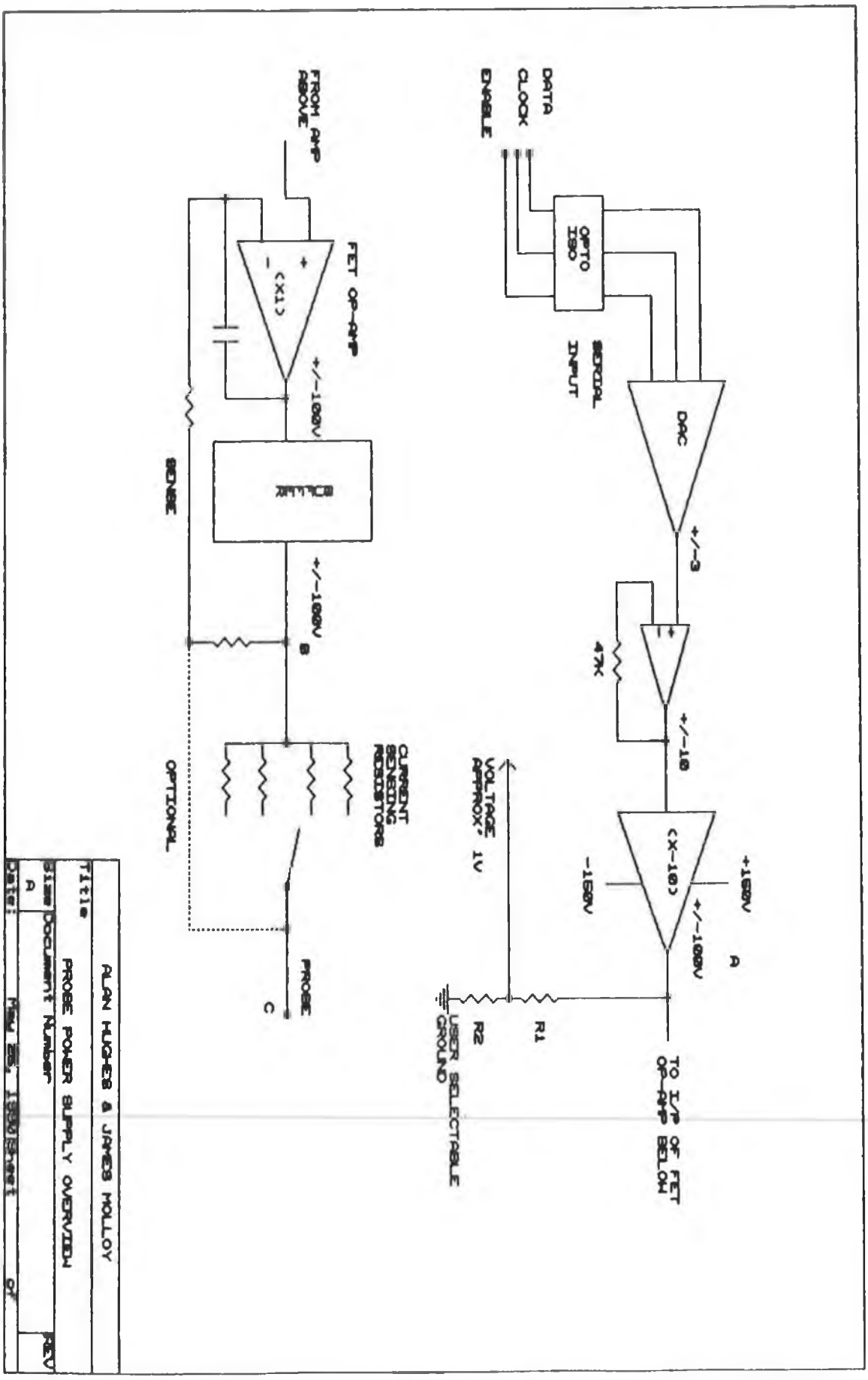
DATA
CLOCK
ENABLE
OPTO ISO
SERIAL INPUT
DAC
+/-3
47K
+/-10
(X-10)
+150V
-150V
+/-100V
A
TO I/P OF FET OP-AMP BELOW
VOLTAGE APPROX. 1V
R2
R1
USER SELECTABLE GROUND
FROM AMP ABOVE
FET OP-AMP
(X1)
+/-100V
SENSE
B
CURRENT SENSING RESISTORS
OPTIONAL
PROBE
C
ALAN HUGHES & JAMES MOLLOY
Title
PROBE POWER SUPPLY OVERVIEW
Size
Document Number
REV
A
Date:
Sheet
of

Figure (3.3)

The chip used is the DATEL shm 91mc dual sample and hold, which can sample the current and voltage simultaneously (this has the effect of reducing random noise) and these are then sequentially multiplexed to the A / D which is a ADC 71jm. All the signals to and from the computer are optically isolated from the measuring electronics which are floating. A PIO - 48 input / output board which uses two 8255 chips is used to generate control signals; a master C program calls up various assembly language routines to control the A / D, D / A and switching relays, as well as the timing circuitry needed to pulse the probe (see below).

The C calling program will process the data and give first approximations for the most important plasma parameters using the real time analysis described in the previous chapter. The user can select a variable number of averages depending on the accuracy and noise elimination needed aswell as the time available for the scan.

An external trigger input (see section on the pulse delay circuit) can be used for time resolved measurements or else the A / D may be triggered using a falling edge from the computer. Figure (3.3) shows an overview of the probe power supply. The DAC is a 16-bit serial input PCMP56P, with a 1.5μs settling time and a ±3V output. Figure (3.4) shows the op-amp arrangement that amplifies the DAC output to the ±10V; this is fed to a pre-amplifier (described below). The D / A has three optically isolated input lines (CLOCK, LATCH ENABLE and DATA), and the output is fed in to the pre-amp input (Figure (3.5)); this stage amplifies the voltage to ±100V but it has limited output impedance and hence cannot supply enough current.

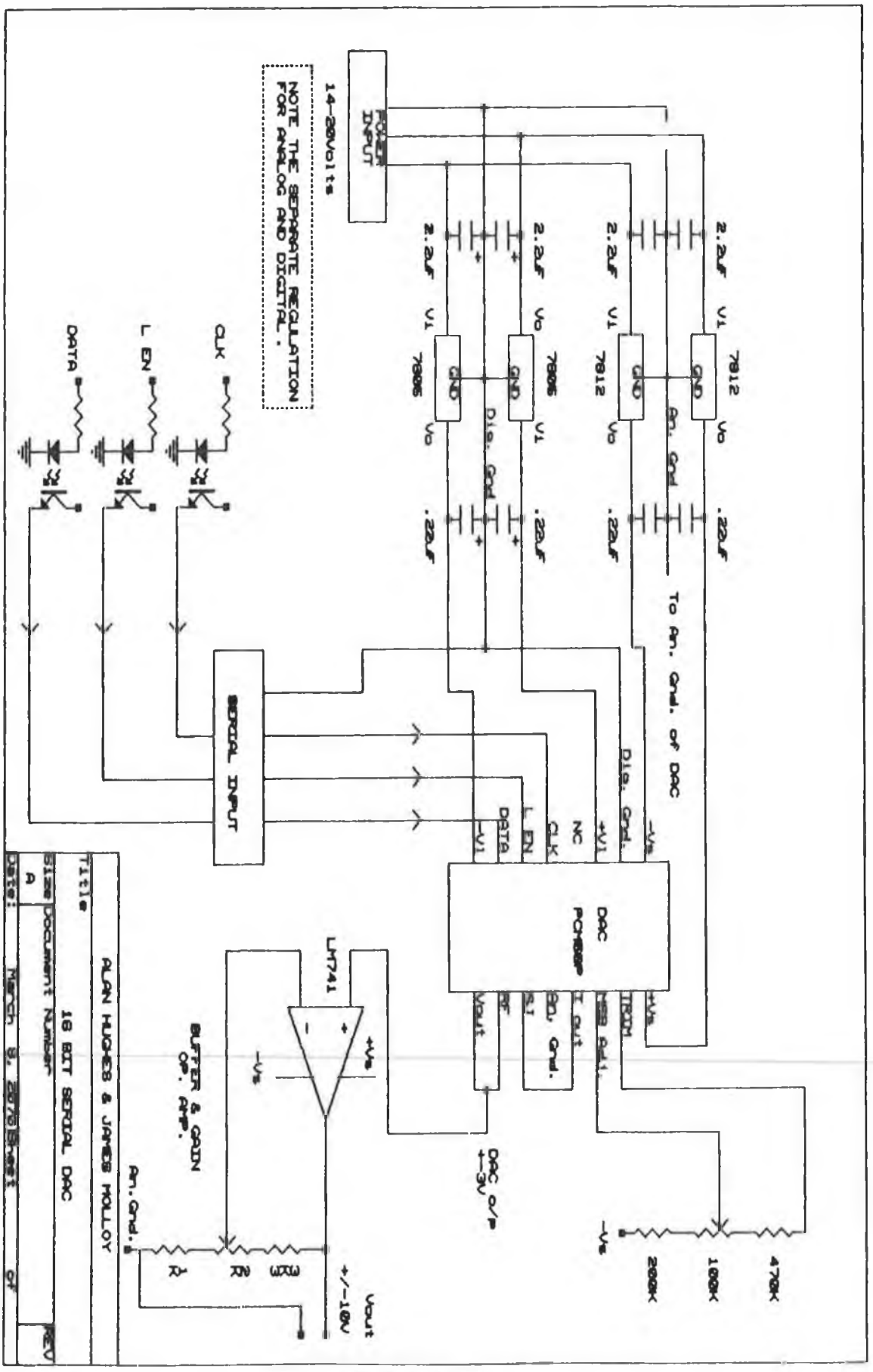
POWER INPUT
14-28Volts
NOTE THE SEPARATE REGULATION FOR ANALOG AND DIGITAL.
7812
7805
GND
Vo
Vi
2.2uF
.22uF
An. Gnd.
Dig. Gnd.
To An. Gnd. of DAC
CLK
L EN
DATA
SERIAL INPUT
DAC
PCM56P
NC
+Vi
-Vi
+Vs
-Vs
I out
Rfb
Vout
LM741
BUFFER & GAIN OP. AMP.
DAC o/p +-3V
Vout +/-10V
470K
100K
200K
R1
R2
R3
ALAN HUGHES & JAMES MOLLOY
Title
16 BIT SERIAL DAC
Size
Document Number
REV
Date: March 8, 2078
Sheet
of

Figure (3.4)

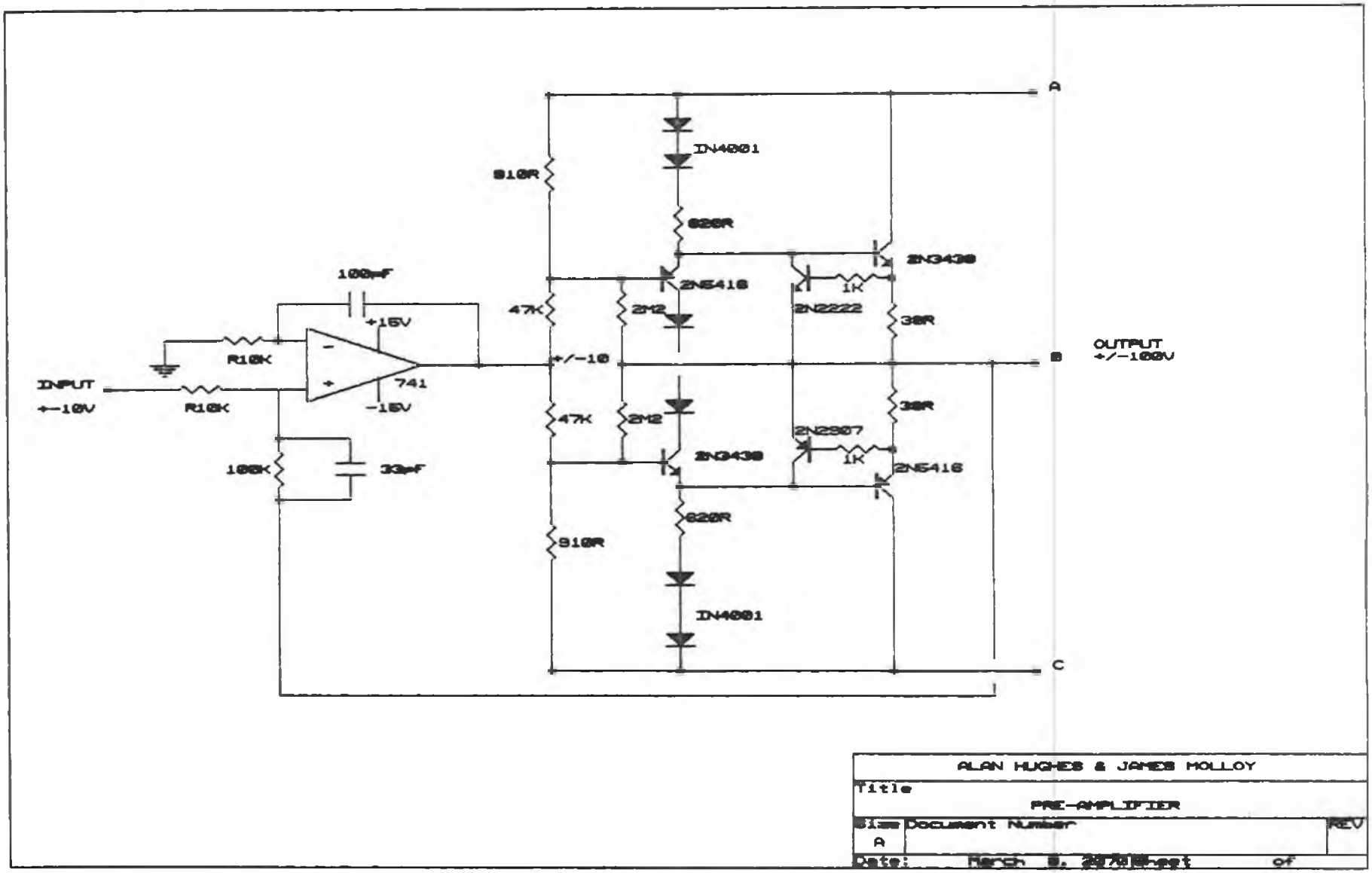
A
B
C
IN4001
910R
820R
2N5416
100nF
+15V
47K
2M2
2N2222
1K
3R3
OUTPUT
+/-100V
+/-10
INPUT
+-10V
R10K
741
-15V
R10K
100K
33nF
2N3439
2N2907
ALAN HUGHES & JAMES MOLLOY
Title
PRE-AMPLIFIER
Size
A
Document Number
REV
Date:
March 8, 2000
Sheet
of

The voltage follower of Figure (3.6) 'drives' the probe; a buffered high power operational amplifier (BURR BROWN 3583) is used and can deliver ± 100 mA at ± 150 Volts; note that the inputs to the 3583 are FET inputs - these draw extremely low currents, and hence do not interfere with the measurement process when 'sensing' the voltage.

3.4 The Pulsing circuitry

An elaborate timing circuit is needed to provide the probe on/off and sample & hold pulses. Figure (3.7) shows a block diagram of the circuit used; the circuit diagram and associated timing diagram is given in full detail in Appendix (C). Looking at Figure (3.7), one sees that the computer clocks the appropriate time delay in bits to a serial to parallel converter (s - p); the counting circuit is disabled by the computer until all the data has been clocked into the s - p; the plasma on - off (pp) pulse gates the clock pulses to the counter, and when the comparators and the counter reach the same state, the monostable m1 is triggered. This pulse is fed through two other monostables yielding the probe pulse, 'pr', and the sample and hold pulse, 'sh', (external trigger). It also disables the counter first, and clears it until the plasma is turned off again.

The probe pulse can then be directly applied to the circuit of Figure (3.8a), and the sh pulse to the sample and hold chip via an opto isolator. The probe pulse produced in the circuit of Figure (3.7) is fed to an op - amp which gives a ± 15V output; this is applied to the gate of the FET which acts as a switch and can either connect or disconnect the probe from the high tension power supply; note the FET used enabled bidirectional current flow through the system i.e. ionic or electronic.

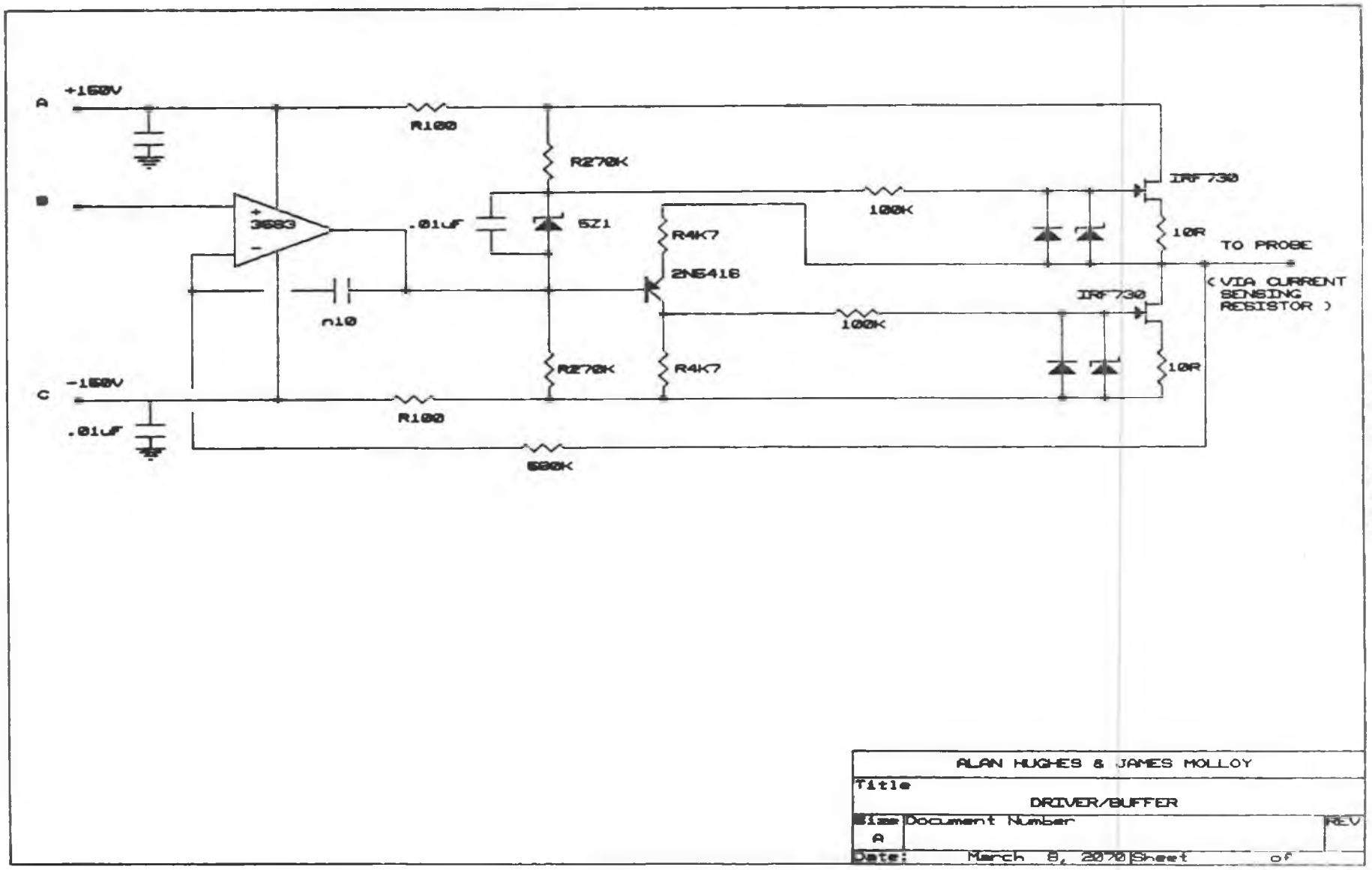
A
+150V
B
C
-150V
.01uF
R100
R270K
3583
.01uF
5Z1
R4K7
2N5416
100K
IRF730
10R
TO PROBE
(VIA CURRENT SENSING RESISTOR)
n10
R270K
R4K7
100K
IRF730
10R
R100
.01uF
500K
ALAN HUGHES & JAMES MOLLOY
Title
DRIVER/BUFFER
Size
A
Document Number
REV
Date:
March 8, 2070
Sheet
of

Figure (3.6)

Figure (3.7)

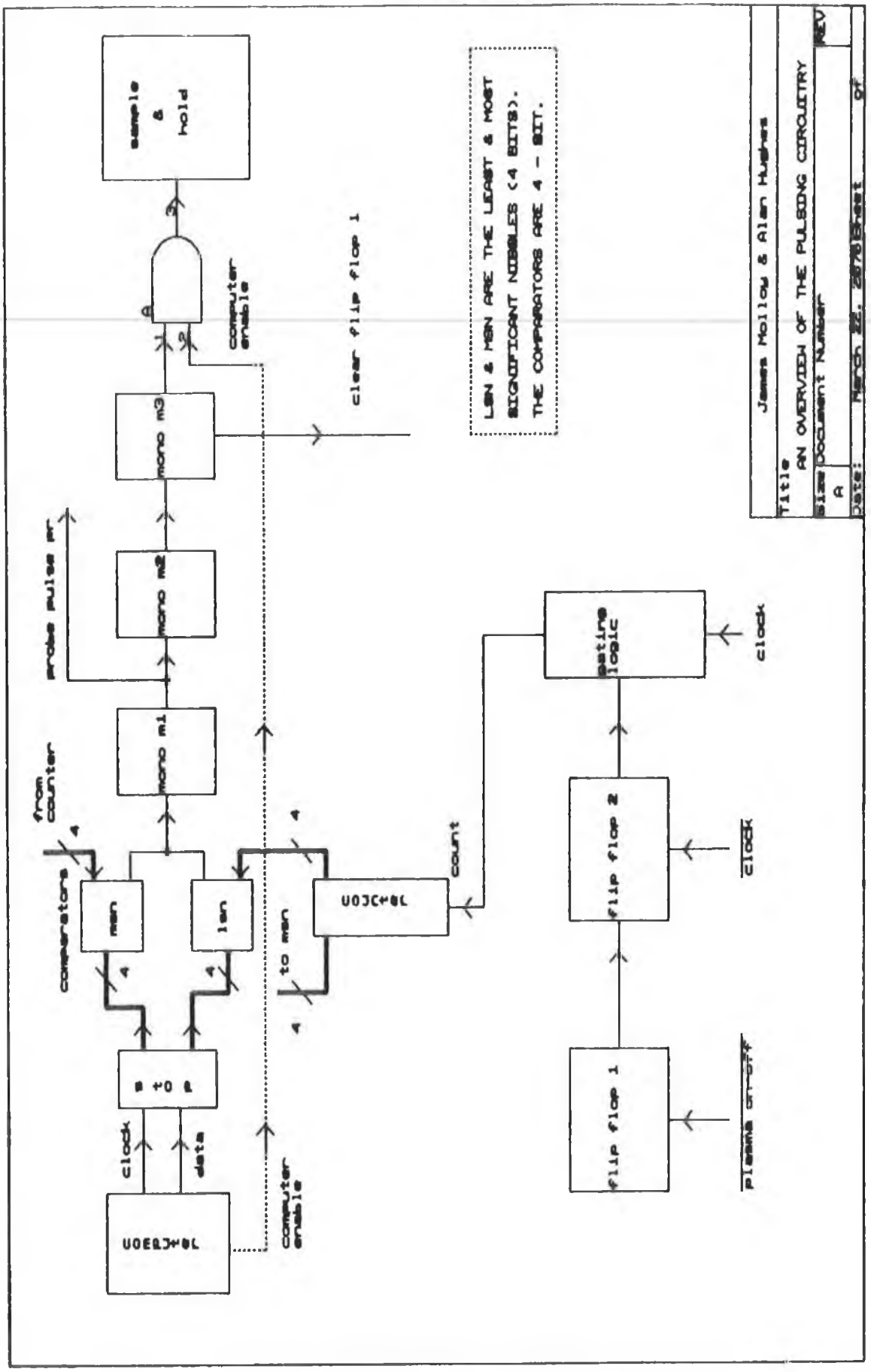
sample & hold
computer enable
clear flip flop 1
mono m3
mono m2
probe pulse pr
mono m1
from counter
comparators
msn
lsn
to msn
count
clock
data
computer enable
flip flop 2
flip flop 1
clock
plasma on-off
LSN & MSN ARE THE LEAST & MOST SIGNIFICANT NIBBLES (4 BITS).
THE COMPARATORS ARE 4 - BIT.
James Mallon & Alan Hughes
Title
AN OVERVIEW OF THE PULSING CIRCUITRY
Size
A
Document Number
REV
Date:
March 22, 1988
Sheet
of

Figure (3.8a)

The probe circuit

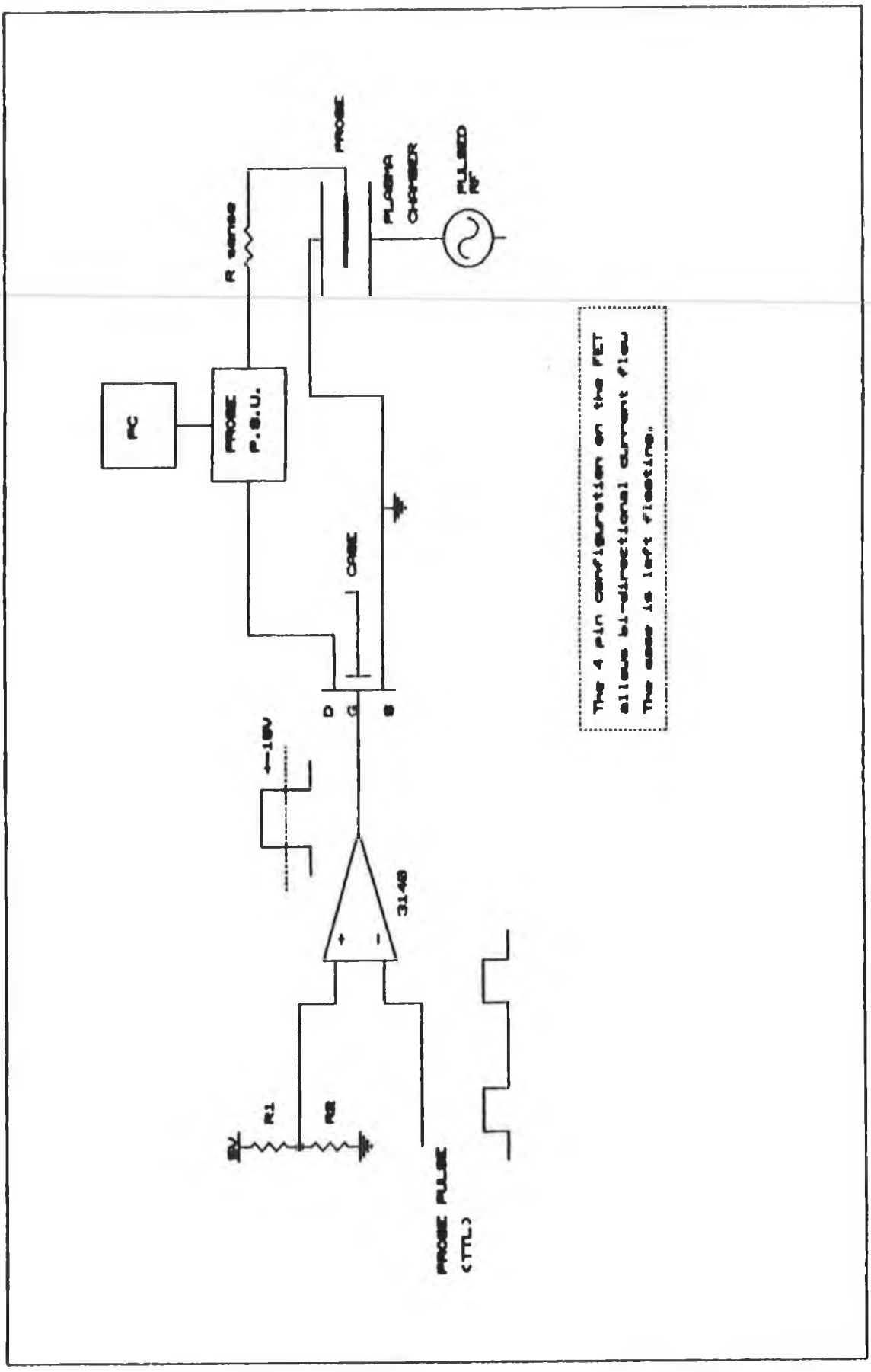

Two scenarios for the application of the bias voltage to the probe were investigated, the first of these being the direct application of a continuous DC voltage and the second was the application of the same voltage in pulse form. This pulse was short in duration relative to the plasma on-off pulse and longer than the sample and hold pulse.

Photograph (3.3) shows such a scheme. The time between switching the probe on and taking the data point is variable and is usually left at 20μs to enable the initial oscillations die away; refer to Figure (3.8b) for a timing diagram.

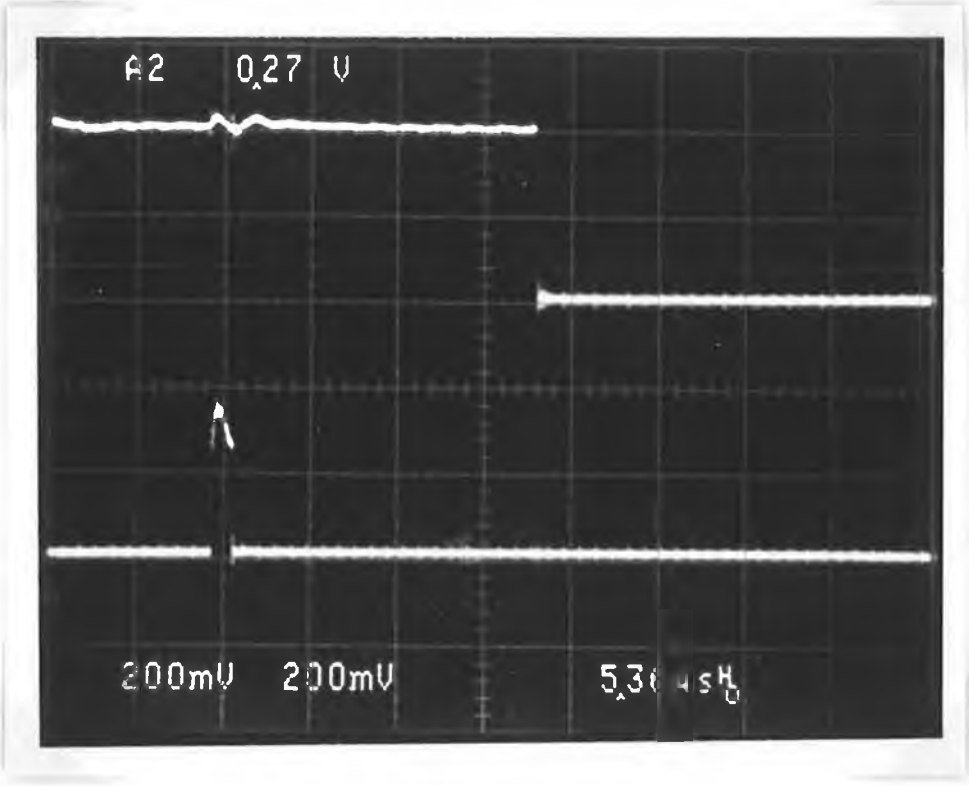

Photograph (3.3)
Probe pulse (top) and sample and hold pulse

Figure (3.8b) **The pulsed probe technique**

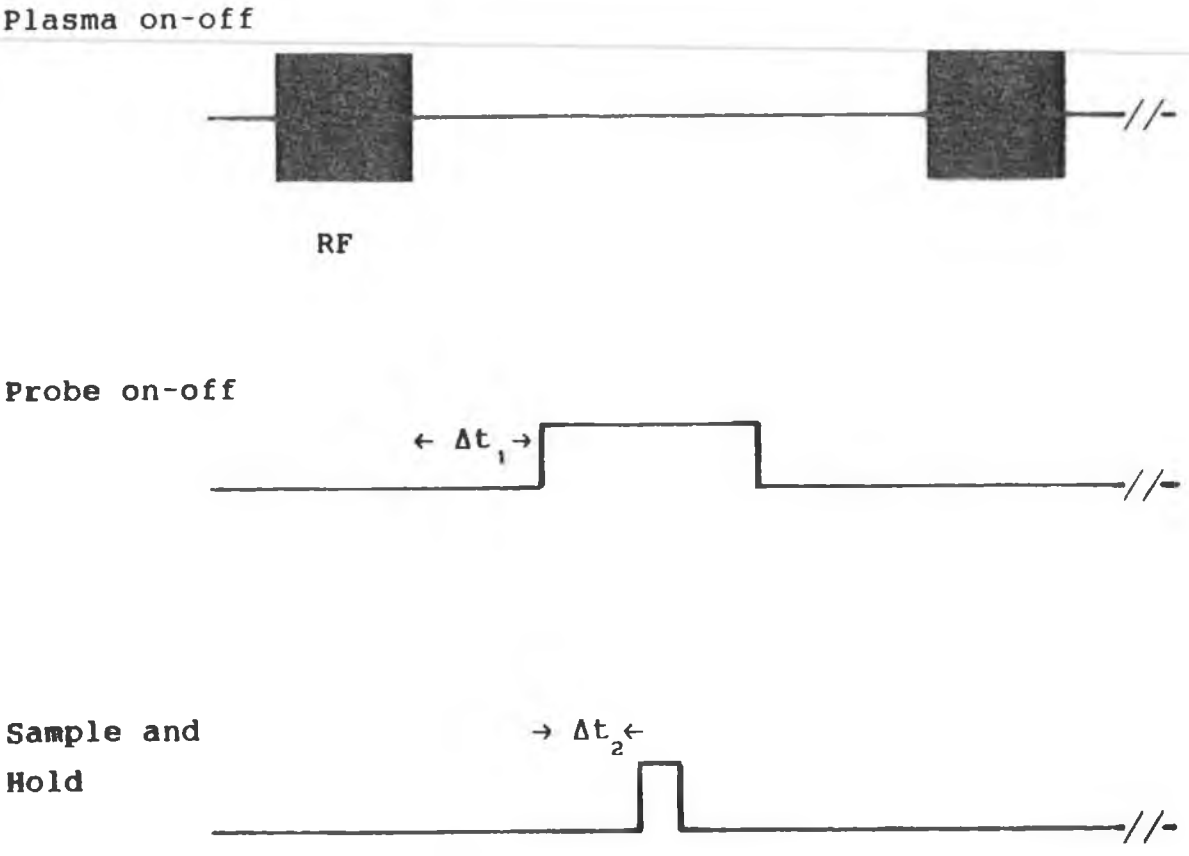

CHAPTER IV

RESULTS AND DISCUSSION

4.1 Introduction

In most probe theories, it is assumed that the plasma is uniform and infinite in extent; the charged particle - neutral collision mean free path is small compared to the dimensions of the plasma container, and the probe does not perturb the plasma i.e. probe measurements are non - perturbative. This last assumption is equivalent to saying that the charged particle density, at large distances from the probe, is not a function of the probe voltage.

The problem of depletion by a biased probe is most acute in slowly decaying plasmas, and can be overcome by using the methods described in the last chapter (pulsing the probe) or using very small radius probes, which have the disadvantage of being susceptible to thermal damage. Although the power in the discharge pulse was not measured accurately, measurements indicate initial electron densities in the range 10^{15} to $10^{16}m^{-3}$ over the range of input powers used. These initial densities are too low for recombination losses to be significant during the period of observation[18].

4.2 The Diffusion model

Ambipolar diffusion is thought to be the main loss mechanism in the afterglow, and is due to the fact that electrons tend to diffuse out of the plasma faster than the colder and much heavier ions, creating a space charge (the plasma potential) that opposes the effect until equilibrium is attained with the electrons and ions diffusing at a similar rate.

A simple model for the plasma density was developed using the diffusion equation

$$\frac{\partial n_e(r,t)}{\partial t} = D_a \nabla^2 n_e(r,t) \qquad (4.1)$$

where D_a is the ambipolar diffusion coefficient ($m^2 s^{-1}$).

The one dimensional case was solved here using the separation of variables technique[30]. This states that the function $n_e(x,t)$ can be split into a product of two functions i.e.

$$n_e(x,t) = R(x)\, T(t) \qquad (4.2)$$

and the time and space dependencies, T(t) and R(x), can be obtained separately. T(t) as given by Equation (4.3) yields the decay times for the different diffusion modes, and R(x), the spatial dependencies of these modes. There is an asymmetry about x = 0 (the centre of the discharge) due to the fact that the boundary conditions $R(x=\Lambda) = R(x=-\Lambda) = 0$ must be satisfied.

$$T(t) = n_0\, e^{-t/\tau_n^{\pm}} \qquad (4.3)$$

with

$$\tau_1^- = \Lambda^2 D_a^{-1} \pi^{-2} \qquad (4.4)$$

for the sine solution, and

$$\tau_1^+ = 4\, \tau_1^- \qquad (4.5)$$

for the cosine solution of the fundamental diffusion mode (n = 1).

The parameter Λ is the characteristic diffusion length from Equation (1.23). The corresponding spatial solutions are

$$R^{-}(x) = \sin(\pi \times \Lambda^{-1}) \qquad (4.6)$$

and

$$R^{+}(x) = \cos(\pi \times \Lambda^{-1}/2) \qquad (4.7)$$

The cosine solution is used in the model since cos(x=0)=1. The values for the diffusion length and diffusion constant are calculated by modelling the discharge volume as a cylinder of effective length, L, and radius, R:

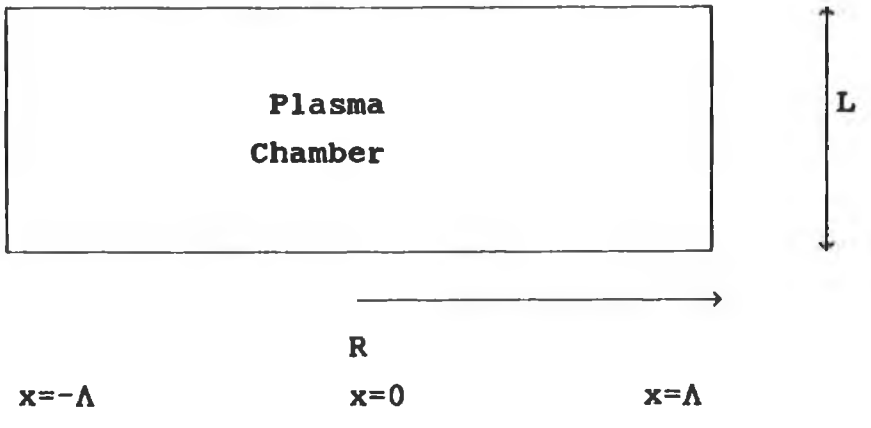

A value of $\Lambda^{-2} = 6261\ m^{-2}$ is obtained from Equation (1.23) and this is used to yield a value for D_a from the following equation:

$$D_a p_o = D_{a1} p_o + \beta p_o^3 \Lambda^2 \qquad (4.8)$$

with D_{a1} as the ambipolar diffusion coefficient for atomic ions and β is the three - body conversion coefficient for the conversion of atomic to molecular Helium ions.

If the reduced pressure, p_0, is approximated as the gas pressure and β = 80 $Torr^{-1}s^{-1}$, $D_{a1}p_0$ = .038 Torr s^{-1} (from Ref. 17), and the value for Λ^2 as calculated above is used, one obtains a value of .052 m^2s^{-1} for D_a. These values can be inserted into the diffusion equation solutions and a comparison with experiment carried out.

Assuming that the electrons lose all their energy when in collision with neutral atoms, it follows that

$$n_0 \tau_e^{-1} = n_0 \lambda_{emfp}^{-1} v_{e,therm} \qquad (4.9)$$

with n_0 the neutral density, λ_{emfp} the electron mean free path and $v_{e,therm}$ the electrons mean thermal velocity

$$(8 \ k \ T_e / \pi \ m_e)^{1/2}$$

This gives us the densities for the different solutions as

$$n_e^{\pm}(x,t) = R^{\pm}(x) \ T^{\pm}(t) - n_0 \tau_e^{-1} \qquad (4.10)$$

This last term is seen to be negligible ($\cong$ 1% loss due to collisions), and can be neglected as ineleastic collisions in monoatomic gases are few and far between. The bulk electron temperature can decay by either of two ways - diffusion cooling to the walls (all electrons above the plasma potential in the EEDF) or collisional cooling of electrons with atoms or molecules.

4.3 Comparison of theory with experiment

Electron density and temperature decay rates were observed in both Helium and Argon afterglow plasmas for the pressures 400mTorr and 1Torr (50Pa and 130Pa). The characteristics were analysed as in the chapter on Langmuir probes, and the parameters plotted versus time. A typical 'family in time' of Lagmuir probe I - V traces is shown in Figure (4.1), and the corresponding $\log_e(I)$ - V in Figure (4.2).

Looking at Figure (4.1), it may be seen that the characteristic is contracting with time, and the density is decaying as expected; it is difficult to state anything definite about the temperature from the exponential region, but this problem is overcome by using the semi - logarithmic plot as shown in Figure (4.2). At early times in the afterglow there are two main groups of electrons, and these can be assigned two distinct 'temperatures'; it should be mentioned again that the 'temperature' of the high energy group is a rather dubious concept because one is approximating a small fraction of the total plasma ($\cong$ 10 %) by a Maxwellian distribution. This high energy tail that corresponds to the source of ionisation in the plasma (the beam electrons) is seen to decay away with time, eventually blending with the colder group (bulk electrons) through collisional processes.

The experimentally observed cold electron temperature decays are shown in Figure (4.3) and Figure (4.4) for .4Torr and 1Torr He afterglows respectively. The experimental rate of decay is not as fast ($\cong$ 44μs and 200μs respectively) as one would expect as the electrons should lose their energy rapidly due to the aforementioned collisions; hence it is suspected that there is either some extra source of fast electrons in the plasma or some unexpected residual source of energy there to give these beam electrons a longer lifetime.

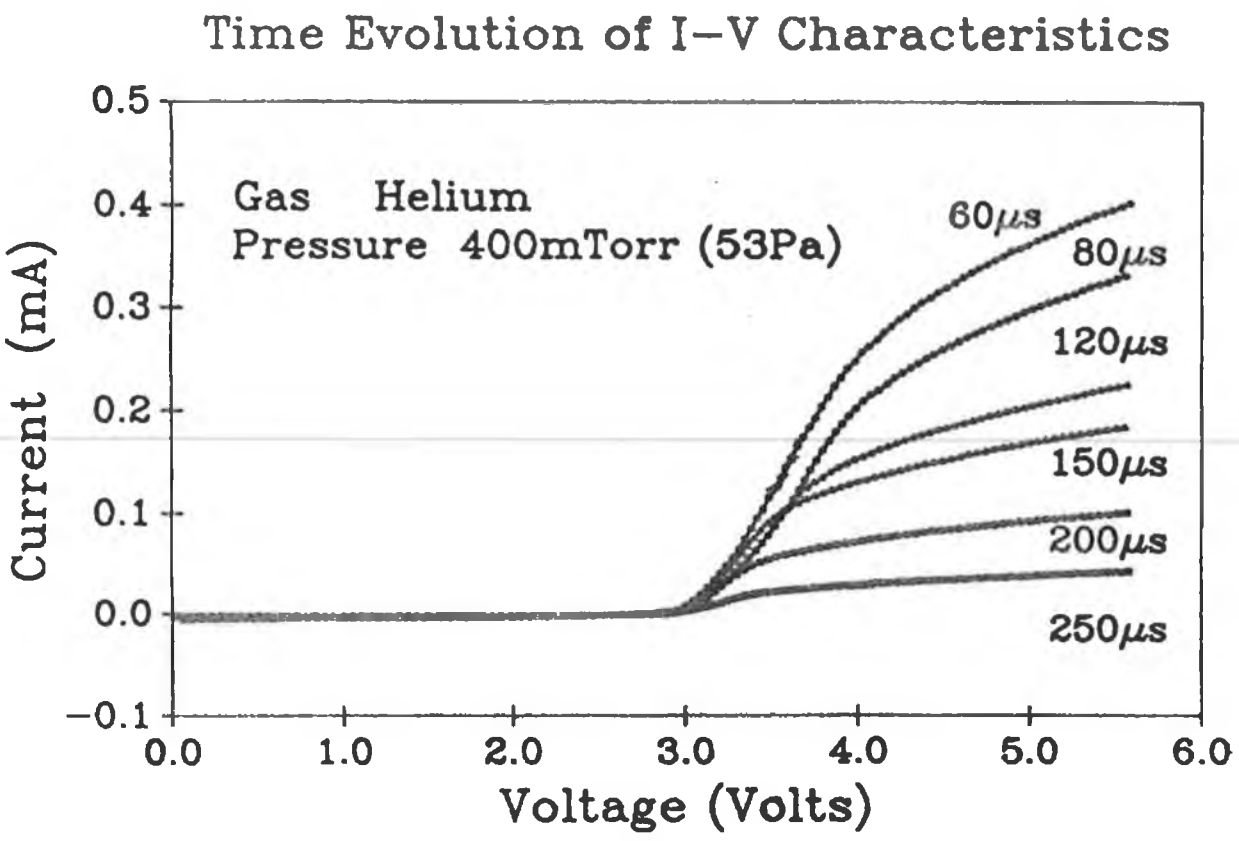

Figure (4.1)

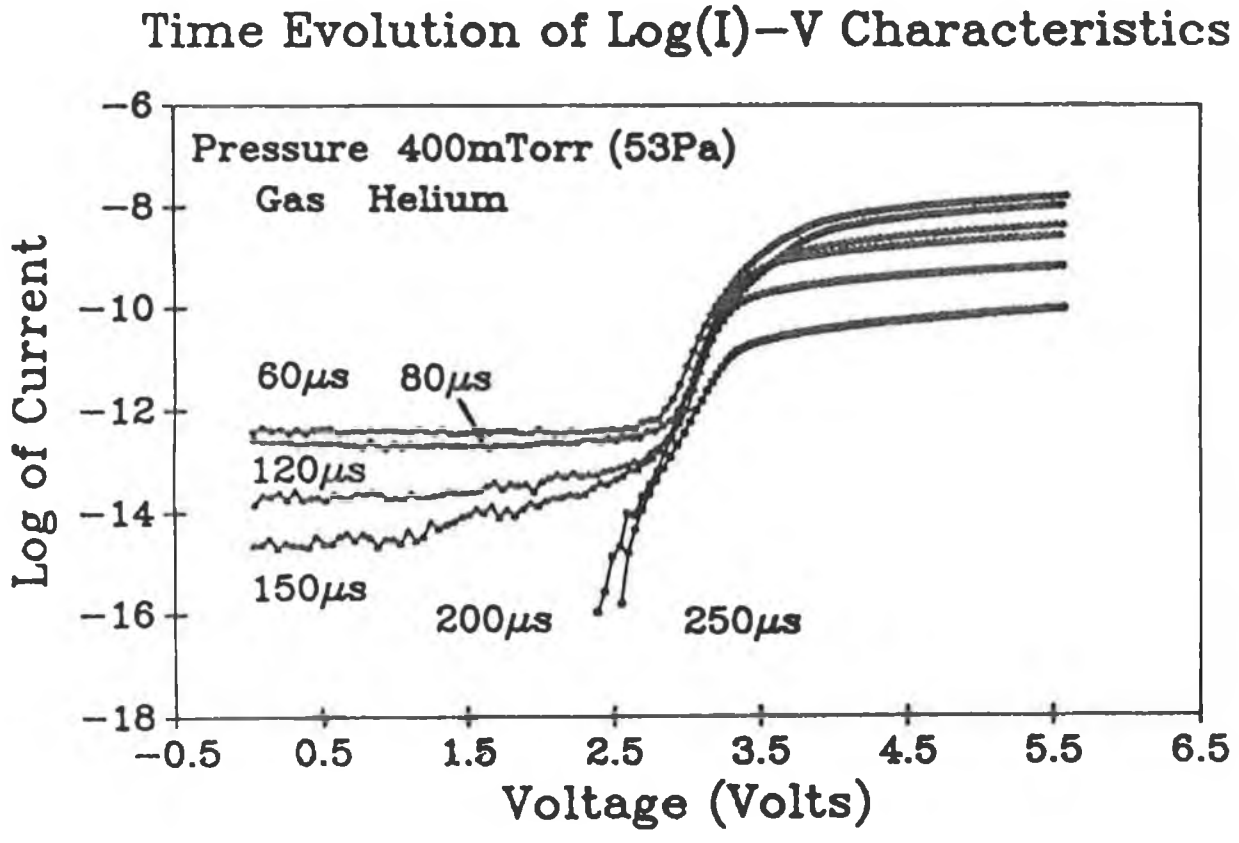

Figure (4.2)

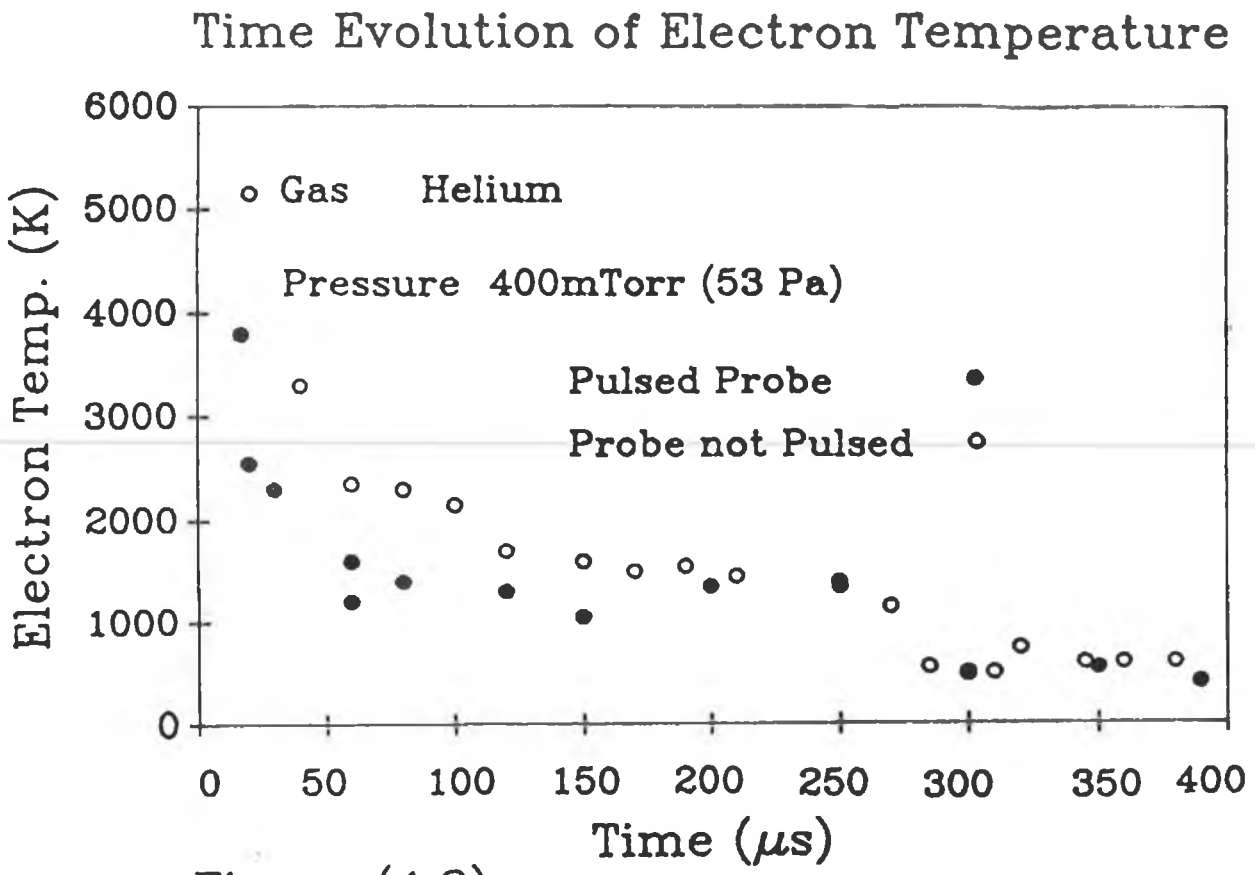

Figure (4.3)

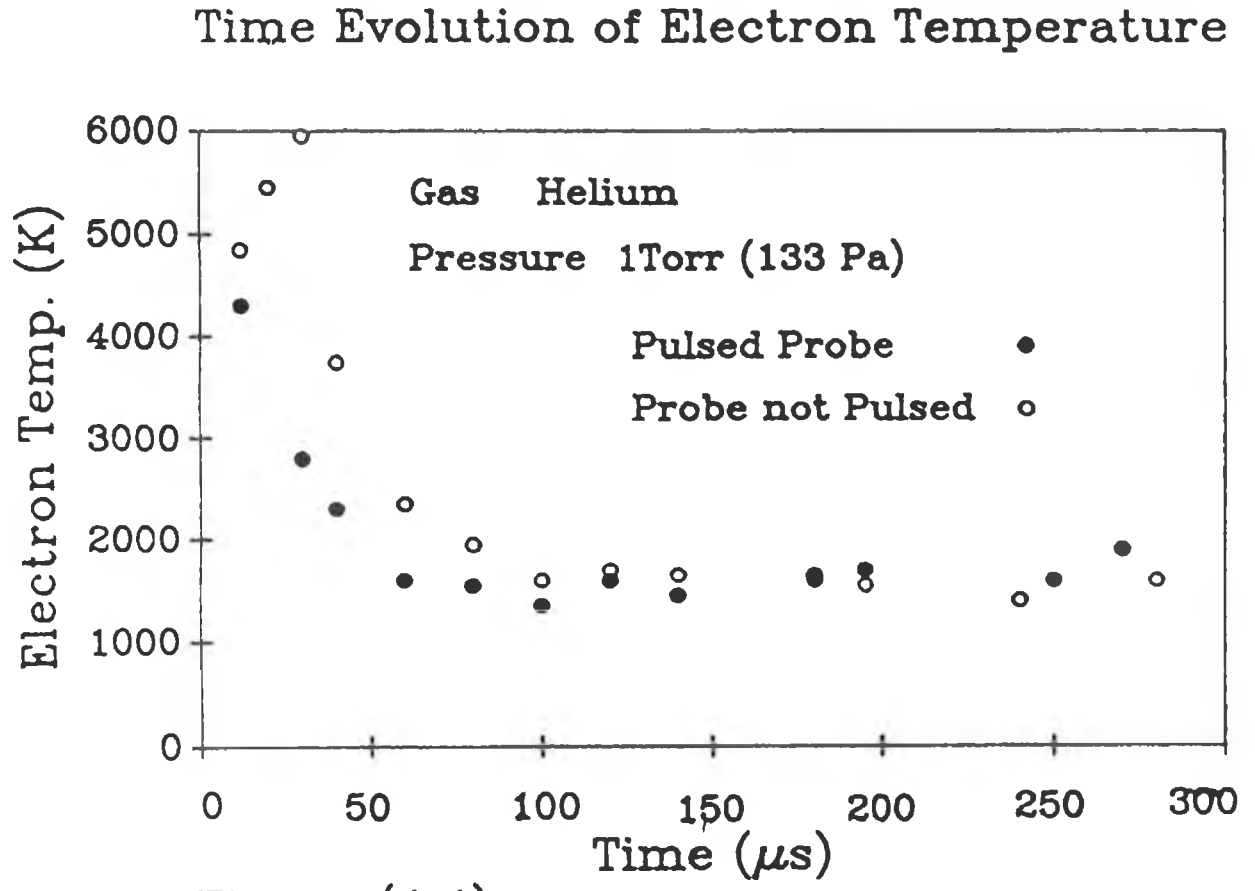

Figure (4.4)

The bulk electron temperature is seen to approach ambient (room) temperature in the temporal limit as is expected due to the fact that the plasma thermalises with the wall at later times in the afterglow. Note the fact that the temperature is lower in the case of the pulsed probe as expected. A number of mechanisms have been suggested (some of which have been mentioned before) for the slower than expected decay in the electron temperature and among these are:

1 the presence of metastable atoms, which due to their long lifetimes could be 'hanging in', and contributing extra energy to the afterglow. Unfortunately no method was available to measure the lifetimes of the metastables. The diffusion coefficients for these metastables in monatomic gases are obviously important and could lead to some interesting physics. These metastable atoms could interact with impurity atoms giving a high energy electron (Penning ionisation). This is highly probable as the lifetime of the metastables is of the order of 100 's of μs, and impurity atoms or molecules tend to cluster, and can become quite large, thus increasing the probability of interaction. The reaction can be characterised as follows:

$$A^* + A_{imp} \rightarrow A + A^+_{imp} + e^-$$

where A^* is the metastable atom,

2 local heating of electrons in the vicinity of the probe can result from the Auger ejection of electrons from the probe due to metastable interactions,

These Auger electrons result from the spontaneous ejection of an electron by an excited positive ion to form a doubly charged ion i.e.

$$A \xrightarrow{-e} A^{+*} \longrightarrow A^{2+} + e^{-},$$

where A^{+*} represents an excited state of a singly charged ion, and A^{2+} a doubly charged ion that may or may not be in its ground state,

3 there could be (not very likely) some residual electric field in the afterglow since the plasma decays capacitively, and Sommerer[43] claims that the weak bulk field is important for heating electrons of all energies.

Figure (4.5) shows the cosine solution and also the experimental density decays in a .4Torr He afterglow. From these plots, the ion and electron confinement times can be obtained from

$$\tau^{-1} = \frac{\log_e(n_1 / n_2)}{t_1 - t_2} \qquad (4.11)$$

where n_1 and n_2 are the densities at times t_1 and t_2; these values can then be used as a comparison with theory.

A number of things are immediately evident[42]

1 the exponential nature of the decays,

2 the increase in density in the case of the pulsed probe, thus indicating the effect of plasma depletion,

3 the particle confinememt times (both electron and ion confinement times are the same due to ambipolar diffusion) for .4Torr are calculated as approximately 80μs using Equation (4.12), and this is a factor of eight out from the theoretically obtained value using the cosine solution (670μs),

4 the rates of temperature and density decay are unequal (the latter being 1.8 and 1.5 times the temperature for the 400mTorr and 1Torr cases respectively). This implies that the plasma temperature decays quicker than its main source, and suggests an unknown additional heating mechanism,

5 the decay is faster than that predicted by the simple diffusion model, and this could be due to the presence of electron attaching impurities, the presence of impurity ions or the existence of surface recombination sites on the body of the probe - sleeve arrangement. This would lead to a decrease in the diffusion length, and hence speed the decay process up.

Figure (4.6) is the electron density decay in a 400mTorr Argon afterglow, and Figure (4.7) shows the electron density as a function of power input to the plasma system. As expected the electron density increases with increasing power as there is more ionisation occurring (more positive ion - electron pairs being created, and the ions incident on the electrodes are of a higher energy thus emitting higher energy beam electrons).

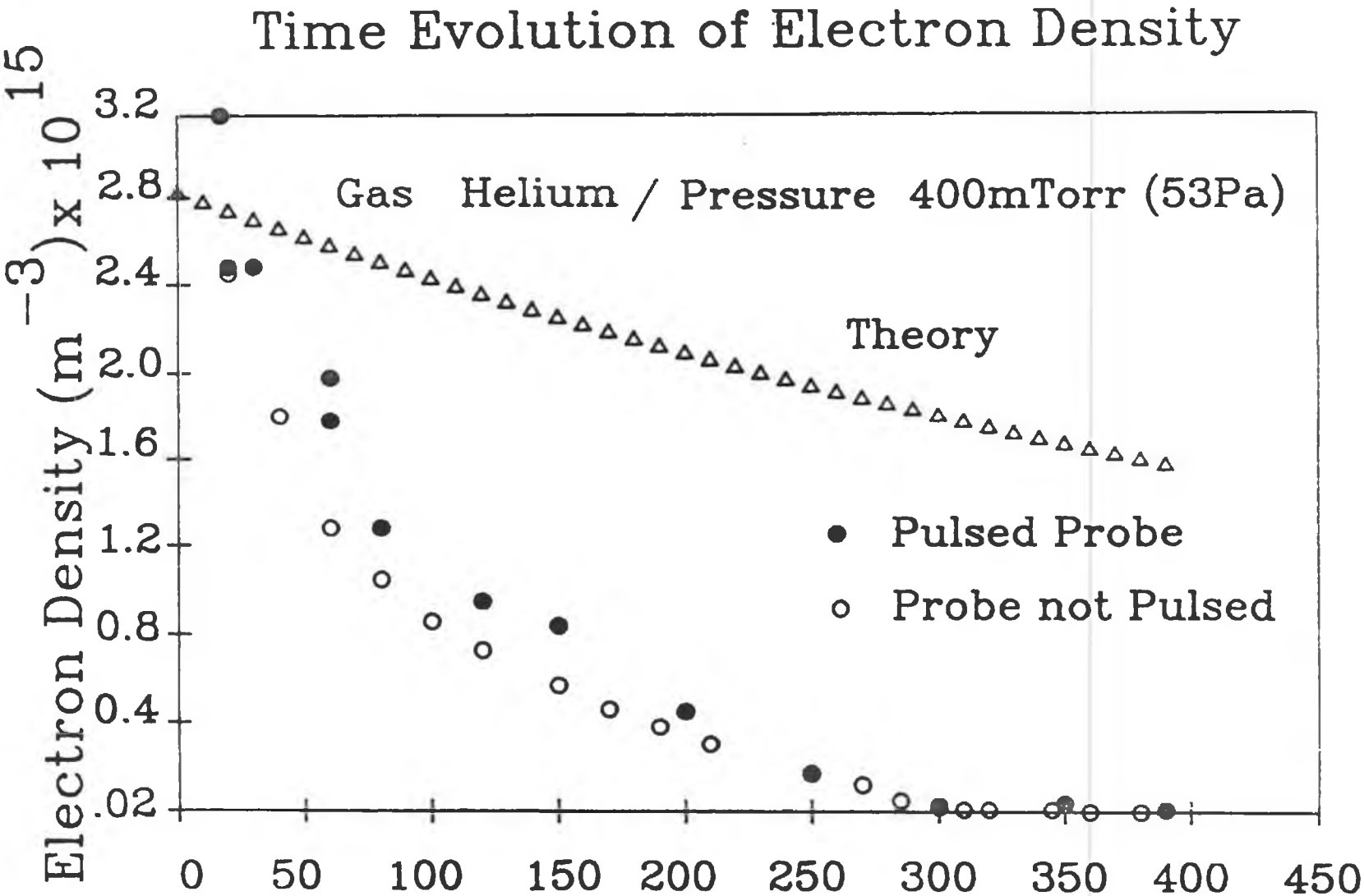
Time Evolution of Electron Density
Gas Helium / Pressure 400mTorr (53Pa)
Theory
Pulsed Probe
Probe not Pulsed
Electron Density (m^{-3}) x 10^{15}
3.2
2.8
2.4
2.0
1.6
1.2
0.8
0.4
.02
0
50
100
150
200
250
300
350
400
450
Time (μs)

Figure (4.5)

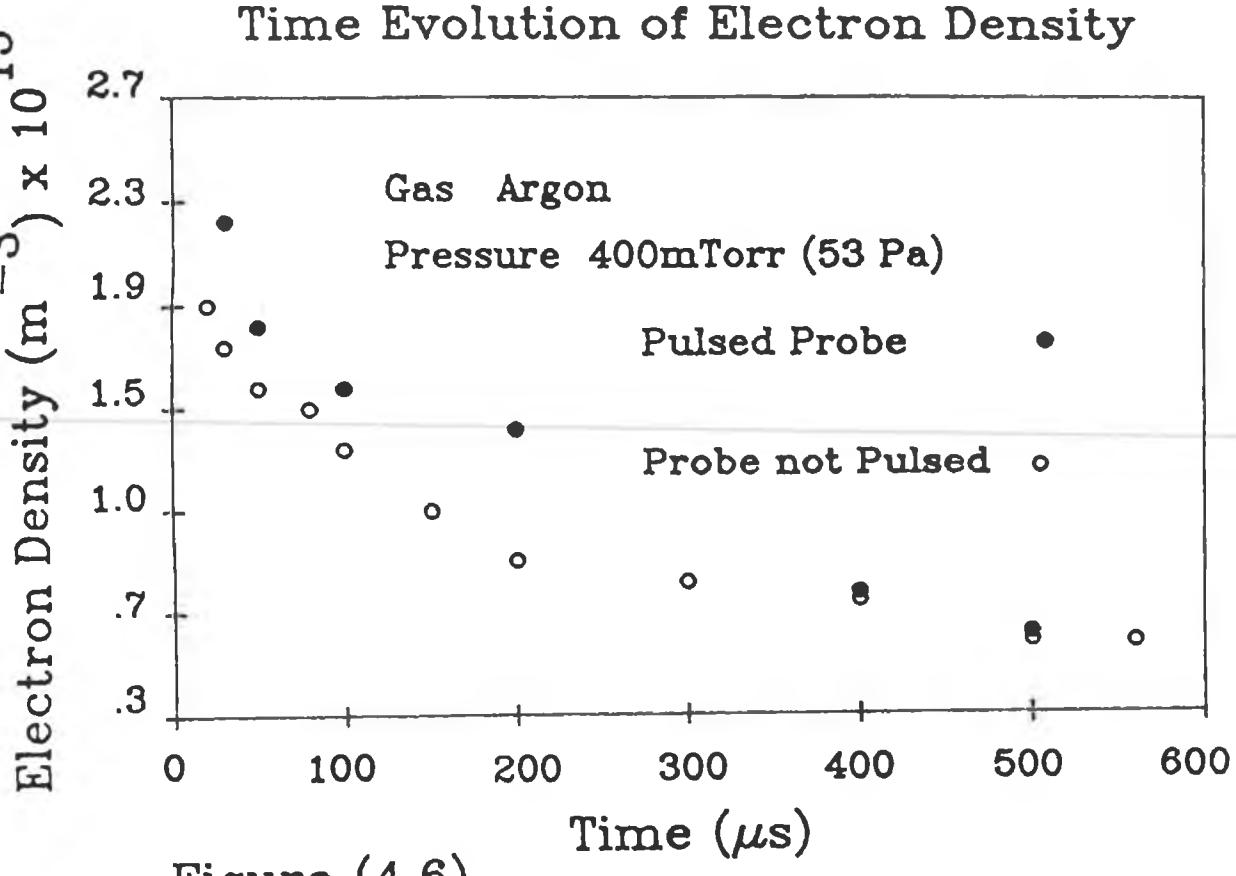

Figure (4.6)

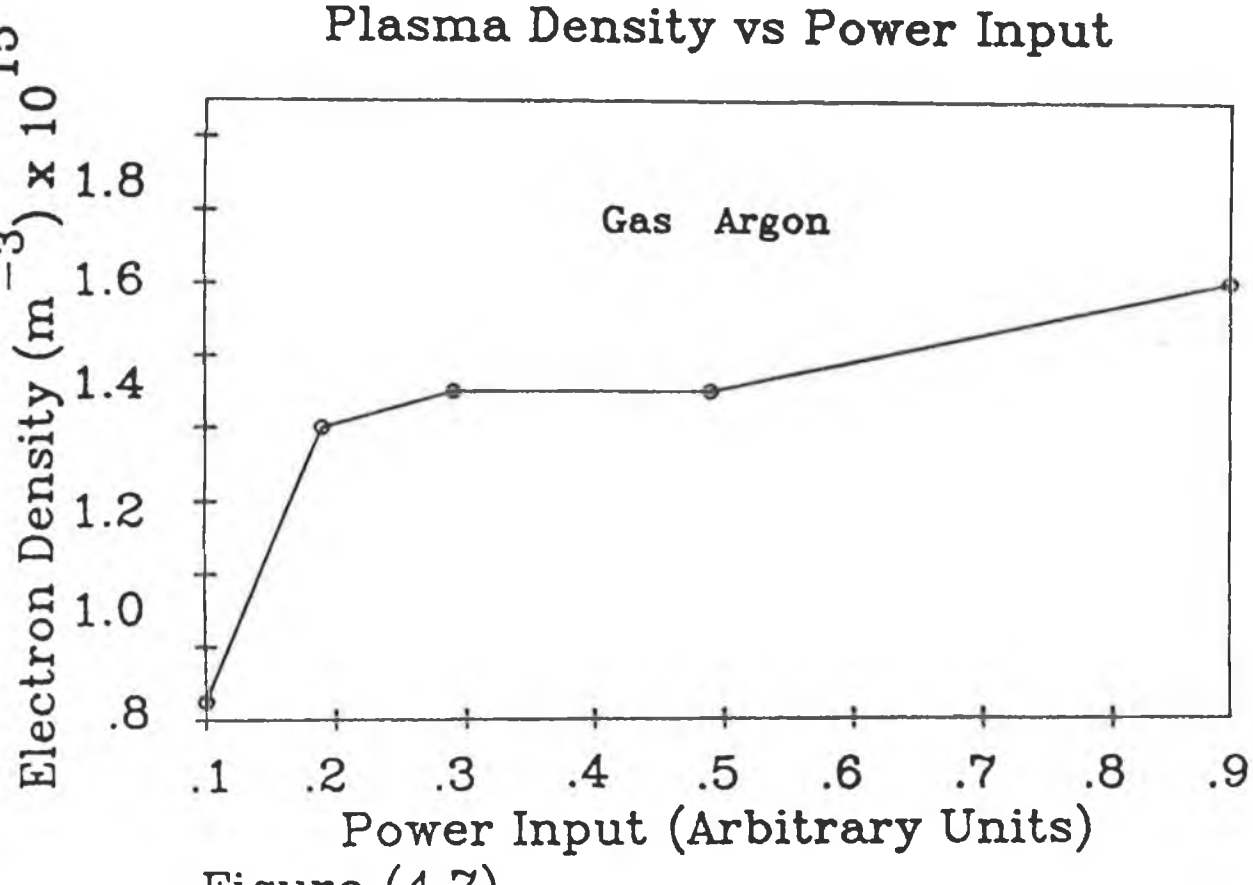

Figure (4.7)

4.4 Conclusions

The acquisistion electronics and software (C and 8086) is developed to a stage where Langmuir probe characteristics can be obtained and analysed to yield the important plasma parameters such as density, temperature and the various potentials; an obvious extension to this would be the ablility to obtain electron energy distributions. The pulsed probe method is seen to work effectively, and is used to minimise the perturbative effect of the measurement process on weak afterglow plasmas. The probe is allowed to float at all times except for a very small fraction of the afterglow time when the scan voltage is applied to it. Initial oscillations are allowed to die away and the current and voltage are sampled at a variable time relative to the probe-on pulse. A characteristic can thus be built up point by point with variable averageing to reduce noise.

It is important to monitor gas purity regularly, and also minimise impurity concentrations, such as water molecules or material sputtered off the walls as it is thought that these can drastically affect the results.

The simple one dimensional theory gives agreement to within an order of magnitude of the experimental results and the next step is to study the spatial variation of the density in the afterglow, thus yielding a density map of the discharge chamber.

A three dimensional model would of course yield a lot more information as would the inclusion of accurate collisional and recombinational effects. The effect of metastable atoms on the afterglow could be studied using laser induced fluorescence, and could yield valuable information on the nature of the temperature decay rates, and also comparison with other diagnostic techniques is advisable.

These alternative tests could include the use of microwaves, mass spectrometry and laser diagnostics; the more comparitive techniques used the better the understanding of the plasma will be.

REFERENCES

1. R.J. Hastie, *Plasma Physics and Nuclear Fusion Research,* R.D. Gill, ed., U.K.A.E.A. Research Group, Culham Laboratory, Abingdon, U.K., Academic Press (1981)
2. M.F. Hoyaux, *Solid State Plasmas,* Pion Limited, London (1970), Chapter 7
3. F.F. Chen, *Plasma Diagnostics Techniques,* R.H. Huddlestone, and S.L. Leonard, eds., Academic Press, New York (1964), Chapter 4
4. K. Wiesemann, *Electrical Diagnostic Methods for Reactive Plasmas,* notes of lectures given at the International Summer School on Plasma Chemistry (ISSCP), Atami, Japan 1987
5. B. Chapman, *Glow Discharge Processes* (Wiley, New York, 1980)
6. A.V Engel, 2nd ed. Clarendon, Oxford (1965)
7. L.B. Loeb, *Basic Processes of Gaseous Electronics,* University of California Press Berkeley (1955), *Recent Advances in Basic Processes of Gaseous Electronics,* University of California Press, Berkeley (1973)
8. W.B. Thompson, *An Introduction to Plasma Physics,* Pergamon Press, Oxford (1962)
9. J.D. Cobine, *Gaseous Conductors,* Dover Publications, New York (1958)
10. S.K. Dhali, *IEEE Trans. Plasma Sci.* 17, 603 (1989)
11. J.P. Bouef and Ph. Belenguer, *Non Equilibrium Processes in Partially Ionised Gases, NATO Advanced Study Institute, Series B: Physics,* edited by M. Capitelli and J.N. Bardsley (Plenum, New York, in press)
12. C.A. Anderson, W.G. Graham, and M.B Hopkins, *Appl.Phys.Lett.* 52, 783 (1988)
13. A.J. van Roosemalen, W.G.M. van den Hoek, and H. Kalter, *J.Appl.Phys.* 58, 653 (1985)
14. J.S. Logan, N.M. Mazza, and P.D. Davidse, *J.Vac.Sci.Technol.* 6, 120 (1967)

15. Ajit P. Paranjpe, Ph.D thesis entitled *Studies of Gas Discharges for Dry Etching*, Technical Reference Number G833-2 (1989)
16. S.C. Brown, *Introduction to Electrical Discharges in Gases*, Wiley, New York (1966)
17. E. Blue and J.E. Stanko, *J.Appl.Phys.* 40, 4061 (1969)
18. D. Smith, C.V. Goodall and M.J. Copsey, *J.Phys.B (Proc.Phys.Soc.)* 1, 660 (1968)
19. R.S. Powers, *J.Appl.Phys.* 37, 3821 (1966)
20. R.M. Clements and H.M. Skarsgard, *Can.J.Phys.* 45,3199 (1967)
21. E. Gogolides, J.P. Nicolai, and H.H. Sawin, *J.Vac.Sci.Technol.A* 7, 1001 (1989)
22. G.R. Misium, A.J. Lichtenberg, and M.A. Lieberman, *J.Vac.Sci.Technol.A* 7, 1007 (1989)
23. P. Bletzinger and Mark J. Flemming, *J.Appl.Phys.* 62, 4688 (1987)
24. M.B. Hopkins and W.G. Graham, *Rev.Sci.Instrum.* 57, 2210 (1986)
25. L.Schott, *Plasma Diagnostics,* edited by W.L Holtgreven (North - Holland, Amsterdam, 1968), Chapter 11
26. C.A. Anderson, M.Sc. Thesis entitled *Time Resolved Plasma Parameter Measurements,* (1987)
27. M.B. Hopkins, A.P. Hughes, J.C. Molloy, and J.V. Scanlan, *International Colloquium on Plasma Sputtering,* Antibes, France, 5 - 9 June (1989)
28. J.F. Waymouth, *J.Appl.Phys.* 37, 4492 (1966)
29. M. Grimley, private communication
30. S.Gasiorowicz, *Quantum Physics* (Wiley, New York 1974)
31. W.G. Graham, Conference on *Gas Discharges and their Applications*, Dublin City University, Ireland, 29 - 30 March 1990
32. G.R. Taylor and K.N. Leung, *Rev.Sci.Instrum.* 47, 614 (1976)

33. M.B. Hopkins, W.G. Graham, and T.J. Griffin *Rev.Sci.Instrum.* 58, 475 (1987)

34. D.C Schram, an article entitled *The Physics of Plasmachemistry,* source and date unknown

35. T. Herbert, Conference on *Gas Discharges and their Applications,* Dublin City University, Ireland, 29 - 30 March 1990

36. M. Kushner, *Non Equilibrium Processes in Partially Ionised Gases, NATO Advanced Study Institute, Series B: Physics,* edited by M. Capitelli and J.N. Bardsley (Plenum, New York, in press)

37. H.R. Koenig and L.I. Maissel, *IBM J.RES.DEVELOP.*, page 168 March 1970

38. K.F. Schoenberg, report entitled *ELECTROSTATIC PROBE DIAGNOSTICS ON THE LBL 10 AMPERE NEUTRAL BEAM ION SOURCE,* Lawrence Berkeley Laboratory, University of California, Berkeley 1978

39. D.G. Bills, R.B. Holt and B.T. McClure, *J.Appl.Phys.* 33, 29 (1962)

40. F. El Hossary, D.J. Fabian and A.P. Webb, *IPAT conference* 1987

41. F. Llewellyn - Jones, *The Glow Discharge and an Introduction to Plasma Physics,* London: Methuen & Co LTD (1966)

42. James Molloy, Conference on *Gas Discharges and their Applications,* Dublin City University, Ireland, 29 - 30 March 1990

43. T.J. Sommerer, W.N.G. Hitchon and J.E. Lawler, accepted for publication in *Phys.Rev.Letters*

44. J.V. Scanlan, Conference on *Gas Discharges and their Applications,* Dublin City University, Ireland, 29 - 30 March 1990

45. Ph. Beleunguer and J.P. Bouef, *Phys.Rev.A* 41, 4447 (1990)

APPENDICES

APPENDIX A

CHARACTERISATION OF RF PLASMAS USING LANGMUIR PROBES

M.B. Hopkins, A. Hughes, J.C. Molloy, and J.V. Scanlan

Dept. of Applied Physics, NIHE, Glasnevin, Dublin 9, Ireland

Abstract

In this paper, a novel method for obtaining a Langmuir probe characteristic in an rf plasma is presented. Although its development is at an early stage, it can, in principle, be used to obtain measurements over the entire rf driving voltage cycle and may be extended to high rf frequencies.

Introduction

Radio-frequency (rf) generated plasmas are widely used in many processing applications. The need for reliable and accurate diagnostics is well established. Spectroscopic diagnostic methods have the disadvantage that they cannot be used to obtain local measurements of plasma parameters. Neither is it possible to measure the electron energy distribution function (EEDF). The Langmuir probe technique is used very successfully in DC glow discharges; measuring such parameters as bulk electron temperature kTe, bulk electron density ne, plasma potential Vp and floating potential Vf [1,2]. In the case of rf plasmas, however, the analysis of the probe current-voltage (I-V) characteristic is hampered by the presence of large fluctuations in the plasma-probe potential. This voltage results in modification of the probe I-V characteristic leading to erroneous measurements of plasma parameters [3,4]. For example,values of kTe are overestimated by a factor of at least 2 or 3, due to the measured I-V characteristic being time-averaged over the rf cycle.

Probe techniques

(A) Single probe

It has been shown that accurate measurements of plasma parameters using a single probe are possible using time resolved measurements of the I-V characteristic [5,6]. Measurements, however, were confined to a small period of the rf cycle. Also, the technique is useful only at low rf frequencies and cannot be used at frequencies approaching the ion plasma frequency.

The problems outlined above have also been approached by attempting to superimpose, on the probe potential, an rf bias of the same frequency, amplitude and phase as the rf component of the plasma potential [4,7]. The rf voltage between the probe and plasma is thus removed and the characteristic is obtained in the conventional manner. This technique ignores the fact that the plasma-probe fluctuations are not sinusoidal and assumes no temporal variation of the I-V characteristic. Also, in the presence of a non-sinusoidal fluctuation of the plasma probe potential, the procedure employed to adjust the amplitude and the phase of the compensating rf bias is not valid.

(B) Double probe

In electrodeless discharges, where no return or reference for the

single probe exists, double probes are frequently used. Two equal area probes are biased with respect to each other and the entire system "floats" with the plasma, provided it is not loaded by capacitive coupling to ground. Therefore, unlike the single probe, the double probe is immune to fluctuations in the plasma potential and valid measurements are possible in rf produced plasmas. The double probe technique suffers from one important drawback. Electron current collected by the positively biased probe must be returned to the plasma. Hence, it cannot exceed ion current to the negative probe. This usually means that only those electrons in the high energy tail of the EEDF are collected by a double probe. In the presence of fast electrons the double probe can not measure the bulk electron temperature [1,2].

(C) The Follower technique

The device presented here consists of two equal area probes, but acts like a highly asymmetric double probe, thus giving a single probe characteristic. One of the two probes feeds the input of a voltage follower. The output of this follower is then treated as a reference to which the voltage on the other probe is varied and measured. The current through the probe system is measured as a voltage drop across a resistor on the driven probe.

The important distinction between this method and the conventional double probe arrangement is that the follower is capable of "sinking" the collected current through the chamber wall. Thus, the current collected by the positively biased probe is not limited by the ion current to the negative probe. Also, the two probes can "float" relative to ground, similar to the conventional double set-up. The system is therefore immune to fluctuations in the plasma potential.

Results

The present measurements were taken in a stainless-steel walled vacuum chamber with two 80mm diameter parallel electrodes separated by 35mm. The electrodes were transformer coupled and driven with 1W of rf power at a frequency of 400Hz. The wall of the chamber was isolated from the electrodes and was connected to ground.

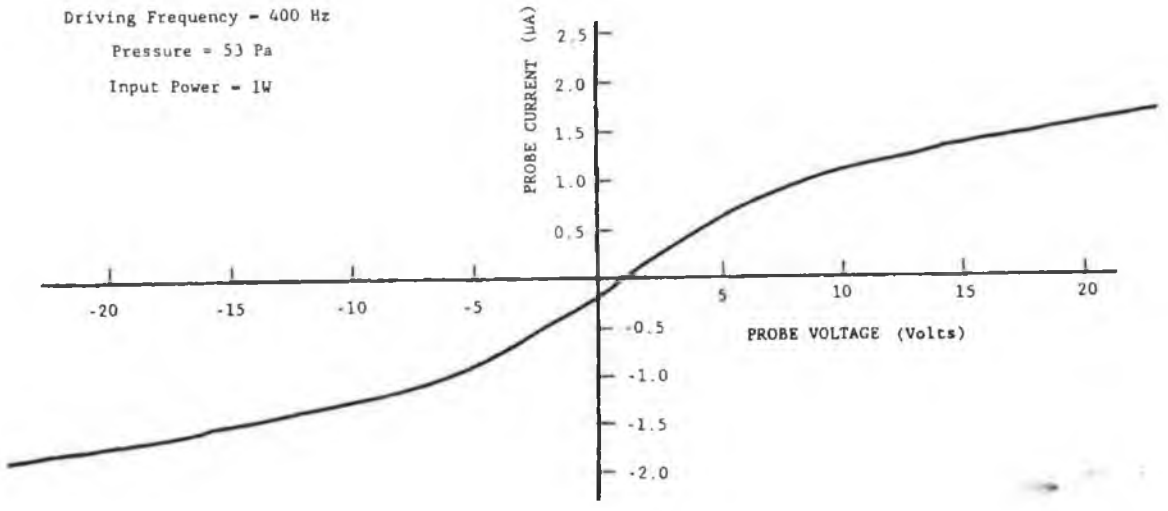

Fig. 1 Double Probe Characteristic

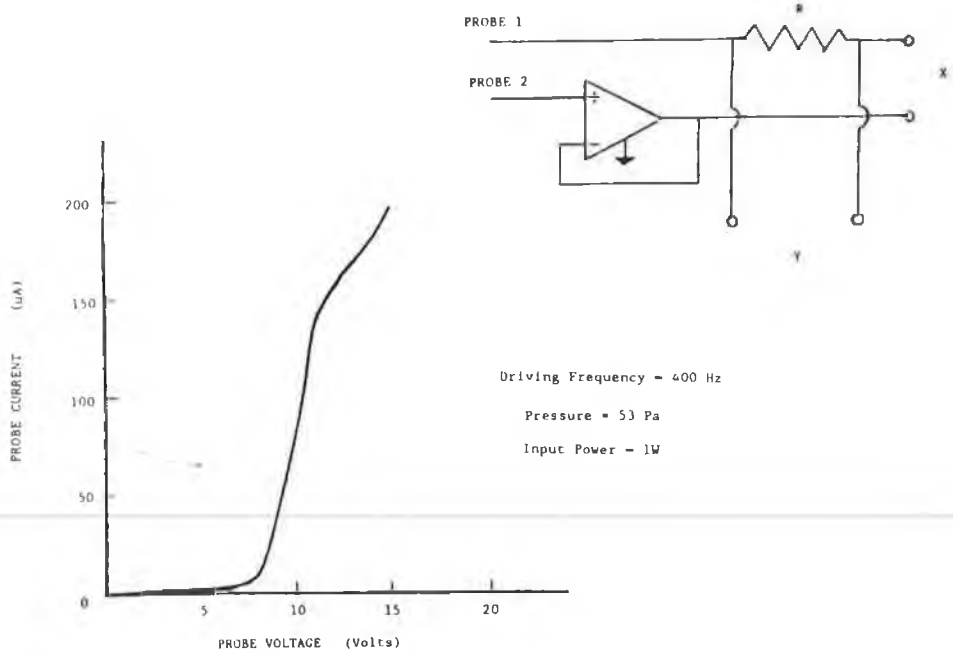

Fig. 1 Double Probe Characteristic with Follower The Inset shows the Probe Circuit

Measurements were taken in the pressure range of 40 Pa to 80 Pa. Both cylindrical probes were constructed from 0.25mm radius tungsten wire with 6.6mm exposed beyond a ceramic sleeve. The probes were separated by a distance of 12.7mm and positioned near the central axis and parallel to the electrodes.

Figure 1 shows a typical double probe characteristic. The displacement of the characteristic from the origin may be due to a difference in plasma potential between the probes. This characteristic, taken at 53 Pa, gives a value of kTe = 3.2eV and ne = 4.8×10^{14} m^{-3} Figure 2 shows the characteristic with the same double probe system but with one probe feeding the follower. As is clearly seen this characteristic resembles that of a normal single probe characteristic. The value of kTe obtained from this characteristic is 0.6eV, representing a much cooler plasma. The plasma does contain a component of fast electrons which accounts for the erroneous measurement produced by the double probe system without the follower. The density measured by both techniques are in reasonable agreement; ne=4.4×10^{14} m^{-3} in the case of the follower and ne=4.8×10^{14} m^{-3} in the case of the normal double probe arrangement.

1. F.F. Chen, in *Plasma Diagnostic Techniques*, R.H. Huddleston, and S.L. Leonard, eds., Academic Press, New York (1964) Chapter 4
2. L. Shott and W. Lochte-Holtgreven, eds., *Plasma Diagnostics*, Wiley, New York (1968) Chapter 11
3. N. Hershkowitz, M.H. Cho, C.H. Man, and T. Intrator, *Plasma Chemistry and Plasma Processing*, Vol.8, No.1, 1988
4. D. Maundrill, J. Slatter, A.I. Spiers, and C.C. Welch, *J.Phys.D.* 20, 815 (1987)
5. C.A. Anderson, W.G. Graham, and M.B. Hopkins, *Appl. Phys. Lett.* 52, 783 (1988)
6. M.B. Hopkins, C.A. Anderson, and W.G. Graham, *Europhys. Lett.* 8, 141 (1989)
7.T.I. Cox, V.G.I. Deshmukh, D.A.O. Hope, A.J. Hydes, N. St. J. Braithwaite, N.M.P. Benjamin, *J. Phys. D.* 20, 820 (1987)

APPENDIX B

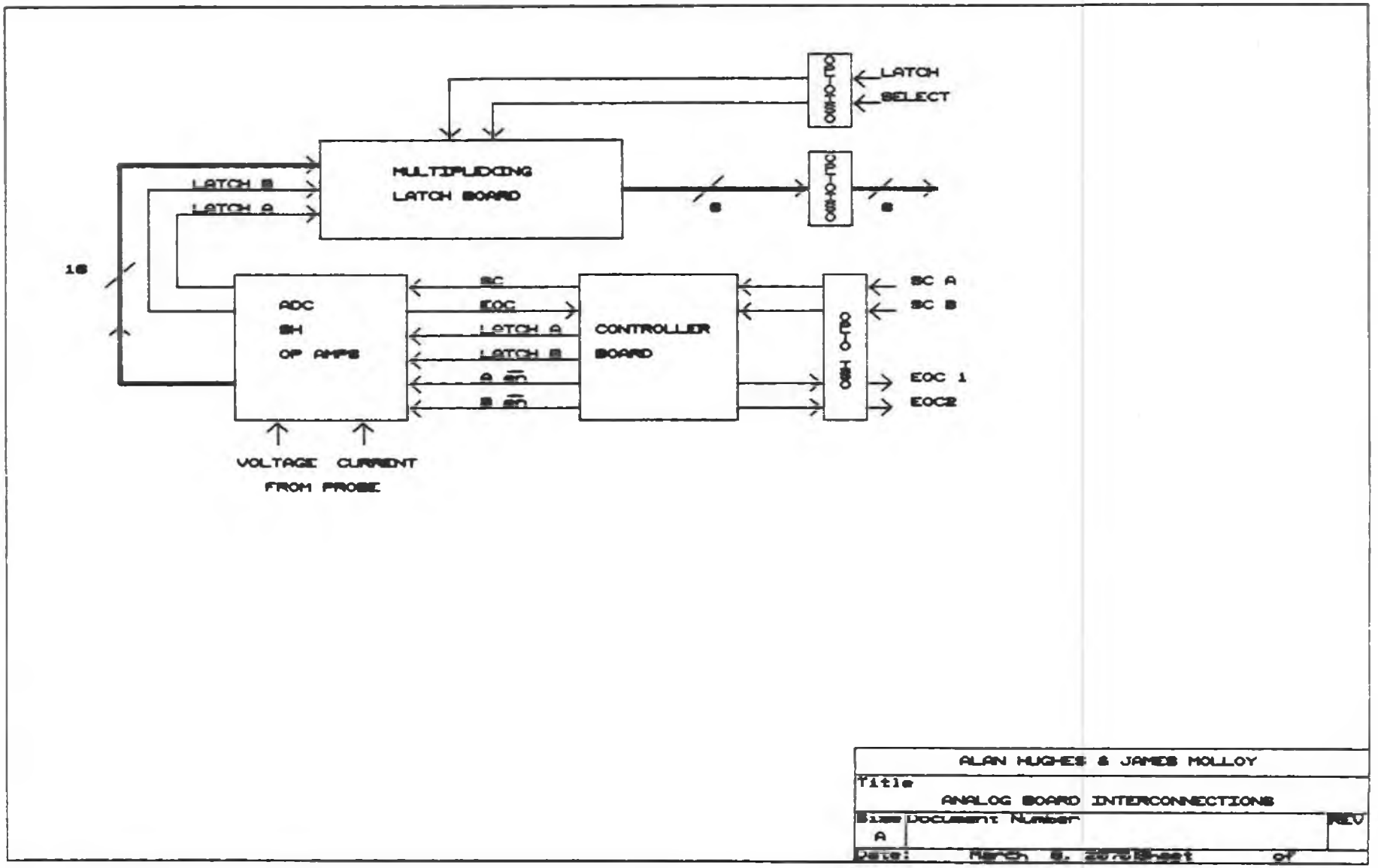
LATCH
SELECT
MULTIPLEXING
LATCH BOARD
LATCH B
LATCH A
8
8
16
ADC
SH
OP AMPS
SC
EOC
LATCH A
LATCH B
A EN
B EN
CONTROLLER
BOARD
SC A
SC B
EOC 1
EOC2
VOLTAGE
CURRENT
FROM PROBE
ALAN HUGHES & JAMES MOLLOY
Title
ANALOG BOARD INTERCONNECTIONS
Size
A
Document Number
REV
Date:
Sheet
of

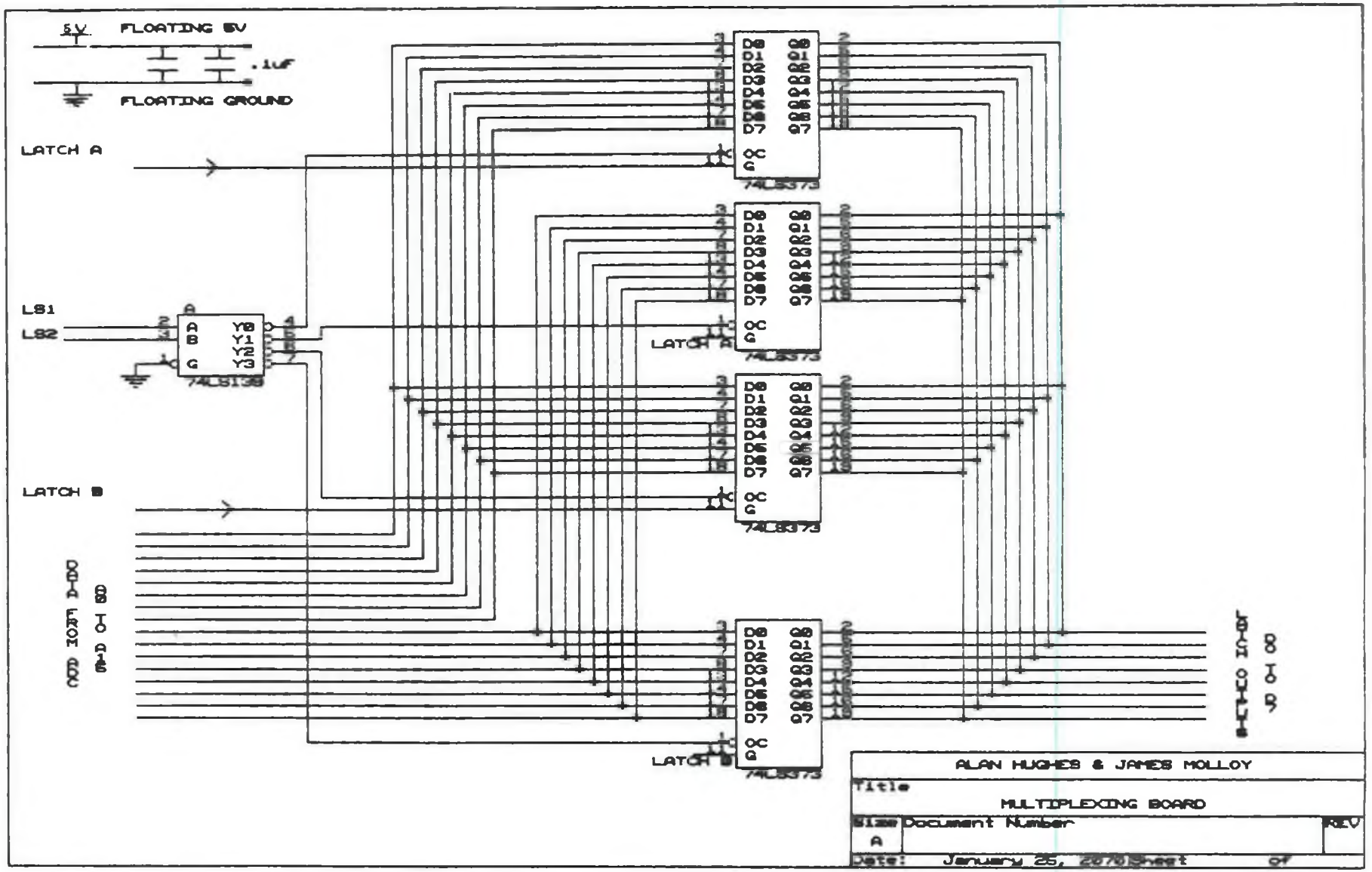
5V
FLOATING 5V
.1uF
FLOATING GROUND
LATCH A
LATCH B
LS1
LS2
74LS138
74LS373
DATA BUS
ADDRESS BUS
ALAN HUGHES & JAMES MOLLOY
Title
MULTIPLEXING BOARD
Size
A
Document Number
REV
Date: January 25, 2010
Sheet
of

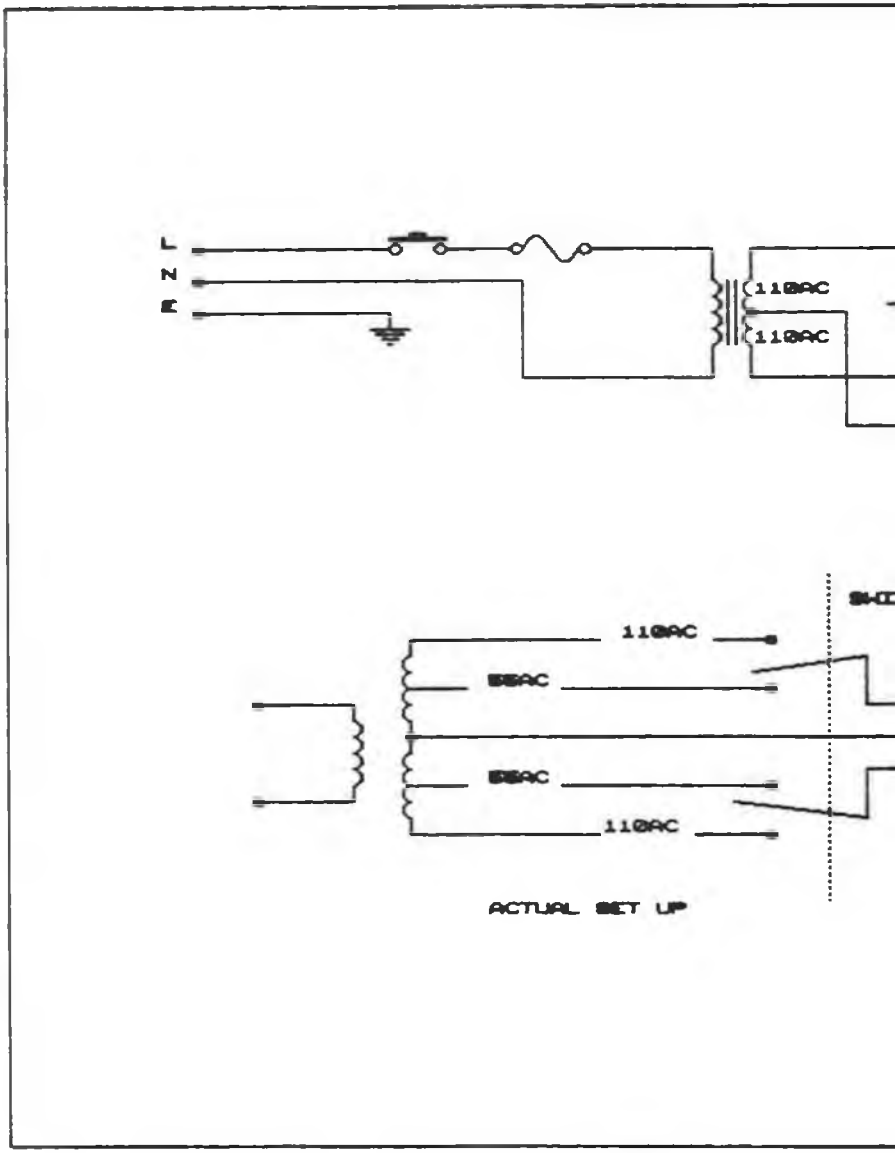
L
N
E
110AC
110AC
110AC
55AC
55AC
110AC
ACTUAL SET UP

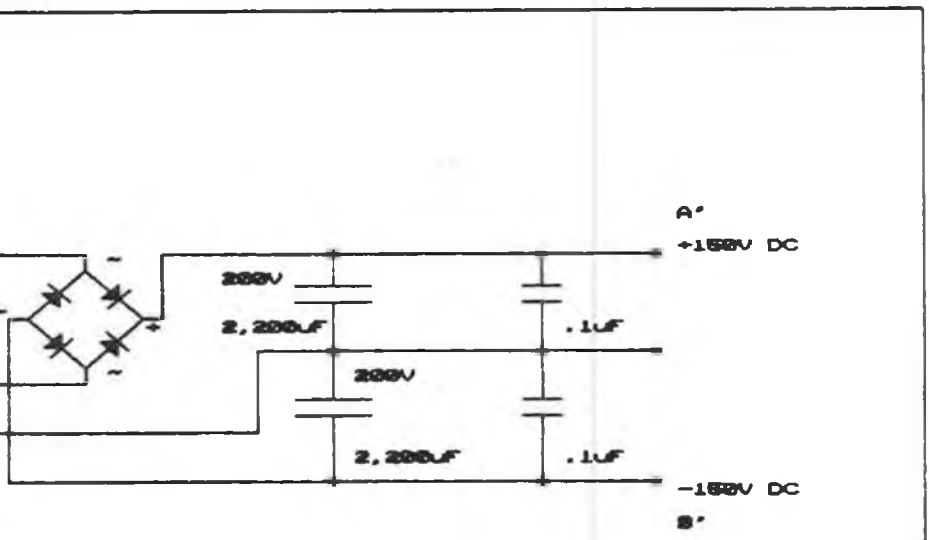

TCHES

ALAN HUGHES & JAMES MOLLOY		
Title: High Tension Power Supply Unit		
Size: A	Document Number:	REV:
Date: March 21, 2070	Sheet: of	

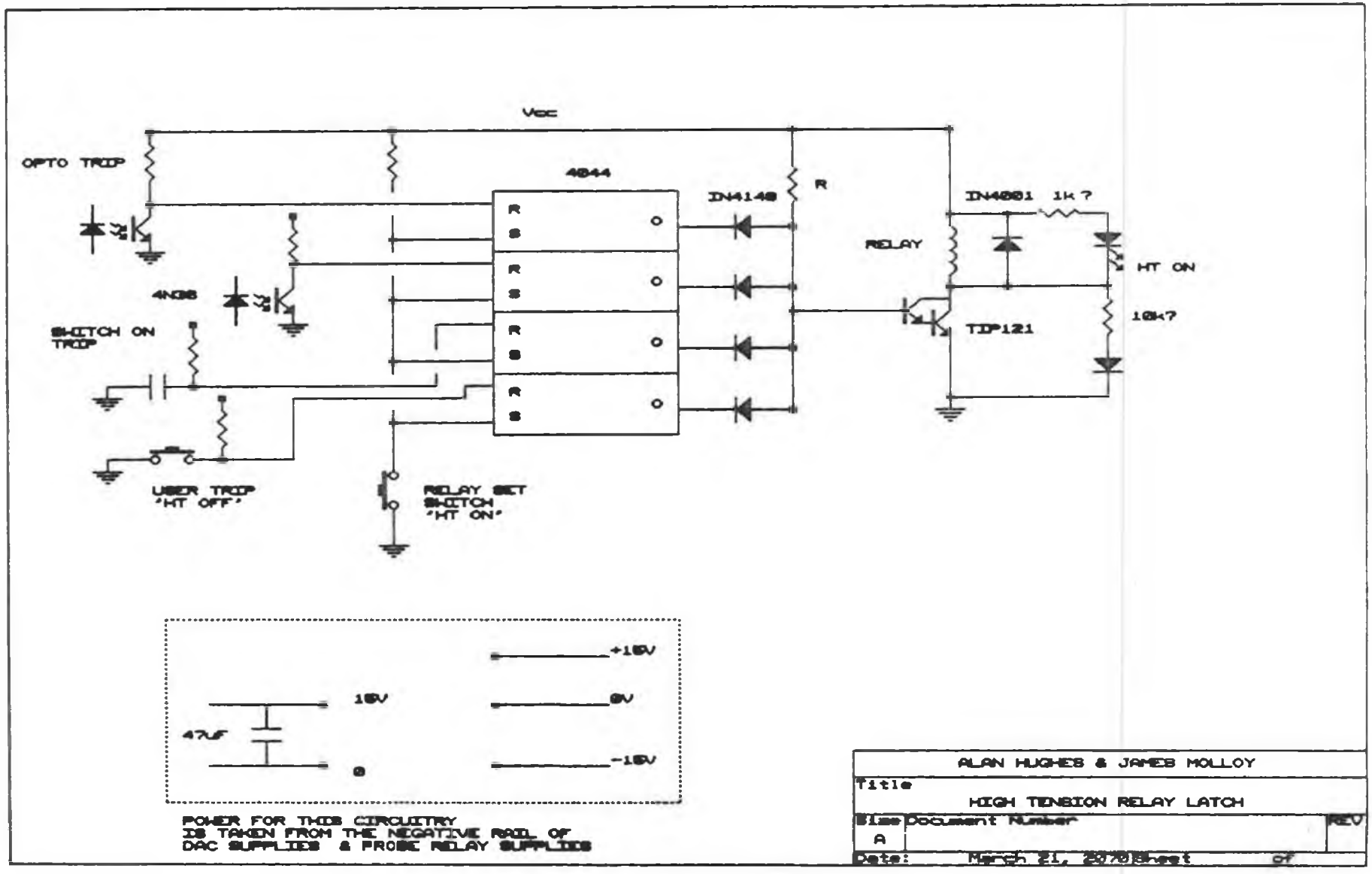
Vcc
OPTO TRIP
4N35
SWITCH ON TRIP
USER TRIP 'HT OFF'
4044
R
S
IN4148
R
RELAY SET SWITCH 'HT ON'
IN4001
1k7
RELAY
HT ON
10k7
TIP121
+15V
15V
0V
47uF
0
-15V
POWER FOR THIS CIRCUITRY IS TAKEN FROM THE NEGATIVE RAIL OF DAC SUPPLIES & PROBE RELAY SUPPLIES
ALAN HUGHES & JAMES MOLLOY
Title
HIGH TENSION RELAY LATCH
Size
A
Document Number
REV
Date:
March 21, 2070
Sheet
of

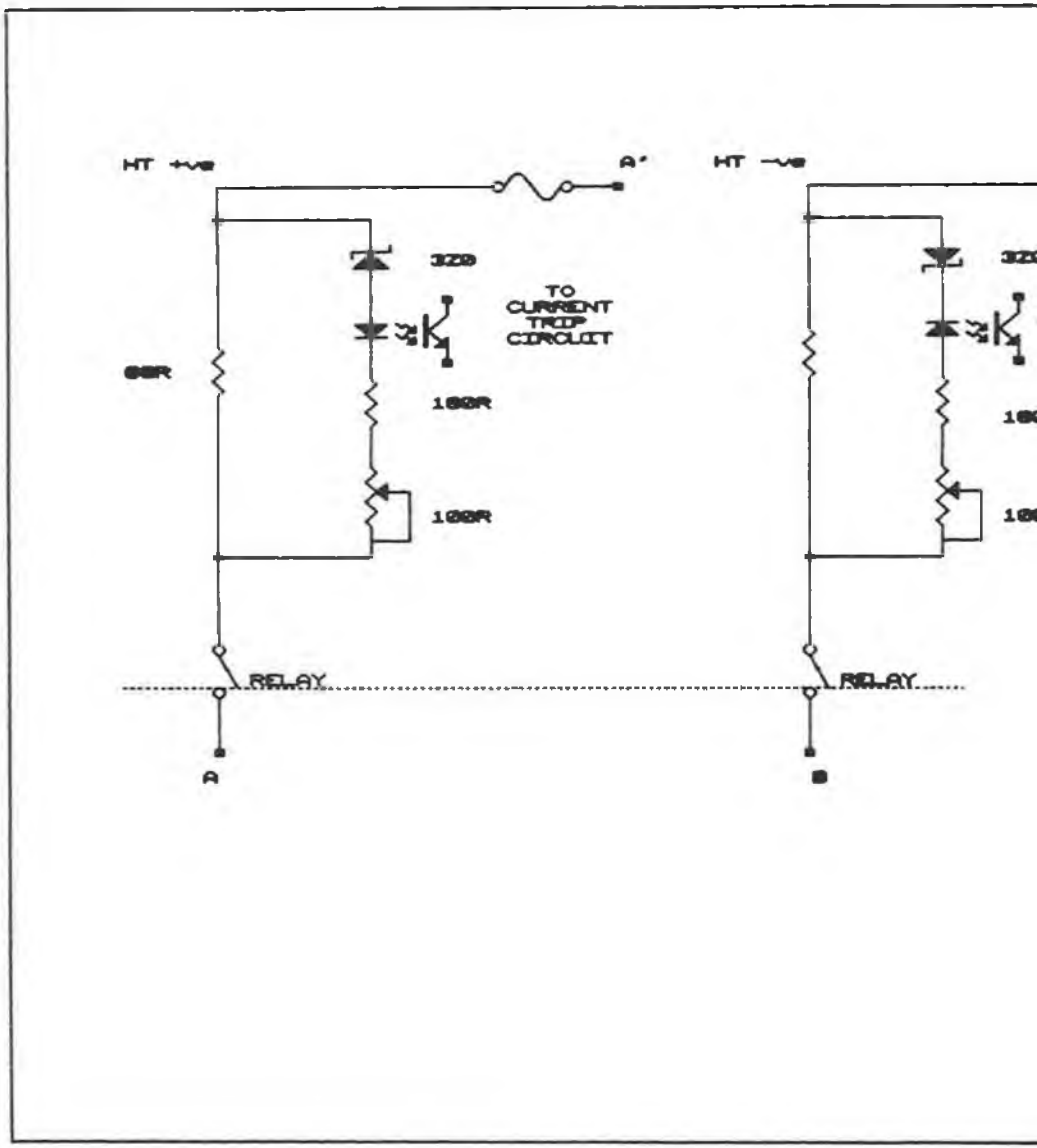
HT +ve
A'
HT -ve
320
TO
CURRENT
TRIP
CIRCUIT
68R
180R
100R
RELAY
RELAY
A
B

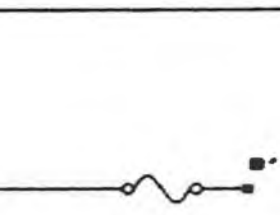

B

4N36

3R

3R

ALAN HUGHES & JAMES MOLLOY		
Title: Current Sense		
Size: A	Document Number:	REV:
Date: March 8, 2010	Sheet of	

APPENDIX C

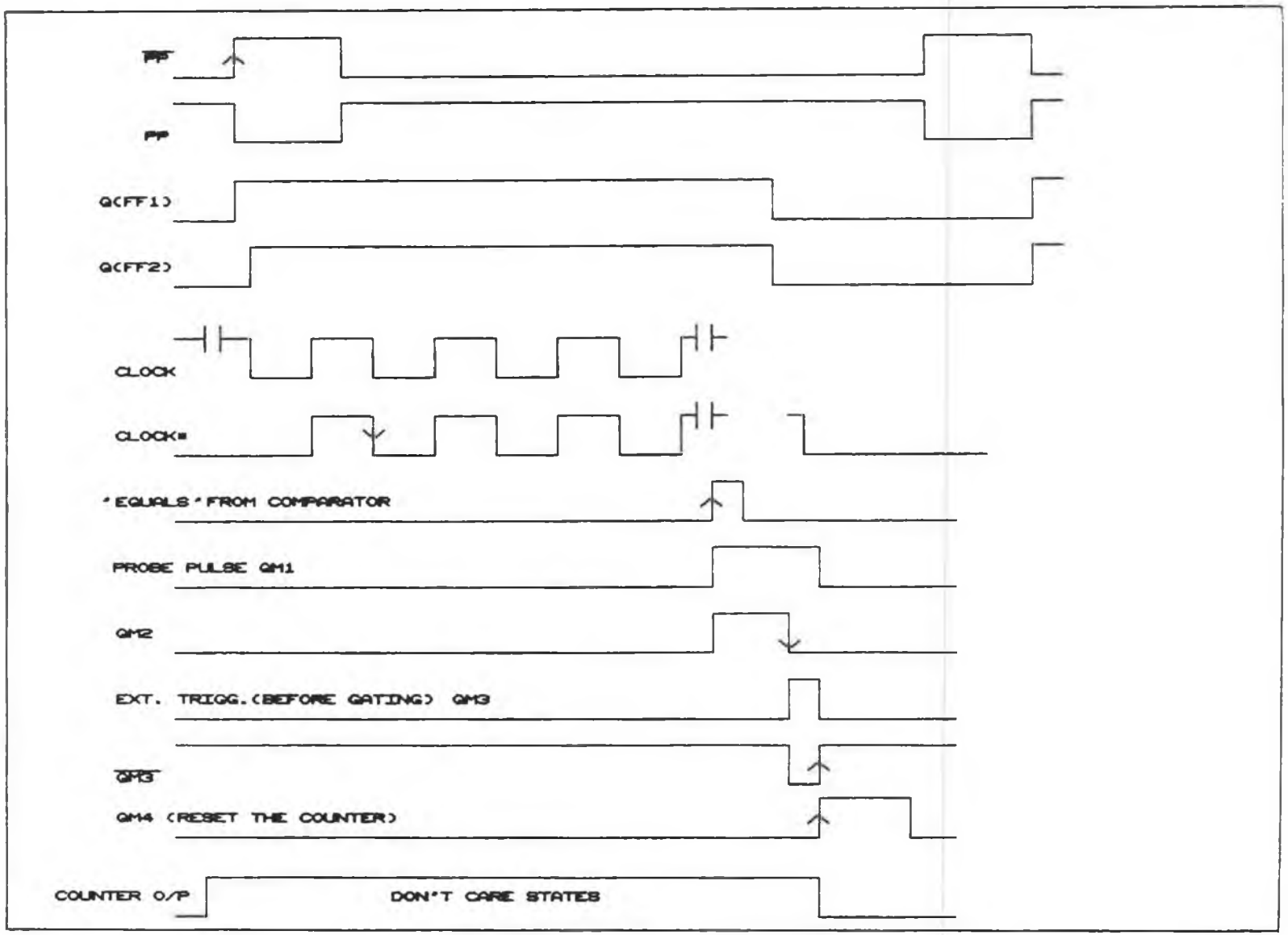
FF
FF
Q(FF1)
Q(FF2)
CLOCK
CLOCK=
'EQUALS' FROM COMPARATOR
PROBE PULSE QM1
QM2
EXT. TRIGG.(BEFORE GATING) QM3
QM3
QM4 (RESET THE COUNTER)
COUNTER O/P
DON'T CARE STATES

APPENDIX D

The Assembly program for non-time resolved measurements

Initialise the segments and allocate stack

```
DOSSEG
.MODEL small
.STACK  100h
.DATA
.CODE
```

Declare the routine as public to enable access by other programs; declare other routines used by this one

```
PUBLIC _vals1
EXTRN snooze:PROC
```

Define the routine

```
_vals1   PROC
```

Define the i/o ports used

```
porta1 equ 200h
portc1 equ 202h
```

Initialise frame pointer

```
push bp
mov bp,sp
```

'push' registers that will be used

```
push si
```

move the C function parameters to the relevant memory locations - cx acts as the counter and si as the memory pointer

```
mov cx,[bp+4]
mov si,[bp+6]
```

clear the data storage locations

```
xor ax,ax
mov [si],ax
mov [si+2],ax
mov [si+4],ax
mov [si+6],ax
```

```
start the routine
     begin:
'start convert' with adequate delay for opto isolators to
settle
     mov al,40h
     mov dx,portc1
     out dx,al
     call snooze
     mov al,20h
     out dx,al
     call snooze
Has END of CONVERT 1 (current conversion complete) changed
state?
     in al,dx
     and al,01h
     jnz begin
     end1:
     in al,dx
     and al,01h
     jz end1
Read the high byte of the current and store
     mov dx,porta1
     xor ax,ax
     in al,dx
     add [si+4],ax
Read the low byte of the current and store
     mov dx,portc1
     mov al,30h
     out dx,al
     call snooze
     mov dx,porta1
     xor ax,ax
     in al,dx
     add [si+6],ax
```

```
Check to see if the voltage has been converted
      mov dx,portc1
      end2:
      in al,dx
      and al,02h
      jz end2
      mov al,00h
      out dx,al
      call snooze
Read the high byte of the voltage and store
      mov dx,porta1
      xor ax,ax
      in al,dx
      add [si],ax
      mov dx,portc1
      mov al,10h
      out dx,al
      call snooze
Read the low byte of the voltage and store
      mov dx,porta1
      xor ax,ax
      in al,dx
      add [si+2],ax
Decrease the counter
      dec cx
      jnz begin
'Pop' the relevant registers off the stack
      pop si
      pop bp
Return to the calling program
      ret
      _vals1  ENDP
      END
```

BLOCK DIAGRAM FOR VALS1.ASM

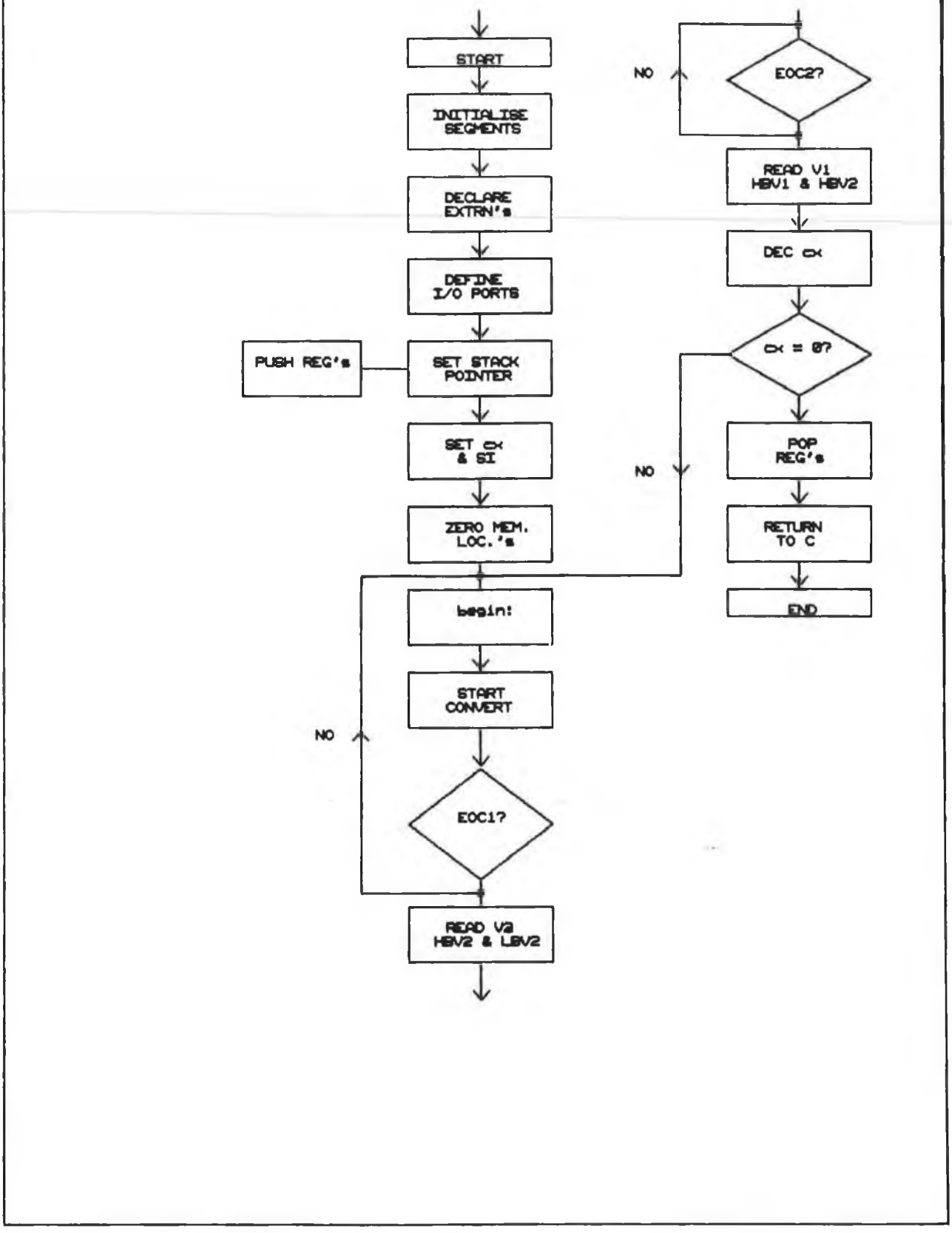

DEFINITIONS

SI - THE STACK INDEX .
DATA IS 'POKED' AT WHERE
THIS POINTS TO IN MEMORY
IT CONTAINS THE SECOND VARIABLE
PASSED FROM C

CX - USED AS A COUNTER & CONTAINS
THE FIRST VARIABLE PASSED FROM C

V1 - THE 16 BIT VOLTAGE

V2 - THE 16 BIT CURRENT

HBV1,HBV2 - HIGH BYTES OF VOLTAGE
AND CURRENT

LBV1,LBV2 - LOW BYTES OF VOLTAGE
AND CURRENT

EOC1 - END OF CONVERSION 1(CURR.)

EOC2 - END OF CONVERSION 2(VOLT.)

ALLOW 8us FOR THE OPTO-
ISOLATORS TO SETTLE

Size	Document Number	REV
B		
Date: March 22, 2070	Sheet	of

APPENDIX E

The function to obtain the experimental data (and analyse it). Note the fact that the relevant library files are included in each C program as the linker does not recognise duplication in this instance.

```
#include <stdio.h>
#include <dos.h>
#include <conio.h>
#include <io.h>
#include <math.h>
#include <stdlib.h>
#include <alloc.h>
```

Declare the Assembly language routines to be used as 'extern'

```
extern void vals1(int,unsigned int *ptr);
extern void relay(int);
extern void snooze(int);
```

Declare any other C functions that will be used in this file. These may be in other C files.

```
void get_data(void);
void pulse(void);
void set(void);
void dac(unsigned int,unsigned int);
float el,begin,end,step,vf,vsat,isat;
int t,o,rmax,rmin,racc;

void get_data()
{
```

Declare variables defined before (in Full.c) as extern so the linker can fetch them and does not give an error.

```
extern float v1[],v2[],zv1,zv2,call;
extern int nost;
```

Define local variables

```
char c;
float area,pi,el,ne,a,me,si,vplas,ion,temp;
int ii,xx,j,i,n,jj;
```

ii is the number of samples to be taken; maximum of 256 at present, but this can be increases ad infinitum by having an extra 'for loop'. ss is defined as a pointer to an unsigned integer i.e. one which can assume a value between 0 and 65535.

```
unsigned int *ss;
float res[5];
```

lbv1 - low byte (8 bits) of the voltage,
hbv1 - high byte (8 bits) of the voltage,
lbv2 - low byte (8 bits) of the current,
hbv2 - high byte (8 bits) of the current,

```
float lbv1,lbv2,hbv1,hbv2;
float gv2,m0,m1,imax,kte,vpl;
float fv1,fv2,vv2,lowlim;
FILE *printer;
```

Accurate values for the resistors (in ohms)

```
res[1]=10.27;
res[2]=105.1;
res[3]=1020;
res[4]=10193;
el=1.6e-19;
me=9.e-31;
pi=3.1415;
area=1.e-5;
```

ss is made point to a certain block of memory. ss will be passed to the assembly language routine vals1.asm (see APPENDIX D), along with ii, the number of samples. The data will then be stored in memory, starting at this memory location and can easily be retrieved by the C calling program.

```
ss=(unsigned int *) calloc(4,sizeof(unsigned int));
```

```
16 bit zeroes for the voltage and current
     zv1=32713;
     zv2=32704;
16 bit equivalent of 10 Volts
     cal1=-3247;
     dac(0,1);
     clrscr();
     printf("I/P starting & finishing voltages for scan,
     time delay between plasma off and sample/hold pulse &
     step  size");
     scanf("%f %f %f %d",&begin,&end,&step,&t);
     clrscr();
Set up delay pulse
     pulse();
     printf("Start relay,lower volt. limit & relay
     for accurate scan?");
     scanf("%d %f %d",&o,&lowlim,&racc);
Get ion current at -45V
     gv2=18.;
     dac(-(65535-326*45),racc);
     delay(20);
     vals1(250,ss);
     hbv1=*(ss);
     lbv1=*(ss+1);
     hbv2=*(ss+2);
     lbv2=*(ss+3);
     ion=zv2-(256.*hbv2+lbv2)/250.;
Convert it to mA's
     ion=1000.*ion/(cal1*gv2*res[racc]);
     clrscr();
     printf("ion current at -45V is %fmA :-Press ENTER to
     continue",ion);
     getch();
     fv1=1;
     fv2=1;
```

```
old slope (used in derivative analysis)
     m1=0.;
     printf("Press any key to go!!");
     getch();
     clrscr();
     printf("SCANNING");
Set array index
     nost=0;
Calibration factor
     si=16.e-6;
Set the max. & min. relay values
     rmax=4;
     rmin=1;
jj=0 ⇒ rough scan; jj=1 ⇒ accurate scan
     for(jj=0;jj<=1;jj++)
     {
For rough scan ii=20 & for accurate scan ii=200
     ii=((jj==0) ? 20 : 200);
Send first voltage to DAC
((begin<=0.)?dac(-(65535+326*begin),o):dac(-(326*begin),o));
The above line is a short way of writing the Boolean
expression:- if(x<0) then y=a; else y=b.  In the above
shorthand this is:- y=((x<0) ? (y=a) : (y=b))
 delay(20);
Probe voltage loop
     for(a=begin+step;a<=end;a+=step,nost++)
          {
Call assembly language routine to take data
          vals1(ii,ss);
Send voltage to DAC and relay
     ((a<=0.) ? dac(-(65535+326*a), o)
     : dac(-(326*a), o));
 Read data from memory
          hbv1=*(ss);
          lbv1=*(ss+1);
          hbv2=*(ss+2);
          lbv2=*(ss+3);
```

vv2 is used as a dummy variable (it represents the current in 16 bits) and relay switching decisions are made using it

```
vv2=(256.*hbv2+lbv2)/ii;
```

If the zeroed current is small enough to allow a higher relay number (and hence a more sensitive/accurate reading to be taken) then switch up in relay

```
if(fabs(vv2-zv2) <= 2900 && o < rmax)
{relay(++o);
```

Take the voltage drop across the sensing resistor into account (depending on the direction of current flow)

```
if(vv2-zv2 > 0) a+=.5;
else a-=.5;
```

Send previous voltage to DAC and do conversions

```
(a<=0.) ? dac(-(65535+326*(a-step)), o)
: dac(-(326*(a-step)), o));
delay(20);
vals1(ii,ss);
```

Send voltage to DAC

```
((a<=0.) ? dac(-(65535+326*a),o)
: dac(-(326*a),o));
hbv1=*(ss);
lbv1=*(ss+1);
hbv2=*(ss+2);
lbv2=*(ss+3);
```

Convert 16 bit numbers to volts and mA's

```
v2[nost]=(zv2-(256.*hbv2+lbv2)/ii);
v1[nost]=(10.*fv1*(zv1-(256.*hbv1+lbv1)/ii)/cal1)
+si*v2[nost];
v2[nost]=1000.*fv2*v2[nost]/(cal1*gv2*res[o]);
}
```

If the zeroed current is too large then switch down relays and repeat as above

```
else if(fabs(vv2-zv2) > 31000 && o > rmin)
{
relay(--o);
if(vv2-zv2 < 0) a+=.5;
else a-=.5;
((a<=0.) ? dac(-(65535+326*(a-step)),o)
: dac(-(326*(a-step)),o));
delay(20);
vals1(ii,ss);
((a<=0.) ? dac(-(65535+326*a),o) : dac(-(326*a),o));
hbv1=*(ss);
lbv1=*(ss+1);
hbv2=*(ss+2);
lbv2=*(ss+3);
v2[nost]=(zv2-(256.*hbv2+lbv2)/ii);
v1[nost]=(10.*fv1*(zv1-(256.*hbv1+lbv1)/ii)/cal1)
+si*v2[nost];
v2[nost]=1000.*fv2*v2[nost]/(cal1*gv2*res[o]);
}
```

If there is no need to change relays then continue taking data on the present one

```
{
v2[nost]=(zv2-(256.*hbv2+lbv2)/ii);
v1[nost]=(10*fv1*(zv1-(256.*hbv1+lbv1)/ii)/cal1)
+si*v2[nost];
v2[nost]=1000.*fv2*v2[nost]/(cal1*gv2*res[o]);
}
```

Rough 1st scan

```
if(jj == 0 && nost > 1)
    {
```

Skips currents less than twice the absolute value of the ion current at -45V

```
    if(v2[nost] < 2.*fabs(ion)) continue;
```

Gets a value for the floating potential (detects zero crossover)

```
vf=((v2[nost-1]*v2[nost]<0.)? (v1[nost]+v1[nost-1])/2.
: lowlim);
```

Get the first derivative

```
m0=(v2[nost]-v2[nost-1])/(v1[nost]-v1[nost-1]);
```

Find the maximum and a rough value fro V_p

```
if(m0 > m1)
{
m1 = m0;
vplas=v1[nost];
printf("old vp%f",vplas);
}
```

Detect saturation in the electronic current & go no further than the max. of the derivative / 3

```
if(fabs(m0) < m1/3.)
{
vsat = v1[nost];
isat = v2[nost];
printf("vsat %f isat %f",vsat,isat);
```

Initialise the variables to their new values for the accurate scan

```
nost=0;
m1=0.;
set();
```

break out of the voltage loop i.e. take the next jj

```
break;
}
```

Accurate 2nd scan (only go to isat/5) with new voltage range and step size etc. Gives a more accurate value for the plasma potential and calculates the bulk electron temperature

```
if(jj == 1 && nost > 4 && v2[nost] > isat/5.)
    {
    m0=(v2[nost]-v2[nost-4])/(v1[nost]-v1[nost-4]);
    if(fabs(m0) > m1)
        {
        m1=m0;
        imax=v2[nost-2];
        kte=imax/m1;
        printf("isat/imax %f",isat/imax);
        vpl=vplas+kte*(log(isat/imax));
        printf("ACC vp %f kte %f",vpl,kte);
        }
    }
}Next probe voltage
}next jj
```

Bias the probe at -45V to clean it by ionic bombardment

```
dac(-(65535-326*45),1);
```

Calculate the bulk electron density

```
ne=isat*(sqrt(2.*pi*me/(kte*el)))/(1000.*el*area);
printf("Accurate Vp %f kte %f ne %e",vpl,kte,ne);
getch();
do_menu1(0);
}
```

Some of the functions used above

Set up parameters for the accurate scan

```
void set(void)
{
begin=vf;
end=vsat+1.;
step/=20.;
```

Sit on the relay selected by the user

```
rmin=rmax=racc;
}
```

Set up delay & probe pulses

```
void pulse(void)
{
int porta2 = 0x204;
int n,i,data,data1;
```

Convert μs to an 8 bit number for output

```
if(t==10)t=12;
t=(t-10)/2;
outport(porta2,0);disables count
```

Load serial to parallel converter

```
for(i=0;i<=7;i++)
{
n=pow(2,(7-i));
data1=2*(t & n)/n;
outport(porta2,data1);
outport(porta2,data1+16);
}
delay(3);
outport(porta2,128) enable count
}
```

Some of the functions used above

Set up parameters for the accurate scan

```
void set(void)
{
begin=vf;
end=vsat+1.;
step/=20.;
```

Sit on the relay selected by the user

```
rmin=rmax=racc;
}
```

Set up delay & probe pulses

```
void pulse(void)
{
int porta2 = 0x204;
int n,i,data,data1;
```

Convert μs to an 8 bit number for output

```
if(t==10)t=12;
t=(t-10)/2;
outport(porta2,0);disables count
```

Load serial to parallel converter

```
for(i=0;i<=7;i++)
{
n=pow(2,(7-i));
data1=2*(t & n)/n;
outport(porta2,data1);
outport(porta2,data1+16);
}
delay(3);
outport(porta2,128) enable count
}
```

APPENDIX F

A table of the line allocation for the interface between the computer and the electronics. The cable is a 50 - way type and even number connections refer to 8255 chip no. 2 on the PIO board ,whereas odd numbered ones refer to chip no. 1.

Cable no.	Function.	Remarks.
1	o/p from A/D	Port A of chip 1
3	''	(all i/p 's)
5	''	
7	''	
9	''	
11	''	
13	''	
15	''	
		Port B of chip 1
		(all o/p 's)
17	Relay select no. 1	LSB RED
19	Relay select no. 2	YELLOW
21	Relay select no. 3	MSB GREEN
23	No connection	
25	Clock	Old DAC Reset
27	Latch enable	Strobe
29	Data	Data
31	No connection	
		Port C (lower)
		chip 1 (all i/p 's)
33	End of conversion 1	
35	End of conversion 2	
37	External trigger	
39	No connection	
41	Latch select no. 1	Port C (upper)
43	Latch select no. 2	(all o/p 's)
45	Start convert	
47	No connection	

49	Ground for chip 1	Port A chip 2 (all o/p's)
50	Ground for chip 2	

EXTRA CONNECTIONS

4	Data for serial to parallel
10	Clock for serial to parallel

APPENDIX G

An introduction to modelling discharge processes using the Boltzmann Equation

G.1 Introduction

The problem of modelling an RF or pulsed RF discharge is far from being a trivial matter. The so - called parameter space can be quite large if an accurate picture is to be obtained. Obviously the more variables included, the more revealing and informative will be the results. This principle must not be allowed to dictate all modelling work as the computer time needed for computation purposes rises in accord with the amount of detail in the model. There are two main interest groups involved in this area - the practical people like NASA (space shuttle re-entry and planetary / solar plasmas), the military with their SDI programs, and finally the industrial community. The latters needs will be dealt with here.

Boeuf[11] states 'it is now generally accepted that the development and extension of such models represent a very promising way of assisting the conception and design of RF reactors used in the processing of semiconductor devices'. A model can be developed to study either the macroscopic physical properties or the plasma chemistry peculiar to a particular type of reactor architecture. The former would predict the temporal - spatial variations in properties, such as the particle densities and temperatures, the electric field and ionisation rates. More advanced models could also produce the variations in the electron energy distribution function $f(\mathbf{r},\mathbf{v},t)$.

The parameters used will obviously have to account for the most important proccsses known to occur in the discharge. These will include the different collisional regimes and losses, excitation methods, sheath dynamics and power deposition.

The experimentalist plays a fundamental role in that he provides the data which enables the theorist to check his ideas, and also the original 'guesstimates' for collisional cross sections, pre - ionisation, current densities and sheath widths etc. On the other hand the theorists models return valuable information on different processes, and perhaps new mechanisms occurring in the discharge. New ways to use and optimise these processes can then be deduced and the experimentalist can further investigate certain mechanisms or interesting results which could lead to a better understanding of the plasma. There should be a continual dialogue between the two parties.

G.2 Modelling using the Boltzmann equation

A number of researchers have used systems of hydrodynamic or continuum equations to model plasmas[11,15,21,22]. Others, for instance Bletzinger[23] use an equivalent circuit model to try and predict plasma behaviour when parameters such as frequency or power are varied. In the continuum modelling[21] of discharges, hydrodynamic or fluid equations are used to express the creation and transport of the charged species and energy. It is necessary that the plasma behaves as a continuum i.e. the mean free path λ < the characteristic dimension R of the plasma.

These models consist of the solution of fluid equations to represent the electron and ion transport, coupled with Poissons equation for the electric field distribution. These equations are remarkably similar to those used to model semiconductor devices in terms of holes and electrons.

The ideal way to represent the electron and ion kinetics is to solve the Boltzmann equation. This is an integro - differential equation of the form

$$\frac{\partial f}{\partial t} + \mathbf{v} \cdot \nabla f + \frac{\mathbf{F}}{m} \cdot \nabla_{\mathbf{v}} f = \left[\frac{\partial f}{\partial t} \right]_{\text{interactions}} \qquad (G.1)$$

where $f = f(\mathbf{r},\mathbf{v},t)$. The function f is called the particle velocity distribution function (EVDF) and it expresses the number density of particles of a given species at a given time t in the vicinity of a point $\mathbf{r} = (x,y,z)$ with a velocity vector whose extremity is in the vicinity of the point $\mathbf{v} = (v_x,v_y,v_z)$. $\mathbf{F}$ is the force per particle; m is the mass of particles of the relevant species; ∇_v is a symbolic vector analogous to the 'grad' operator ∇, but with the components of $\mathbf{v}$ replacing the cartesian (x,y,z) coordinates.

$(\partial f/ \partial t)_{\text{interactions}}$ indicates the influence of collisions or scatterings (it is zero in a collisionless plasma, and the equation becomes the so - called Vlasov equation). The crucial part of the problem exists in getting the correct form of the $(\partial f/ \partial t)_{\text{interactions}}$ term. This can be approximated to

$$(\partial f/ \partial t)_{\text{inter}} = - \frac{f - f_0}{\tau} \qquad (G.2)$$

Here f_0 is a steady state distribution function (i.e. uniform in the space coordinates, Maxwellian in the velocity components and time - independent), and τ is a relaxation time. This approximation fails when the collision time is strongly velocity dependent. When there are several species of mobile particle present (ions and electrons in our case), a Boltzmann equation must be written for each.

In principle the right hand side should include as many terms as there are significant interactions between particles of the species with others of the same species, and in the general case, with every other species as well. Simplifications can of course be made in certain cases where some types of interactions are negligible. Different important rates can be deduced from the electron energy distribution function (EEDF). If the velocity distribution of the electrons is not Maxwellian but is still isotropic (the same in all directions) the shape of the transition region of the probe curve can give information about the distribution function (this has been discussed already in the main text).

If the distribution function is $f(\mathbf{v})$, a function of velocity only, then the electron density can be obtained from

$$n = \int f(\mathbf{v}) d^3\mathbf{v} = 4\pi \int_0^\infty \mathbf{v}^2 f(\mathbf{v}) d\mathbf{v} \qquad (G.3)$$

By taking different moments of the distribution, one can deduce the important plasma properties for comparison for comparison with experiment.